AN INVESTIGATION INTO NON-LINEAR PROPAGATION OF MSK WITH A VIEW A VIEW TO SPECIFYING AN ADAPTIVE EQUALIZER

Prepared by :- DAVID BAIRD HOWIE, B.Sc. (Elec.)
Engineering, Cape Town

A dissertation submitted to the Faculty of Engineering, Department of Electrical and Electronics, University of Cape Town, Cape Town, in partial fulfilment of the requirements for the degree of Master of Science in Engineering.

Cape Town, Feb. 1989

DECLARATION

I declare that this dissertation is my own original work, it being submitted for the degree of Master of Science in Engineering.

Signed by candidate Signature Removed

(Name of Candidate)

10 day of FEB , 19 89

ABSTRACT

The purpose of this dissertation is to investigate the effects of non-linear propagation on a proposed digital microwave radio link which employs MSK modulation, in order to specify a suitable form of adaptive equalization.

MSK is a coherent modulation technique, having improved spectral roll-off over FSK because it avoids the abrupt phase changes at the bit transitions. However computer simulations and field results indicate that MSK digital radio links do suffer from intersymbol interference and crosstalk.

Software and hardware simulations of multipath propagation are based on Rummlers simplified three path model and statistics. The results obtained from the computer simulations of the MSK link and multipath propagation confirm that there is no simple relationship between the multipath parameters and the BER degradation which could be used in the design of an equalizer.

The choice of adaptive equalizer is made based on criteria such as construction cost,circuit complexity, and performance improvement. It is known from ray model analysis that at a transmitting frequency of 23 GHz deep fading will only occur on links longer than 5.24 km's. However even on hops of length 5 km's the fade time is in the order of 1612 seconds/month (calculated using Rummlers model). A 1dB increase in theoretical E_b/N_0 will also be required to overcome potential modem imperfections.

It is necessary to have a time domain equalizer which can compensate for both amplitude and phase distortions simultaneously by acting directly on the ISI. The equalizer structure chosen is a 2-by-2, fractionally spaced, decision feedback, complex adaptive equalizer with zero forcing control algorithm.

ACKNOWLEDGEMENTS

The author is indebted to the following people in particular :-

Dr. Robin Braun, for his supervision and advice.

Mr. Steven Schrire for his help with components for the constructions.

The staff of the Department of Electrical and Electronics Engineering, for assistance during the project.

The CSIR Foundation for Research Development, and Plessey South Africa, for financial assistance.

Most importantly, my parents, without whom nothing would have been possible.

TABLE OF CONTENTS

LIST OF ILLUSTRATIONS

TABLES

NOMENCLATURE

ACI- Adjacent Channel Interference.

AGC- Automatic Gain Control.

AM- Amplitude Modulation.

BER- Bit Error Rate.

Complex equalizer- Equalizer associated with a m-ary modulation scheme.

CMA- Constant Modulus Algorithm.

CP-FSK- Continuous Phase Frequency Shift Keying.

Crosstalk- Intersymbol interference when adjacent bits are associated with different channels.

DFE- Decision Feedback Equalizer.

DFT- Discrete Fourier Transform.

DSD- Differential Steepest Descent.

E_b- Energy per bit.

ENB- Effective Noise Bandwidth.

FFT- Fast Fourier Transform.

Flat fading- Uniform attenuation across the transmission band.

FSE- Fractionally Spaced Equalizer.

ISDN- Integrated Services Digital Networks.

ISI- Inter Symbol Interference.

LFE- Linear Forward Equalizer.

LMS- Least Mean Squares.

LOS- Line Of Sight.

LSI- Large Scale Integration.

LRS- Linear Random Search.

MSK- Minimum Shift Keying.

Minimum phase distortion- Main ray arrives before the delayed ray.

MSE- Mean Square Error.

Non minimum phase distortion- Main ray arrives after the delayed ray.

PM- Phase Modulation.

pdf- Probability Density Function.

PN- Pseudo Noise.

Postcursor- Interfering symbol which follow the symbols that preceed the useful symbol.

Ps- Selective outage probability.

Pso- Outage probability after equalization.

Pt- Probability of exceeding thermal noise threshold.

Precursor- Interfering symbol which preceed the symbols that follow the useful symbol.

QAM- Quadrature Amplitude Modulation.

QPSK- Quadrature Phase Shift Keying.

QPRS- Quadrature Partial Response Signaling.

RLS- Recursive Least Squares.

Selective fading- Non uniform attenuation across transmission band.

SQPRS- Staggered Quadrature Partial Response Signaling.

ZF- Zero Forcing.

INTRODUCTION

In order to specify an adaptive equalizer most suitable to the proposed communication link it is necessary to understand the communication technique to be employed, and the affects of multipath propagation on this technique. Chapter 1 is an introduction to digital communications and discusses the advantages and disadvantages of digital communications, as well as future trends in this area. Details of MSK modulation and MSK transmitters and receivers are discussed in Chapter 2.

Chapters 3,4, and 5 introduce flat and selective fading and discuss methods of modeling non-linear propagation so that quantitative results of outage can be obtained. The information contained in these chapters is used in Chapter 6 which discusses the design and construction of a multipath simulator which can be used in the laboratory.

Multipath propagation can also be studied by means of computer simulations and an example of this method, as well as the results obtained from it are discussed in Chapters 7 and 8.

Chapter 9 is a detailed discussion of adaptive equalizers and explains the advantages and disadvantages of the various hardware and software options available. This information is then used in Chapter 10 to decide on the most effective form of adaptive equalization for the proposed system. Finally Chapter 11 summarizes the results obtained in this dissertation and makes recommendations for the proposed system.

CHAPTER 1

DIGITAL COMMUNICATION SYSTEMS.

Since the early 1970's microwave radio has undergone considerable development, being an ideal transmission medium for digital communications. This sudden growth has also been due to the large scale introduction of digital switching.

Telecommunication networks world wide are currently converting from analogue to digital systems, with the ultimate objective being the creation of Integrated Digital Networks (networks with connections provided via digital switching / transmission), and Integrated Services Digital Networks (multi-service networks with digital access, switching and transmission). In fact it is predicted that by the end of the century almost all new system additions will be digital.

The present transmission networks are either via cables (fibre optic and coaxial), satellite or line of sight radio systems (analogue and digital). The introduction of digital radio systems can be successful only if :-
1. they meet existing transmission performance standards,
2. their spectral efficiencies are compatible with those of their analogue counterparts, and
3. their coexistence with other transmission systems does not lead to performance degradations.

International telecommunication administrations have plans for carrier radio systems from 2GHz to 40GHz, those above 12GHz being mostly used for short haul digital radios (as in this case where the designed carrier frequency is 23GHz).

The major advantage of digital radio over optical fibre is its low installation cost, and its primary advantage over satellite transmission is its much smaller propagation delay.

The major technical issues facing the designer of high capacity digital radio systems can be divided into two broad areas, namely propagation problems (which are discussed in chapter 3), and equipment requirements, which are only briefly discussed in this report. However, the equipment problems that are encountered in modern digital radio arise because of the need, amiss propagation anomalies, to transmit high level modulations. Reference [1.1] explains that a digital radio system must achieve a spectral efficiency of 4.5 bits/sec/Hz in a 4GHz band in order to provide a capacity of 1344 voice circuits. However practical Q.P.S.K. modulators can only achieve an efficiency of approximately 2 bits/sec/Hz.

The modulation technique used in this design is M.S.K. (also known as fast frequency shift keying), and the reason for its choice and its implementation are discussed in chapter 2.

Figure 1.1 shows a simplified block diagram of a digital radio transmitter and receiver. It shows I.F. modulation and demodulation with up and down conversions to the microwave transmit frequency. Most radios use the same receiver structure with down conversion to the I.F. where the automatic gain controlled amplifier maintains a constant level to the demodulator during fading.

References [1.2],[1.3] and [1.1] give a background to digital communication systems, as well as development trends and future implementation techniques.

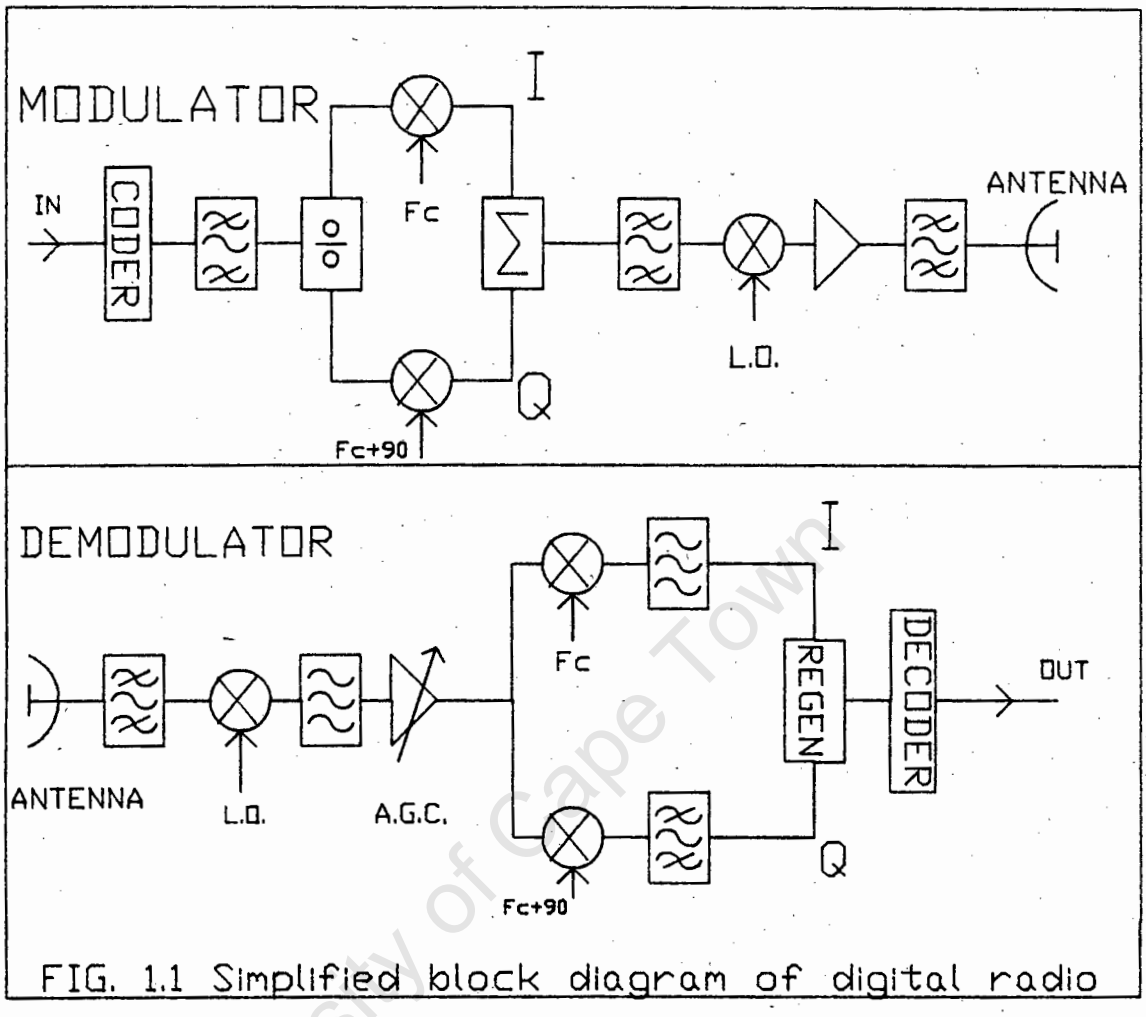

FIG. 1.1 Simplified block diagram of digital radio

CHAPTER 2

M.S.K. MODULATION

There are numerous modulation techniques used in digital radios to date*, which provide a satisfactory spectral efficiency. M.S.K. (minimum shift keying), also called fast frequency shift keying, is a special case of continuous phase frequency shift keying (C.P.-F.S.K.) which avoids the abrupt phase changes at the bit transition instants, resulting in rapid spectral roll-off and improved efficiency. The C.P.-F.S.K. modulation index, d, is 0.5 for M.S.K. ($d = \Delta fT$, where Δf is the separation of the switched frequencies and T is the symbol duration). M.S.K. has the additional advantage of the possibility of a relatively simple self-synchronizing implementation.

References [2.1],and [2.2] provide a quantified comparison of the different modulation techniques most commonly applied to digital radios. Table 2.1 compares the noise performances whilst maintaining a fixed bit error rate. The SNR's have been converted to E_b/N_0 values (defined as the ratio of average signal energy per bit to noise power spectral density) required to achieve a bit error rate of 10^{-4}. Reference values are included with each entry to facilitate obtaining values of required E_b/N_0 for other error rates. From this table it can be seen that M.S.K. performs as well as Q.A.M. and Q.P.S.K. (in fact offset keyed Q.A.M., M.S.K., and O.K.-Q.P.S.K. differ only in the weighting functions applied to the I and Q channels). It is also true that M.S.K. and other C.P.-F.S.K. schemes enjoy a large advantage over the A.M. and P.M. schemes when no post modulation filtering is employed.

---

* A discussion and comparison of these techniques is given in references [2.1], and [2.4].

Table 2.1 Noise Performance Comparisons.

TYPE	MODULATION SCHEME	Eb/No	Reference
AM	OOK-COHERENT DETECTION	11.4	26.77
	OOK-ENVELOPE DETECTION	11.9	77
	QAM	8.4	77
	QPR	10.7	119
FM	FSK-NONCOHERENT DETECTION (d=1)	12.5	24.27
	CPFSK-COHERENT DETECTION (d=0.7)	7.4	1.40
	CPFSK-NONCOHERENT DETECTION (d=0.7)	9.2	1.40
	MSK (d=0.5)	8.4	17
	MSK-DIFF. ENCODING (d=0.5)	9.4	71
PM	BPSK-COHERENT DETECTION	8.4	1.78
	DE-BPSK	8.9	22.1
	DPSK	9.3	22.1
	QPSK	8.4	12
	DQPSK	10.7	100
	OK-QPSK	8.4	50
	8-ary COH. DETECTION	11.8	57
	16-ary COH. DETECTION	16.2	3
AM/PM	16-ary APK	12.4	189

Figure 2.1 shows the position of M.S.K. relative to other modulation techniques as far as implementation cost and complexity are concerned. However it must be remembered that this figure does not take into account trends in the electronics industry.

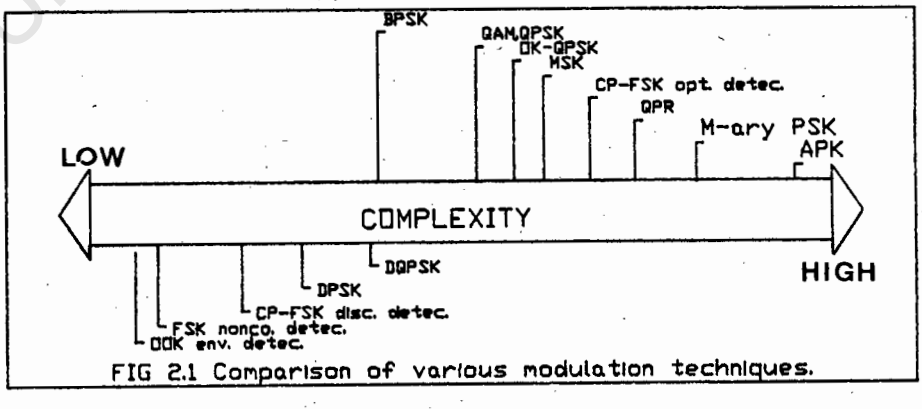

FIG 2.1 Comparison of various modulation techniques.

More detailed information regarding selection of modulation schemes can be found in references [2.1], and [2.4], in particular the topic of band limiting design, but for the moment it is only necessary to understand the operation of M.S.K.. We will first discuss a simplified model for M.S.K. which may help to understand the practical implementation of this scheme.

2.1 THE MSK MODEL.

Figure 2.2a shows the simple block diagram of the transmitter and receiver and the resulting waveshapes are shown in 2.2b. The input data stream, consisting of full length rectangular pulses, is converted into two full length rectangular pulse streams of baud rate half that of the incoming bit rate. These rectangular pulses are converted into sinusoidal pulses by a non-linear circuit known as a sinusoidal pulse shaper. The two sinusoidal pulse streams are now known as the I and Q channels.

The Q stream is delayed by a unit bit duration. After filtering, the I channel is modulated by the carrier signal $\cos(2\pi ft)$, and the Q channel is modulated by the phase shifted carrier signal $\sin(2\pi ft)$. The transmitted signal is then the sum of these two modulated signals.

The receiver is the converse of the transmitter. First the I and Q channels are recovered by synchronous demodulation and then filtered. The decision devices are simple comparators which convert the sinusoidal pulse streams into rectangular pulse streams. The I channel is delayed by a unit bit duration and then the I and Q channels are differentially decoded to reproduce the data stream. The system is similar to offset Q.P.S.K. with the exception that in the transmitter the full length rectangular pulses of the I and Q data streams are processed in a non linear fashion so as to be full length sinusoidal pulses prior to

multiplication with the modulating carrier. Figure 2.3 shows the resulting M.S.K. spectrum, most of the energy of which is within a band width of 1.5 times the bit rate. The MSK spectrum is discussed further in reference [2.3].

Let us now discuss in more detail how the abrupt phase changes are avoided.

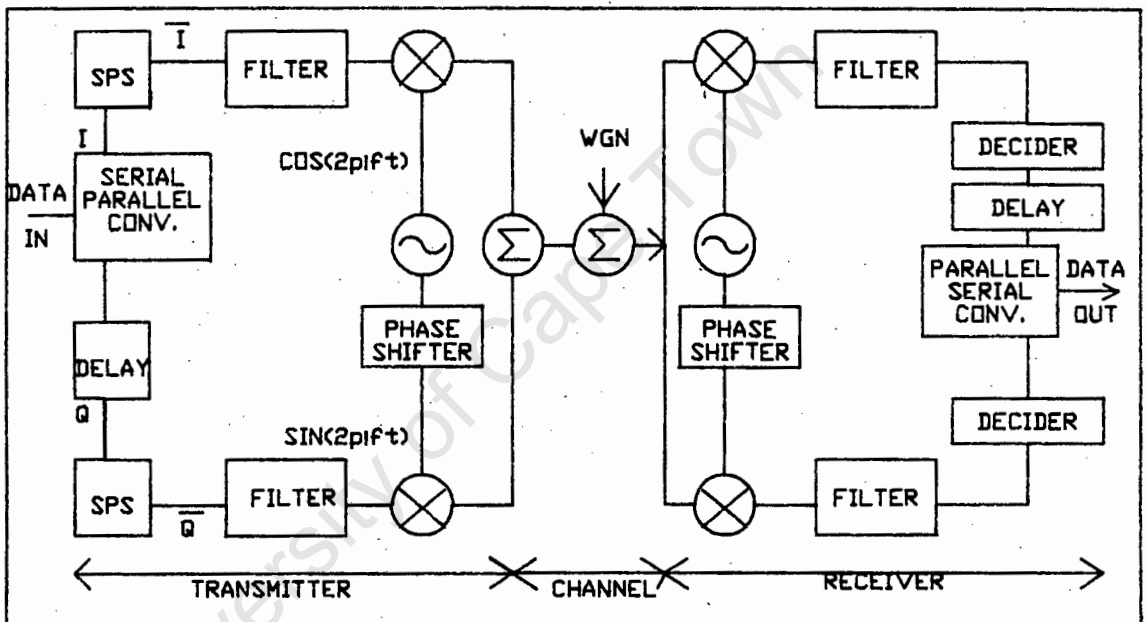

FIG 2.2 a) System Model.

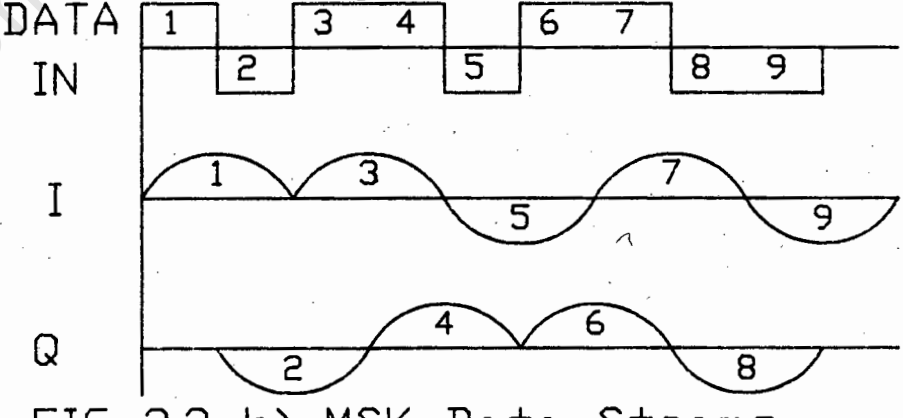

FIG 2.2 b) MSK Data Steams.

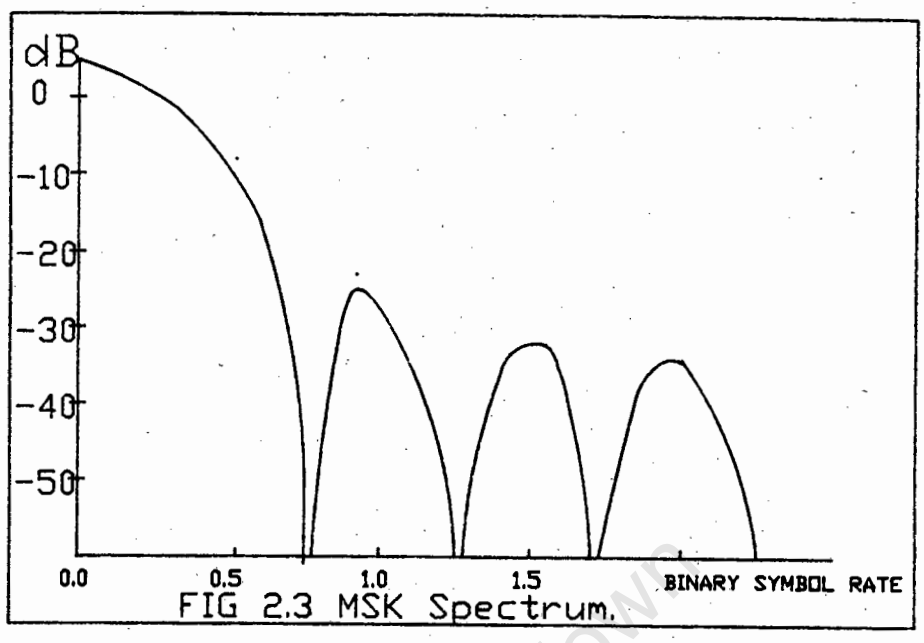

FIG 2.3 MSK Spectrum.

2.2 PHASE COHERENCY.

Consider the digital information to be in the form of a serial stream of marks (representing 1's) and spaces (representing 0's). An arrangement is required where a space increases the phase by πd and a mark reduces the phase by πd. After s spaces and m marks, ie at time (s+m)T, we will have a phase shift

$\phi[(s+m)T] - \phi(0) = (s-m)\pi d$ as shown in figure 2.4 **.

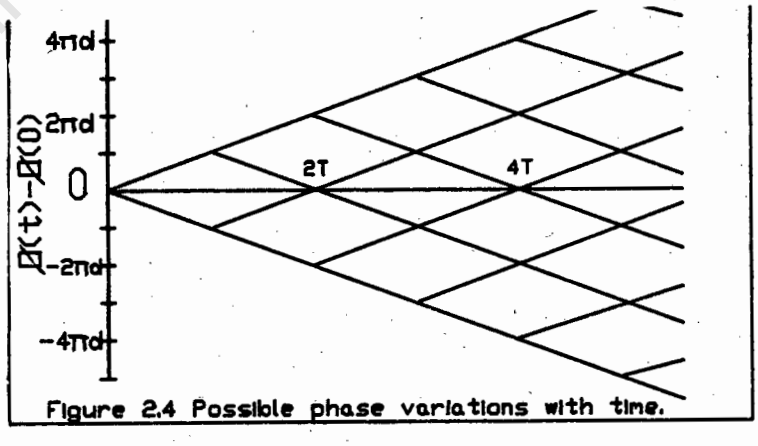

Figure 2.4 Possible phase variations with time.

**This phase shifting is shown and discussed in reference [2.5].

We have an even (odd) multiple of d when (s+m) is even (odd) and the phase at any other time is obtained by linear interpolation. Since $\phi(t)$ is a continuous function of time the signal itself is continuous, and thus has lower spectral sidelobes.

The choice of d, and its affect on the modulation scheme can be read in reference [2.5], however inspection of Figure 2.4 indicates that the phase at times that are odd (even) multiples of T will be odd (even) multiples of d. Since all phases are modulo 2π the case of d=0.5 stands out because the phase can take only two values $\pm \pi/2$ at odd times and only two values 0 and π at even times. Thus one may design a receiver to make a decision between the two permitted phase values.

Reference [2.5] shows that d=0.5 results in an optimum decision scheme provided that the decision is made after observing not the signal in one time interval but the real (imaginary) part of its pre-envelope in two time intervals; the one before and the one after the phase we wish to estimate.

M.S.K. utilizes a frequency shift of exactly $\pm$ 1/4 the bit rate, and requires that the mark and space frequencies be exact even multiples of the shift frequency. This is accomplished by choosing a carrier that is an odd multiple of the frequency shift. For example $\Delta f = \phi f_b/2$

where : ϕ is the phase shift/bit $= \pm \pi/2$ rad/bit

f_b is the bit rate (2.048 Mbits/s)

Δf is the frequency shift $= ([\pm(\pi/2)]/2\pi) f_b$

$= \pm f_b/4$

f_c is the carrier frequency $= Nf_b = N\Delta f/4$

N is an odd integer (choose N=137)

then :

f_c=70.144 MHz

$f=\pm$0.512 MHz

f_{mark}=69.632 MHz

f_{space}=70.656 MHz

Figure 2.5a shows the vector diagram for M.S.K. after one bit. 0(t0) is the signal at the beginning of the bit duration. If a 0 is transmitted the phase is linearly increased resulting in 0(t1) at the end of the bit duration. If a 1 is transmitted the phase is linearly decreased resulting in 1(t1) at the end of the bit duration. Note that the MSK vector always rotates around the circumference of the circle, ie the amplitude of the signal remains constant. Figure 2.5b shows the possible combinations after a 2 bit sequence. A 0,0 results in the signal 0(t2); a 0,1 results in the signal 1(t2); a 1,1 results in the signal 1(t2); and a 1,0 results in the signal 0(t2). Figure 2.6 shows how the two quadrature channels are added to form a single constant amplitude signal.

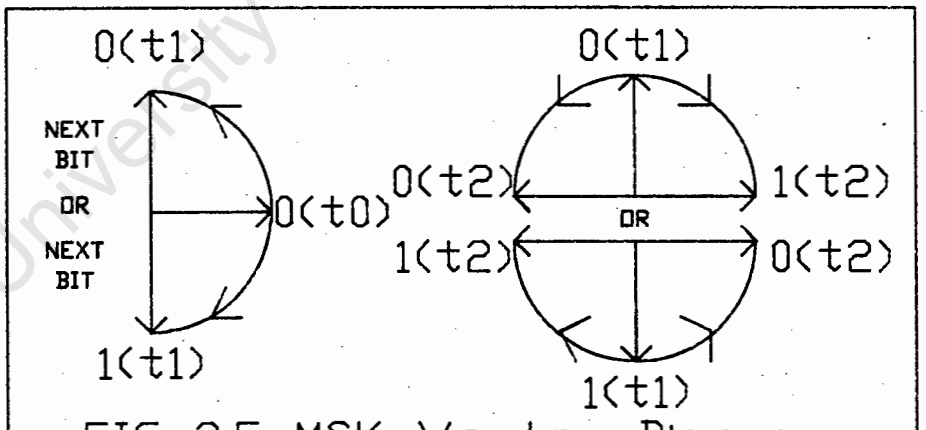

FIG 2.5 MSK Vector Diagram

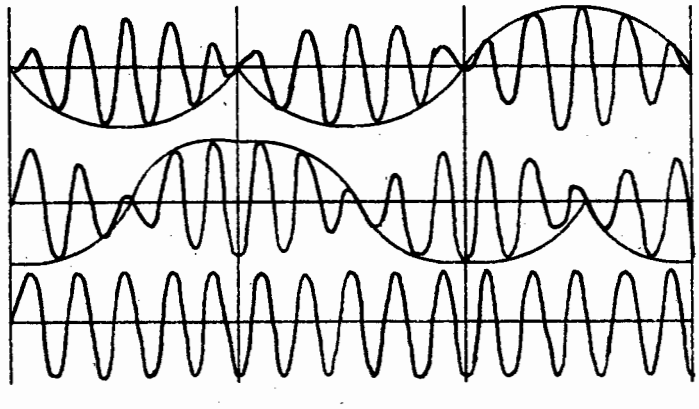

FIG 2.6 Combining the two channels to form a constant amplitude signal.

The M.S.K. receiver is required to generate a phase locked carrier at frequency $w/2\pi$, multiplying the received signal, s(t), with cos(wt) and sin(wt) respectively in two balanced modulators and recovering the second harmonic terms from the two outputs, which by then are usually called the I and Q channels. Two other signals required at the receiver are the clock (that is needed for integrating over 2T) and the precisely phase locked carrier signals cos(wt) and sin(wt). Reference [2.5] describes the self synchronization at the receiver.

A problem may arise if a long sequence of marks or spaces are received as it is possible to loose self synchronization. This can be overcome with coding techniques or by using a scrambler.

2.3 SOLVING PHASE AMBIGUITIES.

Figure 2.7 shows a circuit for the extraction of clock and carrier signals which overcomes any 90 degree phase ambiguity, simply by a more careful layout of the self synchronizing circuit. The outputs of the PLL's are divided by two and then added or subtracted. Since the phase at the divider output is ambiguous by 180 degrees it is not known which adder gives the sum and which the difference, but this does not matter since the outputs are respectively $\pm\cos(wt)\cos(\pi t/(2T))$ and $\pm\sin(wt)\sin(\pi t/(2T))$ and both are the required reference signals when they are gated between the nulls of their respective modulation. The 180 degree phase ambiguity problem can be taken care of by the method of differential encoding.

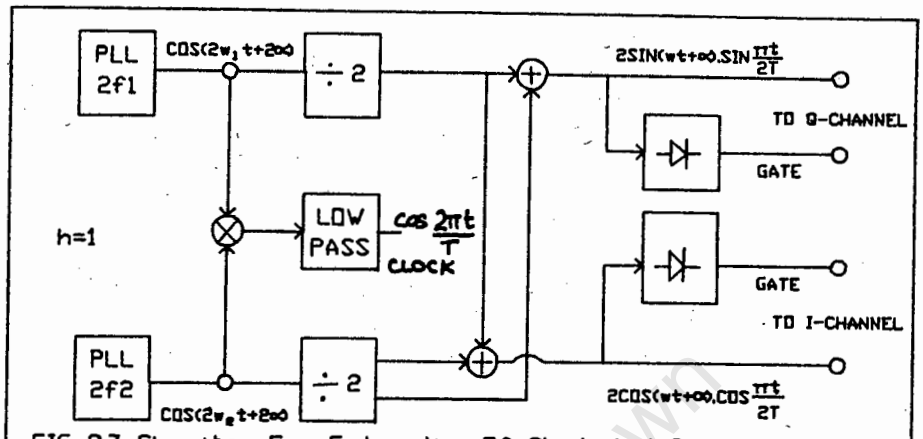

FIG 2.7 Circuitry For Extraction Of Clock And Carrier Signals.

We relate the transmitted bit stream $a_n=\pm1$ (n=1,2,...) to the received signals in the I and Q channels. First we notice that because of the 180 degrees ambiguities only the phase difference $\varnothing[(n-1)T]-\varnothing[(n+1)T]$ can be used. Inspection of Figure 2.4 shows that a sequence mark-space or space-mark leaves the phase unchanged, while a sequence mark-mark or space-space changes the phase by 180 degrees after 2 bit intervals. Thus at time t=2nT a transition at the input corresponds to no transition at the output of the I channel and at time t=(2n+1)T, a transition at the input corresponds to no transition in the Q channel and vice-versa. The circuit of Figure 2.8 shows the various logic operations that recover the differentially encoded input from the outputs of I and Q.

CHAPTER 3

FLAT AND SELECTIVE FADING

First let us repeat that microwave radios are subject to numerous forms of propagation effects, namely :-

1) Low received signals due to flat fading (eg heavy rain),

2) Multipath propagation causing frequency selective fading, which generates intersymbol interference,

3) Interfering signals from satellites and other microwave radios, particularly analogue.

This dissertation will only discuss flat and selective fading.

In order to overcome these serious propagation effects counter measures such as diversity reception (vertically separated antennas providing a combined signal) and adaptive equalizers in the receiver must be employed. The adaptive equalizer cancels out the effect of multipath fade either in the frequency domain at I.F. or in the time domain at base-band. Adaptive equalizers are discussed in chapter 9.

3.1 FLAT FADING

Under many propagation conditions the loss of gain of signal due to the atmosphere is uniform across the radio channel bandwidth; an example is the loss due to extreme rainfall discussed in references [3.1], and [3.2]. For terrestrial systems the lengths of transmission paths may be limited to a few kilometres by the attenuation caused by rain . The severity of input signal attenuation is very much dependent on the operating frequency and we are

particularly interested in attenuation values for an operating frequency of 23GHz.

Flat fading statistics on a microwave path caused by uniform rainfall have been estimated by Bussey and Ryde, and the graphs drawn by them can be used to predict the attenuation of a carrier signal for a certain rainfall rate. The accuracy of these graphs is acceptable for most purposes. For example, at 20GHz the attenuation due to a uniform rainfall rate of 100mm/hr is approximately 10dB/km. The calculations of Bussey and Ryde are shown graphically below in figure 3.0, taken from reference [3.7].

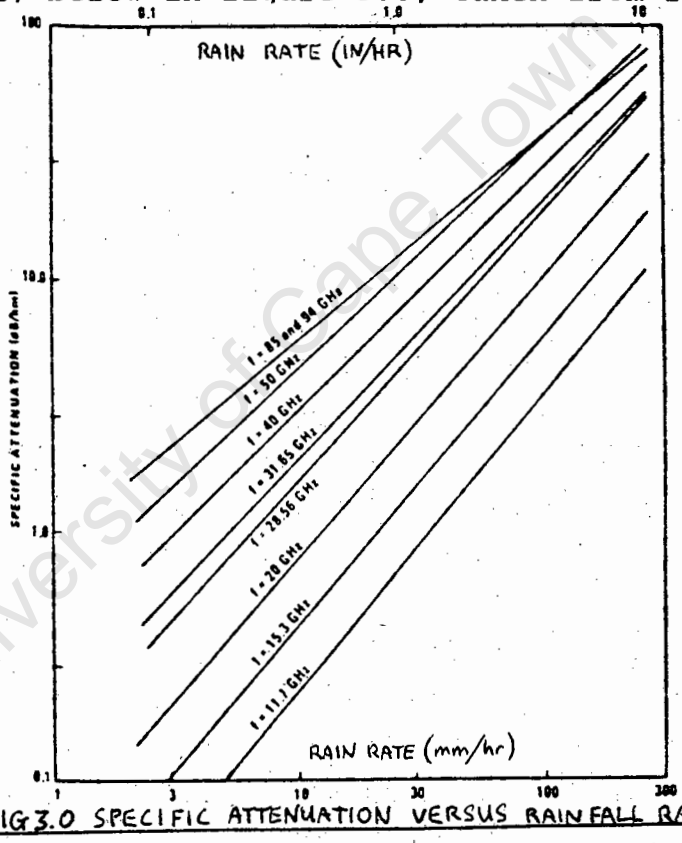

FIG 3.0 SPECIFIC ATTENUATION VERSUS RAINFALL RATE

It is the severity of this attenuation which forces some terrestrial systems to keep a short hop (typically only a few kilometres) , such as that in reference [3.4].

The figures calculated by Bussey and Ryde can only be assumed to be of acceptable accuracy if the rainfall is uniform along the hop length. However as operating

B is the factor to convert worst month probability to annual probability :-

=1/2 for Great Lakes or similar hot, humid areas

=1/4 for average inland areas

=1/8 for mountainous or very dry areas.

3.2 SELECTIVE FADING

Multipaths are caused by a layer of atmosphere above the transmission path which has a negative gradient in the index of refraction. Generally the energy travelling over the separate paths will undergo unequal phase shifts.

Under normal conditions the decrease in refractive index with height imparts a downward curvature to the direction of propagation over the path as shown in figure 3.1. Allowances for the reduced rates of decrease with height which sometimes occur (sub-refractive conditions), are the controlling considerations in determining tower heights to clear the intervening terrain, and are discussed in reference [3.1].

For a large fraction of the time in most locations, propagation conditions do not vary significantly from those shown in figure 3.1 and digital radios operate essentially error free. However at other times meteorological conditions lead to the formation of unusual temperature and humidity profiles; these in turn impose structure on the index of refraction profile.

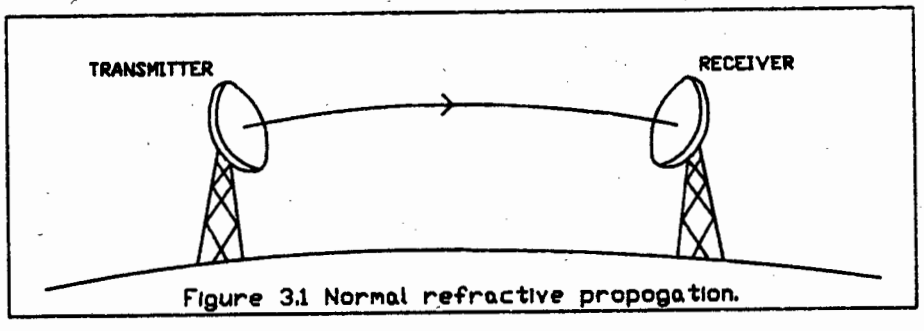

Figure 3.1 Normal refractive propogation.

In a layered atmosphere, energy that would normally be radiated into space can be refracted down to the receiving antennas by other paths as shown in figure 3.2. The receiver sees a weighted sum of time shifted replicas of the transmitted signal from these multiple atmospheric layers, and possibly from ground reflections as well.

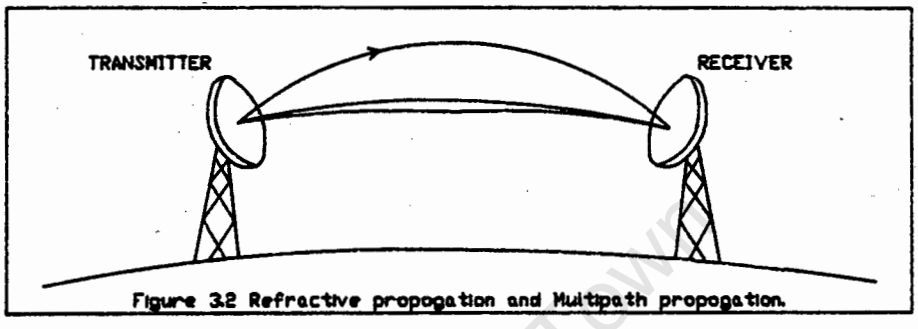

Figure 3.2 Refractive propogation and Multipath propogation.

Since multipath fading is a function of the magnitude of the gradient in the index of refraction, it is reasonable to assume that there is a maximum value of this gradient which occurs in a climatic region. Reference [3.2] shows that a path length D exists such that for any path of length d<=D, (called a short path), deep multipath fading cannot occur. Fading on long paths is also discussed and it is shown that the path attenuation distribution is a function of d^3/λ where d is the path length and λ is the wavelength in air.

Figure 3.3 shows the relationship between f and D and from this graph it can be seen that for a frequency of 23 GHz the maximum hop length that avoids deep fading (assuming a similar index of refraction) is 5,24 kms. Obviously since this is the maximum length under mild atmospheric conditions and calculated independently from flat fading it is reasonable to assume that on a 5km hop selective fading will occur and must be compensated for.

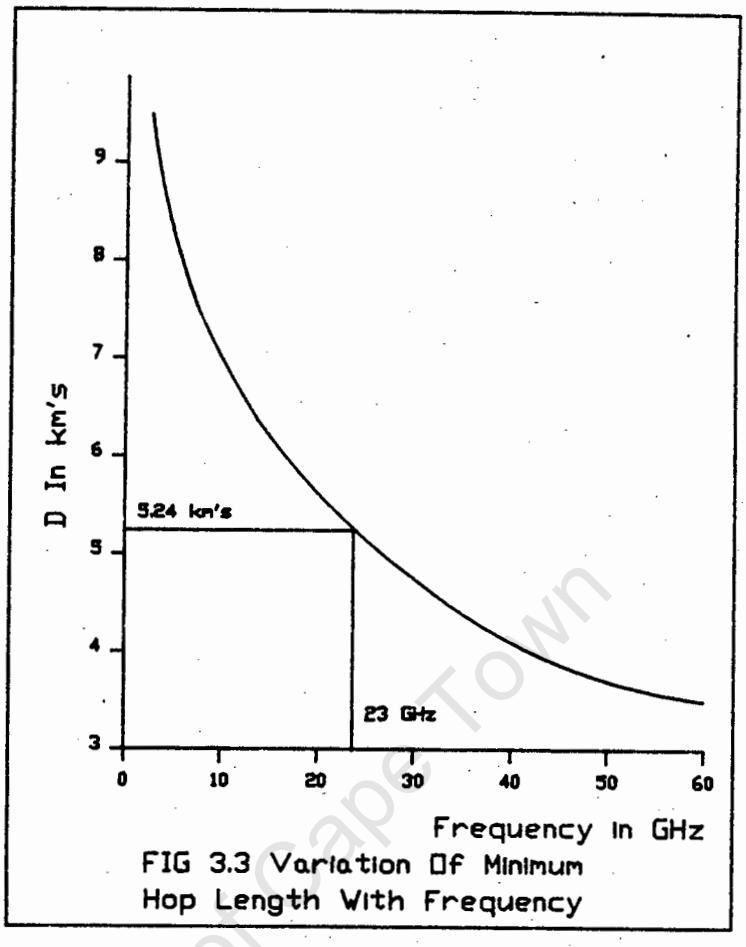

FIG 3.3 Variation Of Minimum Hop Length With Frequency

Most severe selective fading occurs during clear summer nights when temperature inversions and associated meteorological effects produce negative gradients in the index of refraction of the atmosphere. It has also been noted that severe selective fading occurs when a large percentage of the transmission is over water.

Frequency selective fading gives rise to notches or slopes in the amplitude response across the channel bandwidth, as discussed in reference [3.3]. The group delay is similarly affected, and as is shown in figure 3.4, the shape will invert if the fade becomes non-minimum ie if the secondary beam amplitude is greater than the direct beam.

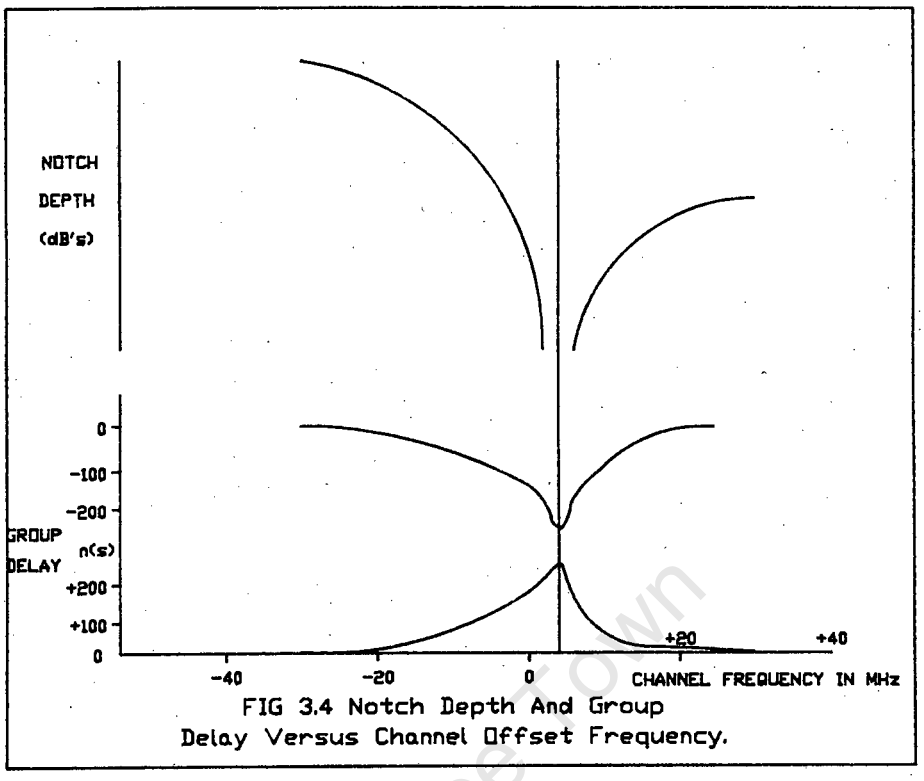

FIG 3.4 Notch Depth And Group Delay Versus Channel Offset Frequency.

The depth and frequency of the notch vary continuously during multipath fading and create very serious intersymbol interference in the digital radio. The result is short periods of very high error rate which can cause loss of synchronization in the radio itself or in associated multiplex equipment.

From equations of system gain and fade margin, it is seen that when the magnitude of a multipath fade exceeds the fade margin a condition of potential service failure exists. Protection will be required if the duration of the fade exceeds the time limit imposed by the reliability specifications. The time during which a signal fades below a given level L is called the fade duration of that level and the statistics of these values are discussed in chapter 5. The reduction in available system gain increases costs because shorter hops and more complex

antenna systems are required. The option of using adaptive equalizers to reduce costs is discussed in chapter 10.

CHAPTER 4

MULTIPATH PROPAGATION MODELS

The description of multipath models is wide and well published in technical magazines. Although the methodology is considerably variable this dissertation considers only two main classes, "ray models" and "channel models".

4.1 RAY MODELS

Multipath fading is a function of the magnitude of the gradient in the index of refraction of the refracting layer. Figure 4.1 illustrates a simple profile of the index of refraction which can produce two or three transmission paths between the transmitter and receiver. The index of refraction is assumed to change only in the vertical direction.

From geometric optics the position of the elevated negative gradient in the index of refraction allows a direct ray between transmitter and receiver and causes another ray, launched upward at a small angle θ_0 to be refracted into the receiver. This is a simple approximation to the actual variations in the index of refraction and is generally not used*. Reference [3.2] explains that if the gradient in the index of refraction is constant the refracted ray will follow the arc of a circle with radius R with $1/R=-10^{-6}dN(z)/dz$, and z being the height above the earth, n(z) the index of refraction, and $N(z)=[n(z)-1]10^{6}$.

*See figure 4.1

The phase shift between transmitter and receiver for this model is given by :-

$\Theta = 2\pi/\lambda \int n(z)ds$ where n(z) is the index of refraction, is the free space wavelength, and ds is the element of length along the ray.

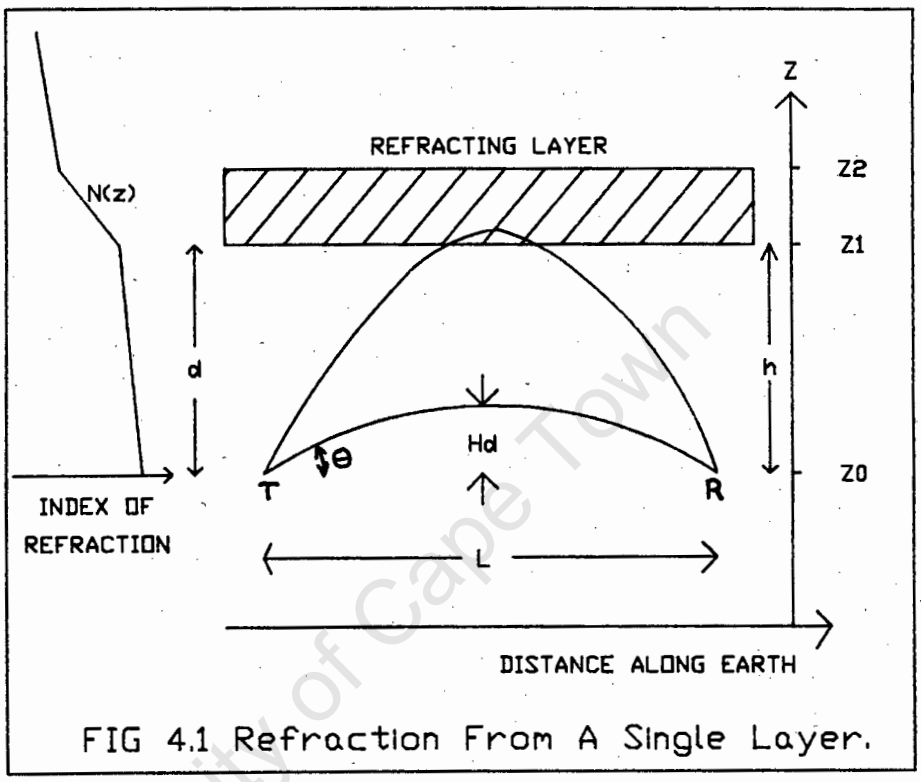

FIG 4.1 Refraction From A Single Layer.

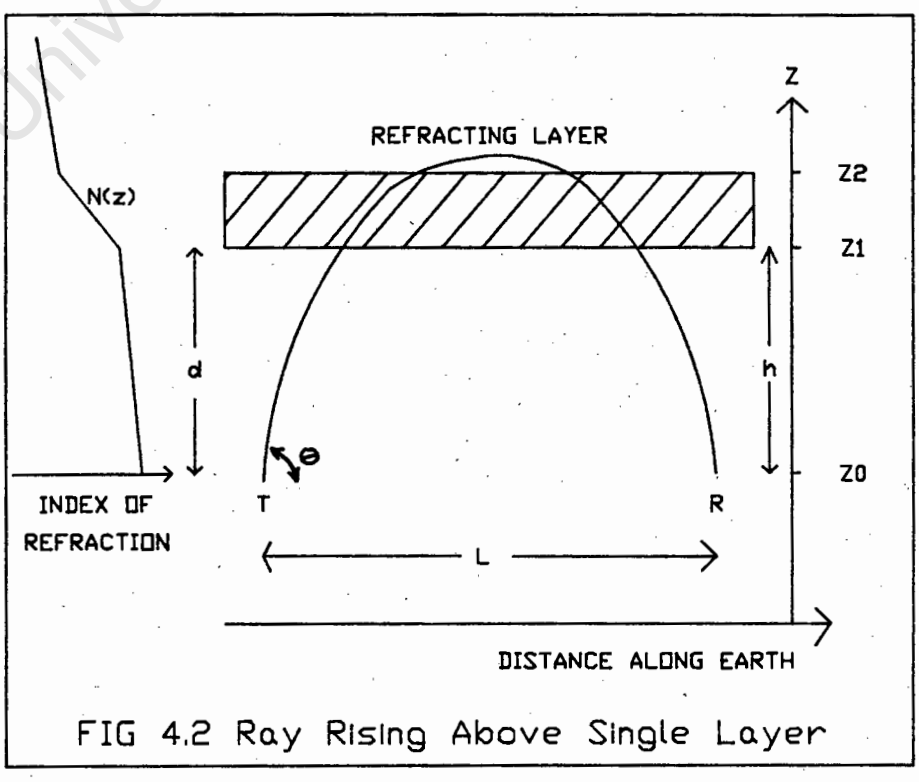

FIG 4.2 Ray Rising Above Single Layer

It is possible for the refracted ray to rise above the refracting layer and still reach the receiver, as shown in figure 4.2 and the phase shift for this model is derived in reference [3.2].

The worst case of interference, that is the largest difference in phase between the direct ray and refracted rays, occurs when the layer is thick enough that no ray which reaches the receiver rises above the layer. Reference [3.2] mathematically predicts that either one, two or three rays reach the receiver depending upon the height of the refracting layer. Examples of this are shown in figure 4.3.

In figure 4.3a the layer height is $2.2H_d$ (where H_d is the maximum distance that the direct ray rises above the path axis). In addition to the direct ray two other rays are refracted into the receiver. As the layer height decreases the vertical separation between the two refracted rays increases as indicated in figure 4.3b. When the height of the layer equals the height of the direct ray, $h=H_d$, the direct ray coincides with one refracted ray; only two rays reach the receiver. Finally when the layer height is less than H_d only one ray reaches the receiver as shown in 4.3d. Reference [3.2] derives numerous formulae and statistical information relating the variables of this type of model.

The main problem with this type of model is that it is very system dependent ie it requires information regarding launch angles, path length, and information relating to geographical conditions.

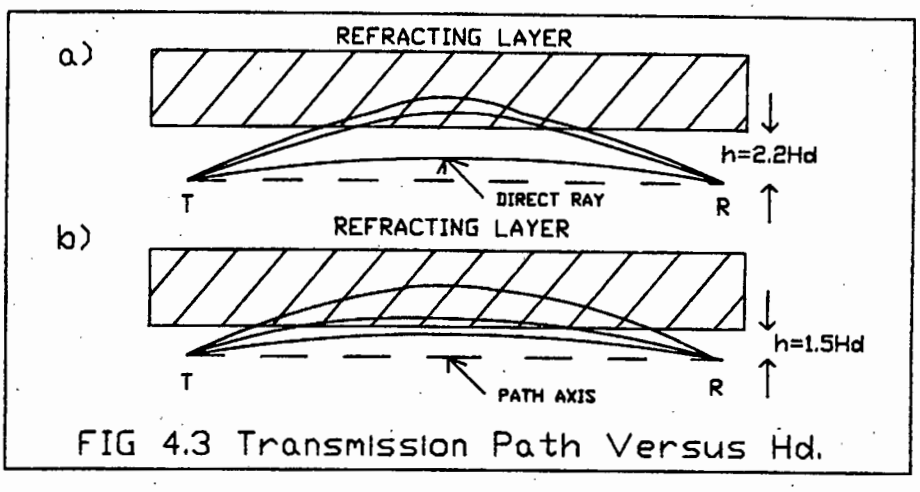

FIG 4.3 Transmission Path Versus Hd.

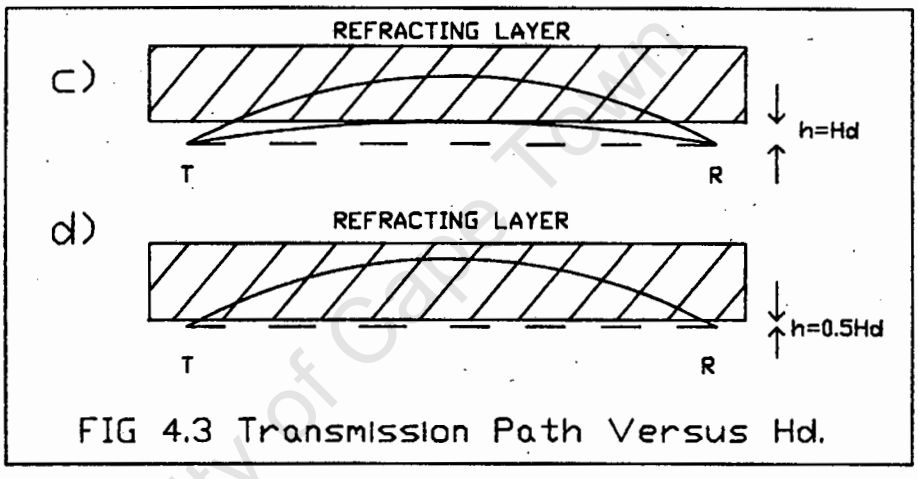

FIG 4.3 Transmission Path Versus Hd.

4.2 CHANNEL MODELS

In most digital radio studies, the model for the complex channel transfer function begins with the same representation. Starting it somewhat formally :-

$$H(f)=\begin{cases} 1+j0 & \text{during normal propagation} \\ F(f;\{c\}) & \text{during multipath fading} \end{cases}$$

with $-w/2 \leqslant f \leqslant w/2$ and where w is the channel bandwidth, f is measured from the centre of the channel, and F() is a complex function of f containing a finite set of parameters (the c's) that change randomly with time. Because the c's change very slowly compared to the signaling rate used over the channel, F() can be regarded

as a quasi-stable function of f whose parameters are random variables.**

The statistical model then consists of
1) the form of the function F(f;{c}),
2) the joint conditional probability density function (pdf) of its random variables, and
3) a number or formula for the effective number of multipath fading seconds per year, Tf. Typically Tf is chosen so that the yearly distribution of power fading at a single frequency, as derived using 1),2), and 3), is consistent with known results of single frequency fading. (At the discretion of the user, Tf can be made to represent the number of fading seconds per heavily fading month rather than per year.)

Note that this discussion does not include models for multiple channels, that is channel models associated with space diversity reception and/or dually polarized transmission, but is confined to single polarization non-diversity channels. The primary distinction among models described in the literature resides in the function F(f) used to characterize the complex response over the channel bandwidth.

Two of the most popular models use a function of the form $F(f)=a[1-b*\exp(\pm j2\pi(f-f_0)\tau)]$ where the + is for non-minimum fading (ie the main ray arrives after the secondary ray), and the - is for minimum fading (ie the main ray arrives first). In the so called "two path" model there is no amplitude scale factor (equivalently a=1) and b, f_0 and τ are the variable parameters. In the so called "simplified three path" model τ is a parameter related to

**Reference [4.1], and [5.1] give a detailed description of this topic.

the channel bandwidth whose value is set to 12.5 ns; and a,b and f_0 are the variable parameters.

For the purpose of discussing either model we recast the parameter b in terms of the decibel value of maximum fade depth

$$B = \begin{cases} -20\ \log_{10}(1-b) & \text{if } b<=1 \\ -20\ \log_{10}(1-1/b) & \text{if } b>1 \end{cases}$$

Also the a parameter in the simplified 3 path model is recast in terms of its decibel value

$$A = -20\ \log_{10}(a)$$

Thus A+B gives the total fade depth at the response minimum.

Confusion often arises from the observation that F(f) in the above formula has the appearance of a two path response rather than a three path response. However it can be thought of as arising from three paths (or propagation rays) wherein two of the paths are so close in time delay that there composite response is a constant (a) over the channel bandwidth and frequency selectivity is attributed to a third path, at relative delay τ. This useful picture gives the simplified three path model its name.

On the other hand radio links with terrain reflections (from either land or sea) can have a more physical motivated three path situation. In such cases, a so called general three path model may be appropriate. For this model we denote the path gains by a0, a1, and a2 and the relative delays between the primary and two secondary paths by $\tau 1$ and $\tau 2$.

4.2.1 THREE PATH MODELS

These models as previously stated have a voltage transfer function of the form $H(w)=a[1-b*\exp(\pm j(w-w_0)\tau)]$

where the real positive parameters a and b control the scale and shape of the fade respectively.

The relative amplitude b ranges from zero to one , providing a minimum phase function for τ positive. The response is non-minimum phase when the sign of the delay is reversed ($0<b<1, \tau<0$). The non-minimum phase state is also obtained when the relative amplitude of the delayed ray is greater than unity ($b>1, \tau>0$).

The channel modeling function has been found to provide a good fit to almost all measured responses of narrow band radio channels. During multipath fading these channels usually have only simple transmission defects that can be described as either attenuation slopes or single notches. For this purpose of representing the responses of such channels this modeling function has too many parameters if all are regarded as free. That is, within measurement errors, one cannot uniquely determine all four parameters from a given channel response measurement. The simple three path fade over-specifies the channel transfer function if the delay is less than 1/6 B, where B is the observation bandwidth. Unless the channel response can be determined to an accuracy of the order of 0.001 dB's, a unique set of a, b, τ, f_0, cannot be determined for more than half the faded channel conditions encountered.

To avoid this problem one must suppress or fix one of the model parameters. While a model with a fixed delay may appear to be a strange choice , it has all the required characteristics for modeling the channel transfer function. This is shown in reference [4.3] where the data collected on field tests on a 26.4 mile hop in Atlanta Georgia was used to test the affects of fixing the different parameters. Figure 4.4 shows the amplitude of the channel transfer function of the above equation on a

power scale and a specibel scale for a fixed τ=6.31 ns. This value of τ has been accepted as standard for many workers, whilst we have followed the factor of six rule giving a τ of 12.5 ns.

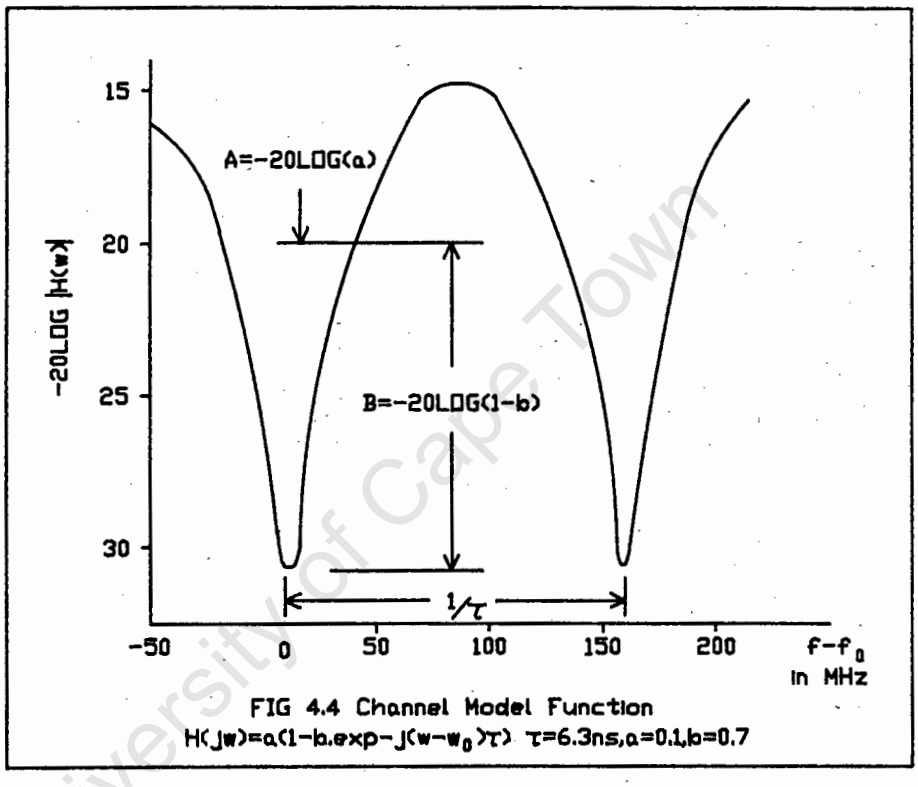

FIG 4.4 Channel Model Function
$H(jw)=a(1-b.exp-j(w-w_0)\tau)$ τ=6.3ns,a=0.1,b=0.7

With τ fixed the response minimum is shifted with respect to frequency by varying f_0. If the minimum is within the bandwidth the fixed delay model can generate notches with a wide range of levels and notch widths. With the minimum out of band it can generate a wide range of combinations of levels, slopes and curvatures within the channel bandwidth.

The complete characterization of a radio in terms of this model requires a three parameter signature which interrelates the values of A,B and w_0 that cause a prescribed bit error rate, (usually 10^{-3}). The characterization is presented as a family of A-B curves for a set of values of the notch frequency parameter. The dispersion signatures which are more commonly used characterize the relative sensitivity of a given radio to fade shapes in terms of the notch frequency and the relative notch depth. Figure 4.5 shows the dispersion signatures for a 16-QAM radio for a BER of 10^{-3}. For all points below the curve the radio will exhibit a higher BER.

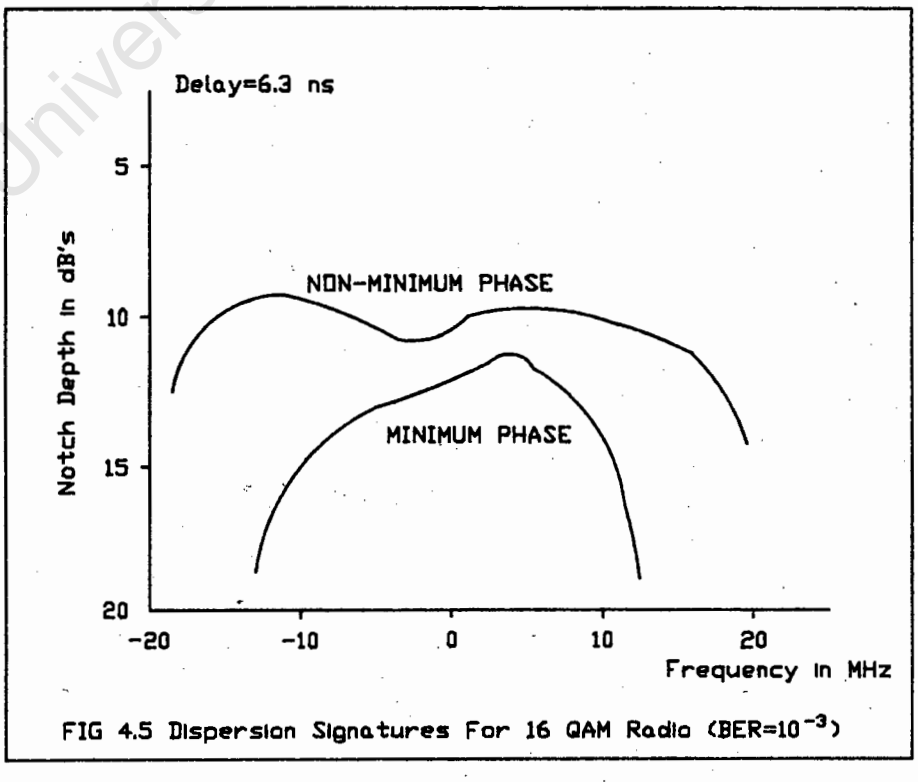

FIG 4.5 Dispersion Signatures For 16 QAM Radio (BER=10^{-3})

4.2.2 TWO PATH MODELS

Two path models describe the multipath propagation in terms of a primary and a dominant interfering ray and is introduced in reference [3.1]. The earliest application of two path models to digital radio used the most simple form of the modeling function

$$H(jw) = 1 + b*\exp(-jw\tau)$$

This function has strictly only two parameters, the relative echo delay τ and the relative amplitude b. Furthermore the frequency w is measured at R.F.

In most subsequent applications of this model, a random phase component has been added to the delayed ray. This is achieved by introducing a notch frequency offset so that the above expression becomes :-

$$H(jw) = 1 - b*\exp(-j(w-w_0)\tau)$$

The addition of the notch frequency term allows w to be measured from any convenient frequency since H(jw) depends only on frequency differences. Both of these expressions are minimum phase for a positive delay ($\tau>0$) if the relative amplitude b is less than 1.

The two path model has been most often used to represent the dispersive component of fading, first because of its simplicity, and secondly because dispersion is usually the dominant cause of system outage for high capacity systems.

Adaptations of this model have introduced a constant factor a to be applied to the modeling function, to represent a medium depression or flat fade component. This factor is assumed to be independent of the dispersive component characterized by the other parameters. With its inclusion the modeling function is identical to that used in the simplified three path model; however the models themselves remain distinct.

The statistics of the parameters of the two path function are derived from simple approximations to the atmospheric model of propagation. Normally, the delay and relative amplitude are both considered as random variables with statistically independent distributions if nothing but for simplicity. Digital radios experience excessive BER under stress only when the response has a deep notch close to the operating frequency band. Consequently the signatures consist of a series of disjoint outage regions in b-τ space as illustrated in figure 4.6.

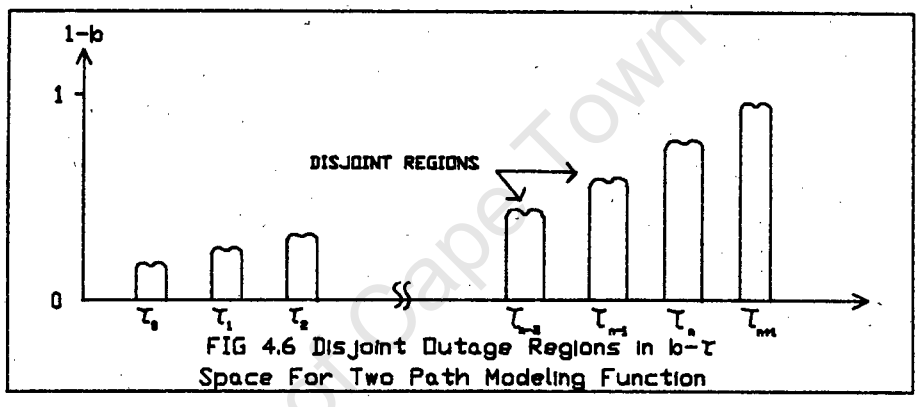

FIG 4.6 Disjoint Outage Regions in b-τ Space For Two Path Modeling Function

The centres of these regions are the delays for which the notch is at the radio channel centre frequency w_c. Thus the nth region is centreed at delay $\tau_n = 2n / w_c$. At 6GHz for example adjacent regions are separated by 0.17 ns. Within each region small changes in τ have the effect of moving the frequency of the notch across the band. If τ is assumed to be constant in a region the variation can be obtained equivalently by introducing a variable notch frequency with an independent and uniform probability distribution.

4.2.3 POLYNOMIAL MODELS

Models have been used which describe the attenuation and group delay responses with the help of polynomials. This is equivalent to describing the logarithm of the

H(jw) by a complex polynomial as discussed in reference [4.2].

Scan by scan records of the attenuation response, A(f), of a channel can be fitted with a polynomial of order M, that is :-

$A(f) = a_0 + a_1 f + a_2 f^2 + \ldots\ldots + a_M f^M$

Coefficients have been obtained using least squares fitting with polynomials of orders M=2,4 and 6. For highly selective events, the most suitable polynomial order is M=4; however for most fading periods polynomials of order M=2 can be used to provide acceptable accuracy. The representation with a second order polynomial has the advantage of familiarity and simplicity.

The M+1 coefficients derived from fitting the channel response can be used to provide a statistical description of the channel. One set of coefficients $(a_0, a_1, \ldots, a_M)$ represents an element in an (M+1)-dimensional probability density function $p(a_0, a_1, .., a_M)$. Figure 4.7 shows an example of a 2-dimensional density function obtained from an 11GHz experiment.

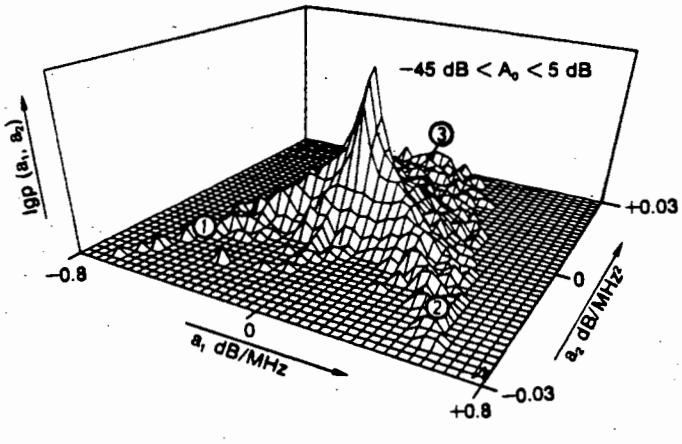

FIG 4.7 Probability Density Function Of The Linear And Quadratic Coefficients Of The Polynomial Model For A 111 km Path At 11 GHz

A quite different approach to polynomial modeling begins with a representation suggested by Bello, in which H(jw) itself (not its logarithm) is characterized by a complex polynomial. Thus :-

$H(jw) = A_0 + (A_n + jB_n)(jw)^n$ where w is measured from the centre of the channel and A and B vary slowly relative to the speeds of typical digital radio systems. This polynomial function can fit frequency responses of any shape with arbitrary accuracy merely by choosing n sufficiently large. Moreover the difficulty of fitting coherently measured responses does not grow significantly with n since H(jw) is linearly related to the characterizing parameters (the A's and B's).

CHAPTER 5

STATISTICAL ANALYSIS OF SIMPLIFIED THREE PATH MODEL

Although statistical analysis of the models described in the previous chapter have been presented in numerous references, this dissertation confines itself to examining only the simplified three path model which has been tried and tested against measured field results and been proven reliable.

Reference [4.3] has analysed the model based on measurements in 1977 on a 26.4 mile hop near Atlanta Georgia. The channel data consisted of 25000 scans at 24 selected frequencies 1.1 MHz apart, and parameter estimation was used to determine a,b and f_0.

Although the statistics have been tied to the "Rummler" model, which has a fixed 6.31 ns delay, carrier frequency of 6 GHz and channel bandwidth of 30 MHz reference [4.4] shows that the results should hold in practice for other systems if they have narrow band (0.5 % bandwidth) ie the model is independent of operating frequency and antenna characteristics within the limits tested to date.

The relative joint frequency of occurance of the three parameters a,b and f_0 by the set of distribution functions is shown in figures 5.1 to 5.5.

5.1 NOTCH DEPTH

The distribution of the parameter b is described in figure 5.1 in terms of the distribution of B, with B= -20log(1-b).

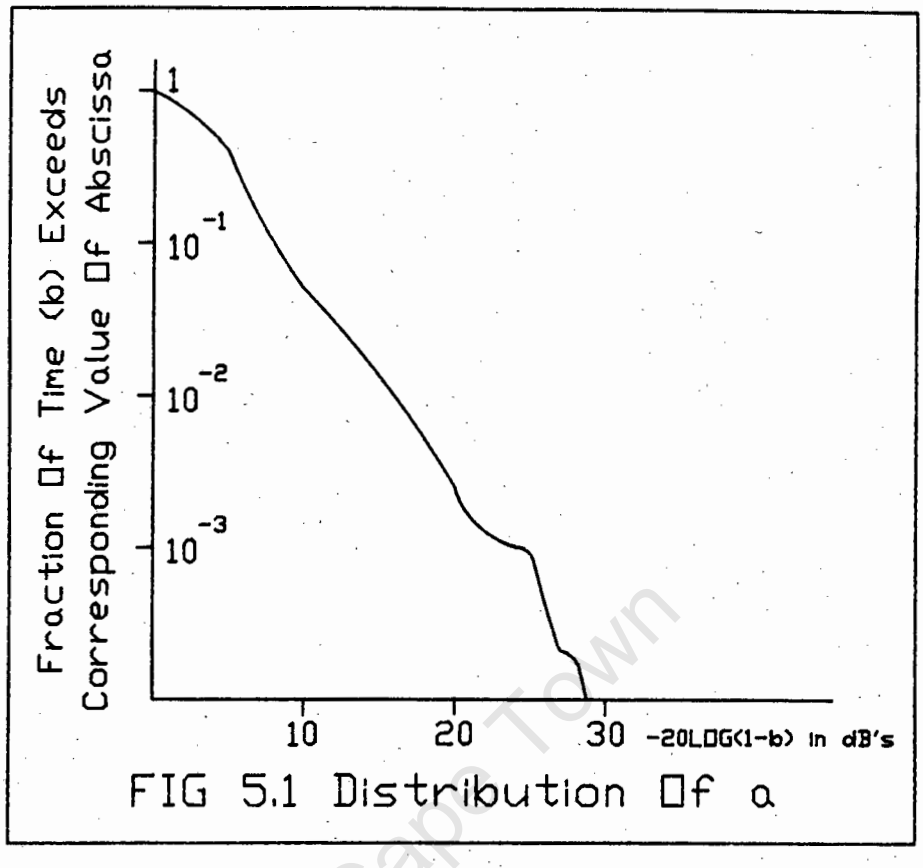

FIG 5.1 Distribution Of a

This distribution is approximately exponential with a mean of 3.8 dB and gives the time that b exceeds the value given by the abscissa X, as a fraction of the time in a heavy fading month that the RMS level in the channel is depressed by more than 15 dB. From the graph it can be seen that 40 % of the time when the channel is depressed the value of b exceeds 0.3 . It exceeds 0.7 for 4 % of the time and 0.99 about 0.3 % of the time. Thus the B description can be approximated by a probability that B exceeds X :-

$P(B>X) = \exp(-X/3.8)$

5.2 SCALE PARAMETER

Although the distribution of the parameter a is dependent upon the value B, the dependence is limited and may often be ignored (ie the distribution of a is conditioned on b and is lognormal as shown in figures 5.2 and 5.3).

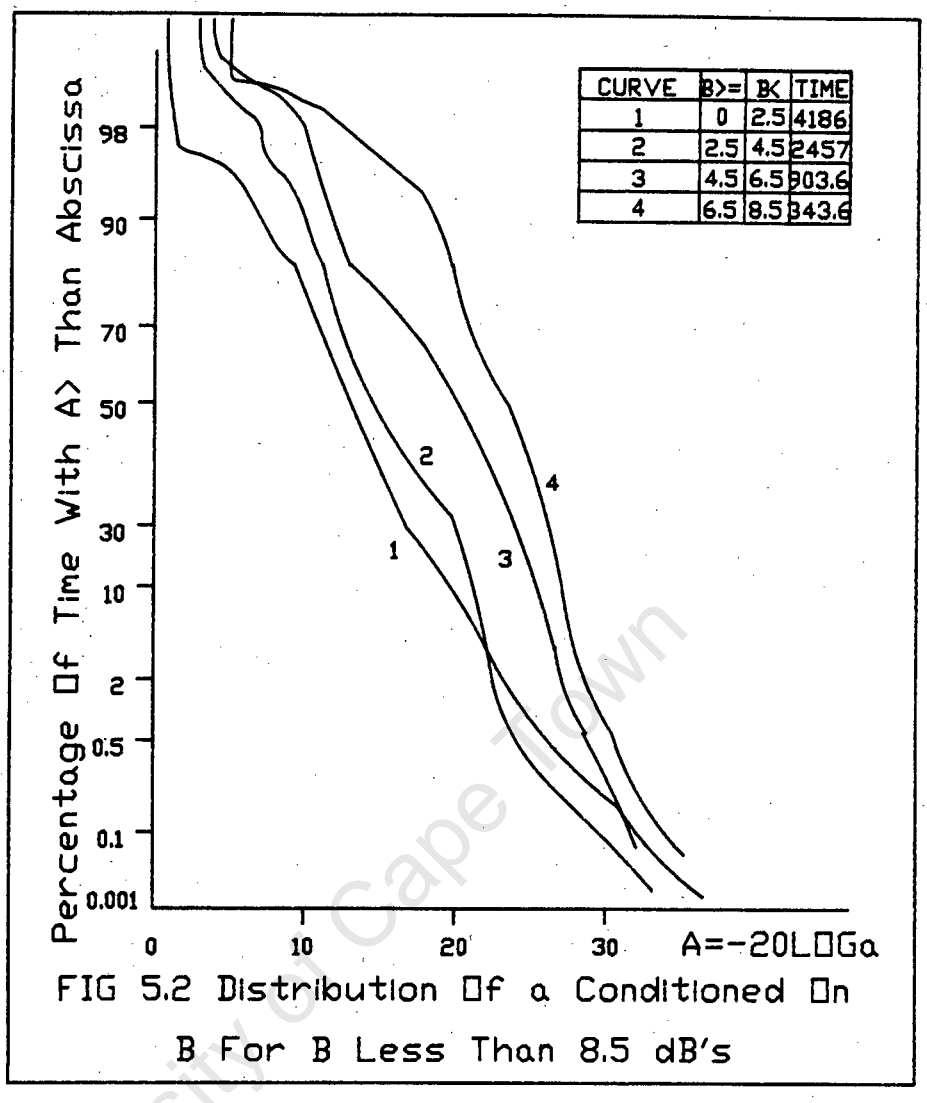

FIG 5.2 Distribution Of a Conditioned On B For B Less Than 8.5 dB's

From figures 5.2 and 5.3 it can be seen that least shapely fades tend to occur at less depressed values. We note that the shape occurs when the average depression is 20 to 25 dB, that the average depression is near 25 dB for b greater than 0.7 and that it falls off gradually to 15 dB for small b. The distribution of A = -20log(a) is conditioned on b and may be modeled as :-

$$P(A>Y) = 1 - P[\{Y - A_0(b)\}/5]$$

where P is the cumulative distribution function of a zero mean, unit variance, and Gaussian random variable, and $A_0(b)$ is the mean of A for a given value of b as given in figure 5.4.

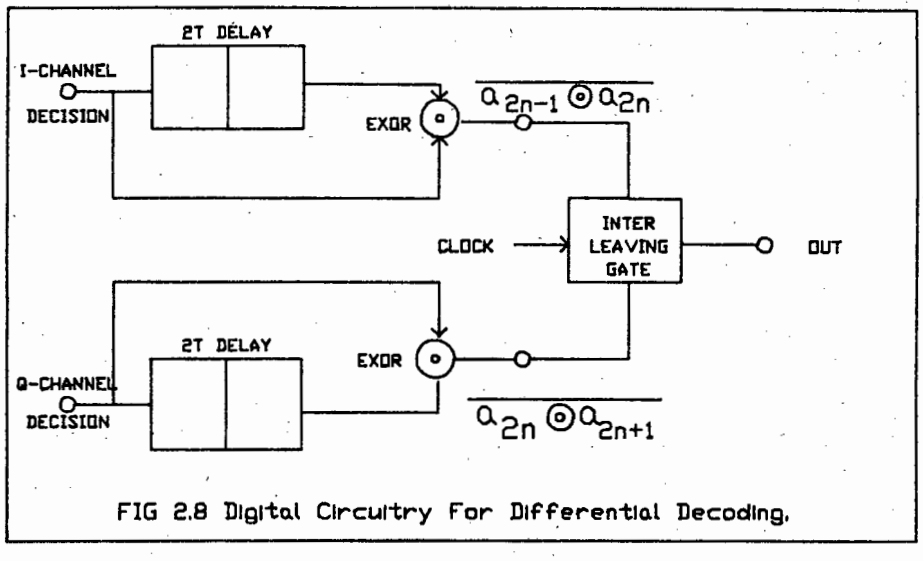

FIG 2.8 Digital Circuitry For Differential Decoding.

Two types of interference may occur:

1) within each channel, and/or

2) between I and Q.

Careful filter design can prevent method 2) although multipaths cause both 1) and 2). The intersymbol interference within the I (or Q) channel limits the speed with which we can transmit bits through a given system, but in each of the two baseband channels bits occur at half speed (1/2T) and the signaling function is continuous since switching occurs only at the nulls of $\cos(\pi t/2T)$. Thus the intersymbol interference will be considerably smaller than when rectangular pulses are transmitted in an I.F. band of 1.2/T.

Computer analysis described in reference [2.6] showed that M.S.K. could permit the transmission of 20 Mbits/s in only slightly more than 21 MHz occupied bandwidth.

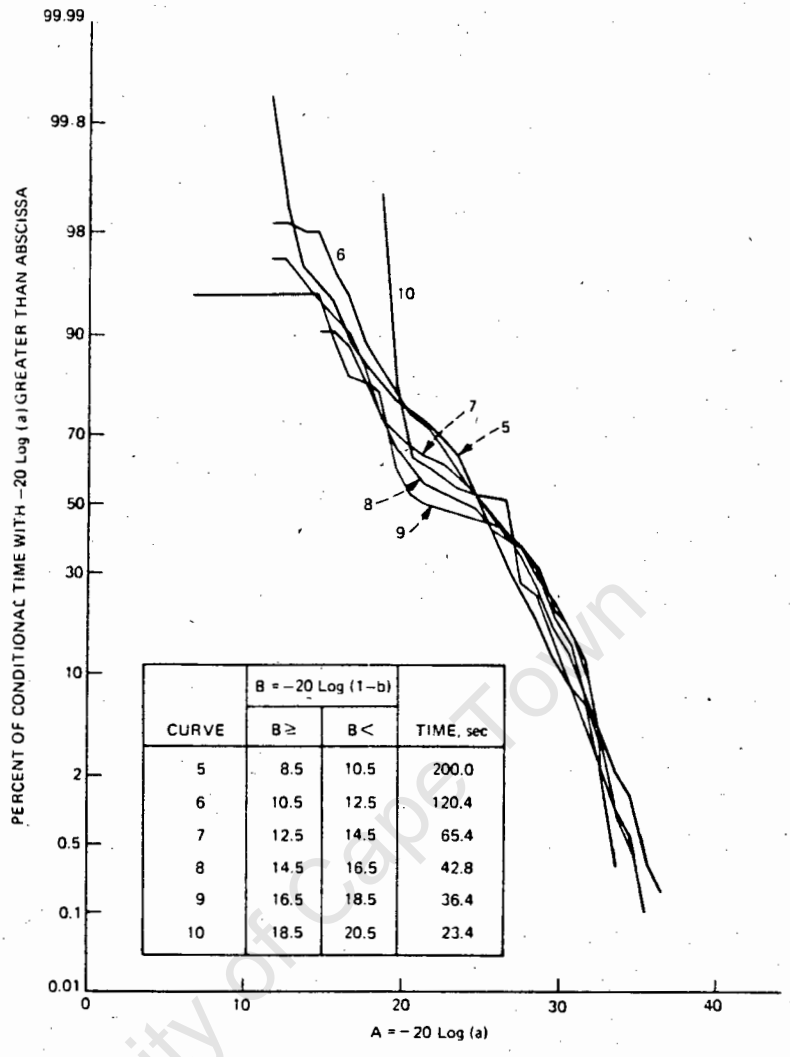

CURVE	B = −20 Log (1−b) B≥	B<	TIME, sec
5	8.5	10.5	200.0
6	10.5	12.5	120.4
7	12.5	14.5	65.4
8	14.5	16.5	42.8
9	16.5	18.5	36.4
10	18.5	20.5	23.4

FIG 5.3 Distribution Of a Conditioned On B For B Greater Than 8.5 dB's

We see from figure 5.4 that the standard deviation of A may be taken as 5 dB regardless of the value of b. The mean value of the A distribution, A_0 is nearly constant for B greater than 8 dB. A_0 as a function of B may be represented by

$A_0(B) = 24.6(B^4 + 500)/(B^4 + 800)$ although this may be very system related. One may interpret figure 5.4 as indicating that the distribution of A is independent of B during well developed fading (B greater than 8 dB). Reference [4.4] indicates that in their case 99 % of the

time the channel was observed to have a flat transmission characteristic (B=0) and no deep fading (small A).

Discussing figure 5.4 further, any terrestrial radio system which operates satisfactory in the common carrier bands must be capable of withstanding a flat fade of more than 30 dB. If the system is adversely affected by selective fading within the band, the precise form of $A_0(B)$ for small B becomes less important. There are more seconds for which B
exceeds say, 10 dB than for which A exceeds 30 dB. In many cases it may service to use $A_0(B)=24.6$ in the P(A>Y) formula.

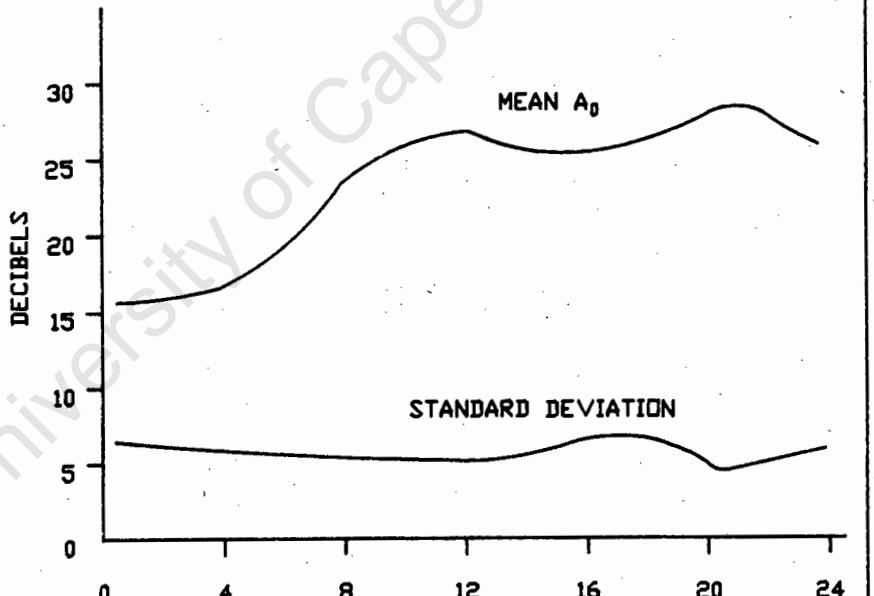

Fig 5.4 Mean And Standard Deviation Of A As A Function Of B

5.3 NOTCH FREQUENCY

The distribution of the notch position f_0, has been found to be independent of both A and B. To represent its

distribution we note that the model function is periodic in f_0 with a period $1/\tau$ =80MHz in our case. Alternatively, we may present the distribution of $\Theta = 360 f_0 \tau$ which is the relative phase at midband of the second path in the model.

For the nominal case the distribution has been described as constant at two levels stated below, with values of less than 90 degrees 5 times more likely than values greater than 90 degrees. Thus we ascribe to the probability density function per degree :-

$$P(\Theta) = \begin{cases} 1/216 & |\Theta| <= 90 \text{ degrees} \\ 1/1080 & 90 < |\Theta| < 180 \text{ degrees} \end{cases}$$

Figure 5.5 shows the time during which the scans had f_0 in 4*1.1 MHz frequency intervals.

While on physical grounds one would expect f_0 to have a uniform distribution, the fixed delay model is decidedly not a physical model.

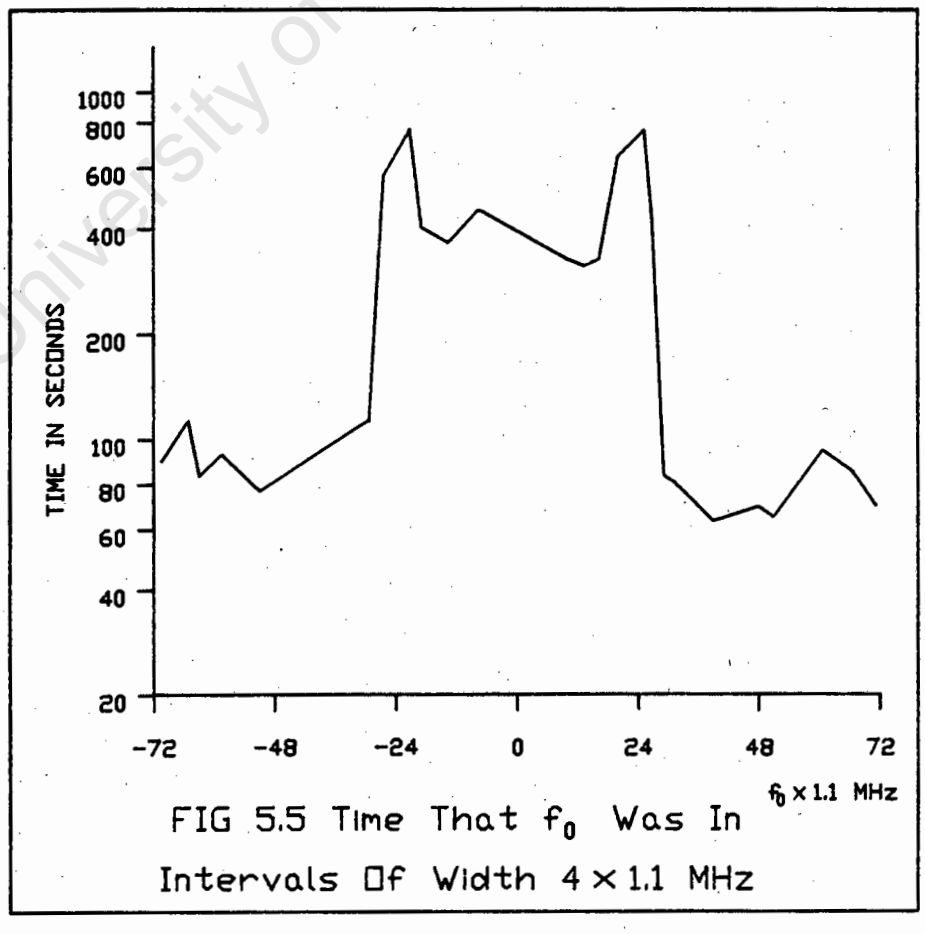

FIG 5.5 Time That f_0 Was In Intervals Of Width 4 x 1.1 MHz

Reference [4.3] claims that figure 5.5 is characteristic of a channel with a considerable fraction of delay differences greater than 6 ns. This leads to systems which have τ fixed at values other than 6.31 ns (ie 12.5 ns) in which case the probability density function for f_0 may be approximated by

$$P(f_0) = \begin{cases} 5\tau/3 & |f_0| \leq 1/(4\tau) \\ \tau/3 & 1/(4\tau) < |f_0| < 1/(2\tau) \end{cases}$$

5.4 SCALING TO A HEAVY FADING MONTH

For the model to be useful in practical situations and outage calculations, the probability distributions discussed earlier and shown in the previous figures must be scaled to seconds of occurrence in a heavy fading month.

Reference [4.4] shows how data for three different radio systems was used to calculate the time scale factors and which has led to the time scale factor being formulated as :-

$$\text{time scale factor} = 0.073cfD^3$$

where f is the frequency in GHz, D is the path length in miles, and c is the terrain factor varying between 0.25 and 4. For our link this formula gives us a fade time of 1612 s/month. It is during this time that the previously discussed probabilities will hold.

CHAPTER 6

MULTIPATH HARDWARE SIMULATOR

As discussed in the previous chapters the form of the multipath simulator which has been chosen relies on the formula :-

$H(w) = a[1-b*\exp(\pm j(w-w_0)\tau)]$.

To understand how the simulator works it is constructive to discuss the above formula in terms of phase vectors.

Figure 6.1 shows how H(w) can vary in amplitude and phase rotation with

$H(w) = a - ab*\exp(\pm j(w-w_0)\tau)$ for two values namely $w=w_1$ and $w=w_2$. More specifically figure 6.2 shows the variation of H(w) if a and b are held constant and w is varied from +1.5 MHZ to -1.5 MHz. It becomes clear from these vector diagrams how the simplified model can simulate various levels and notch depths.

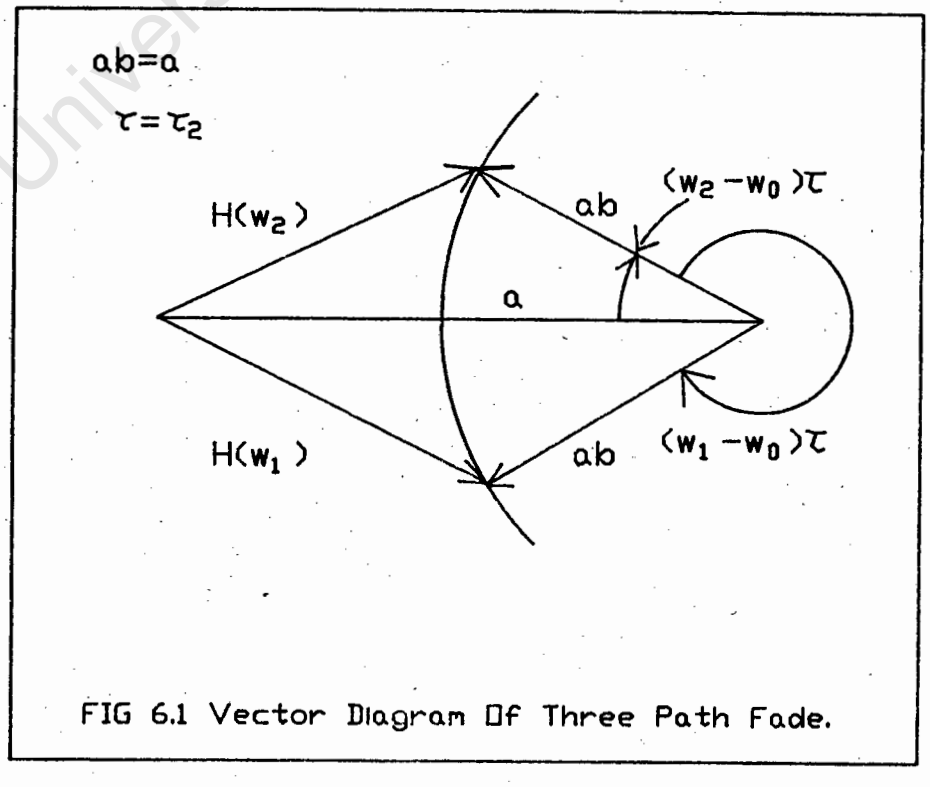

FIG 6.1 Vector Diagram Of Three Path Fade.

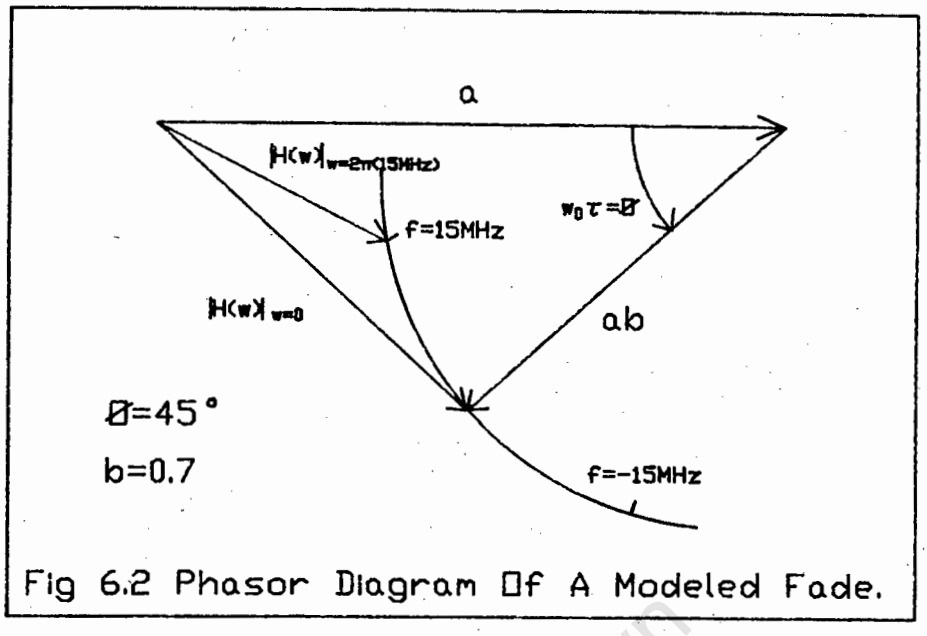

Fig 6.2 Phasor Diagram Of A Modeled Fade.

Figure 6.3 illustrates splitting the desired IF signal into an arbitrary phased, adjustable "main" component and a "delayed" component fixed in delay 12.5 ns but adjustable in magnitude. The main component is further resolved into orthogonal components as shown in the inset to figure 6.3. Reference [4.5] discusses a similar method.

The 0 and 180 degree power splitters (apart from the final 0 degree power splitter) are toroidal transformers, the design of which is complicated at an operating frequency of 70 MHz, by the fact that the transformer also acts as a transmission line and so is also an impedance transformer. The design of these transformers is explained in appendix A and discussed in references [6.1], [6.2], and [6.3].

The final 0 degree power splitter is a hybrid PSC 2-1 manufactured by **MINICIRCUITS** and is guaranteed to operate over the range 0.1 MHz to 400 MHz, have a typical isolation of 25 dB's, a typical insertion loss of 0.3 dB's, and a maximum phase unbalance of 3 degrees. It was used in preference over the toroidal power splitter

because of its improved isolation, thus reducing the overall feeding back to the other channels when the amplitude or phase is changed.

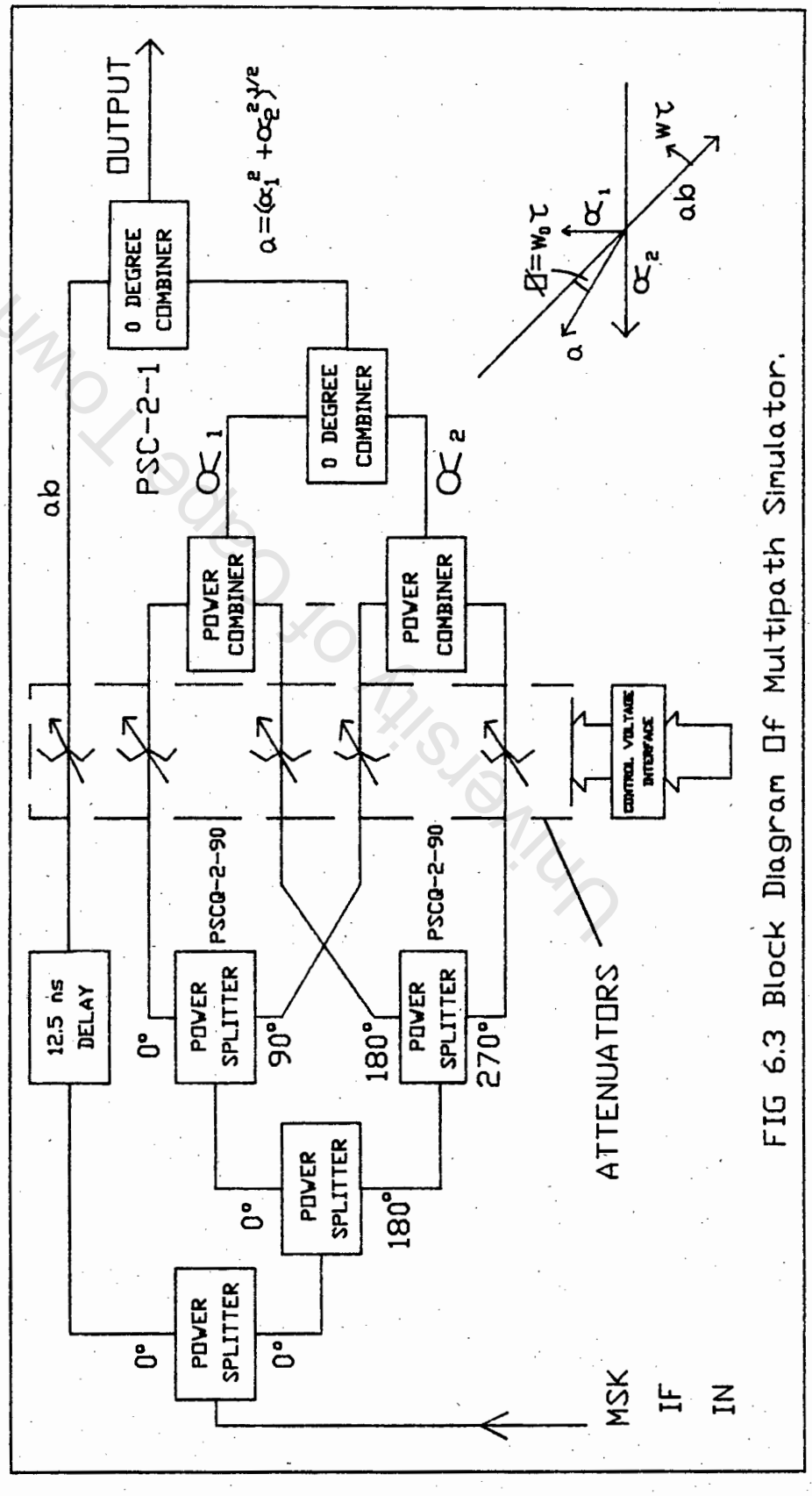

FIG 6.3 Block Diagram Of Multipath Simulator.

The 90 degree power splitters are hybrid PSCQ-2-90's which operate over the range 55 MHz to 90 MHz, have a typical isolation of 30 dB's, a typical insertion loss of 0.3 dB's and a maximum phase unbalance of 3 degrees.

A particular sum vector is constructed by adjusting the orthogonal components to establish a simulated fade notch frequency. This is achieved in practice by varying the voltage controlled attenuators via a programmable voltage interface controlled by a GPIO bus.

The 12.5 ns fixed delay, generated by a 2.475m length of 50 ohm coaxial cable, added to the main path imparts a phase shift of 315 degrees relative to the 0 degrees transmission path. The delayed vector is fixed in direction opposite the midrange position of the adjustable main vector (by the choice of $\alpha 1$ and $\alpha 2$), corresponding to the channel centred fade (Θ = 0 degrees).

Since $1/\tau$ = 80 MHz, a change of 1 degree of the main vector corresponds to a frequency displacement of the fade notch location of 0.22 MHz. For Θ = -45 degrees the notch location is displaced 10 MHz below the channel centre (f_0= -10 MHz). The magnitude of the delayed component is then adjusted to achieve the desired notch depth.

6.1 VOLTAGE CONTROLLED ATTENUATORS

The voltage controlled attenuator is a matched attenuator using pin diodes discussed in reference [6.4]. The schematic of figure 6.4 shows a PI attenuation circuit using resistive elements. The attenuator requires resistive values that vary in accordance with the following equations

$$R_p = Z_0 \left[1+\frac{2}{(10^{dB/20}-1)}\right]$$

$$R_S = \frac{Z_0}{2}\left[\frac{(10^{dB/10})^2 - 1}{10^{dB/10}}\right]$$

and these values for a matched 50 ohm attenuator are shown in table 6.1.

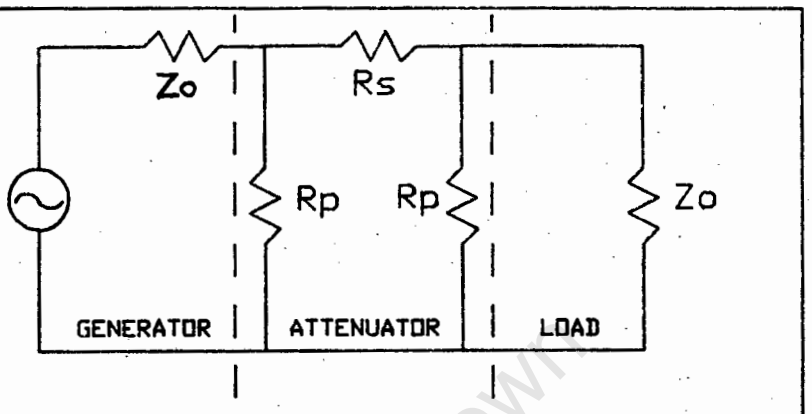

FIG 6.4 Schematic Of A PI Attenuator.

TABLE 6.1 Resistor Values For PI Attenuator

ATTENUATION (dB)	Rp (Ohms)	Rs (Ohms)
1	870	5.7
2	436	11.6
3	292	17.8
4	221	24
5	178	30
6	150	38
8	116	53
10	96	71.2
12	83	93
14	75	120
16	69	154
18	64	196
20	61	248

The PIN diode that was chosen for an attenuator operating at 70 MHz was the MA-47111 which has minimal intermodulation distortion. Three MA-47111 PIN diodes were used to replace the resistors shown in figure 6.4. The complete RF circuit including diodes, chokes and blocking

capacitors is shown in figure 6.5 which is reproduced from the MA-4711 data sheet , reference [6.4].

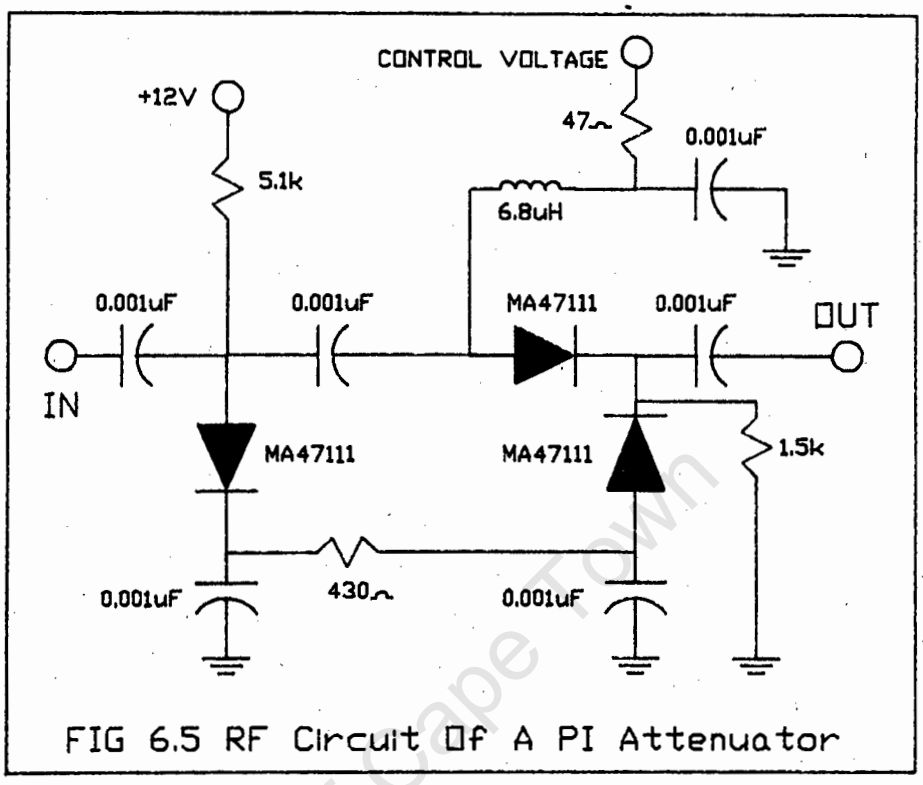

FIG 6.5 RF Circuit Of A PI Attenuator

The control voltage-attenuation response for this circuit is extremely non-linear but is acceptable for this application since the voltage is being digitally controlled and so has the necessary flexibility. A plot of voltage against attenuation is shown in figure 6.6.

The graph shows that there is a significant difference in the response of the channels. It also shows that the attenuation values possible are not as great as the predicted values. The reason is that, as indicated in table 6.1, the resistive values need to be very small for small attenuations, and again for large attenuations. However the resistance of the capacitors becomes significant at these values and their values vary from component to component. The performance could be greatly improved by careful circuit construction using strip line

techniques, which employ chip capacitors and metal film resistors.

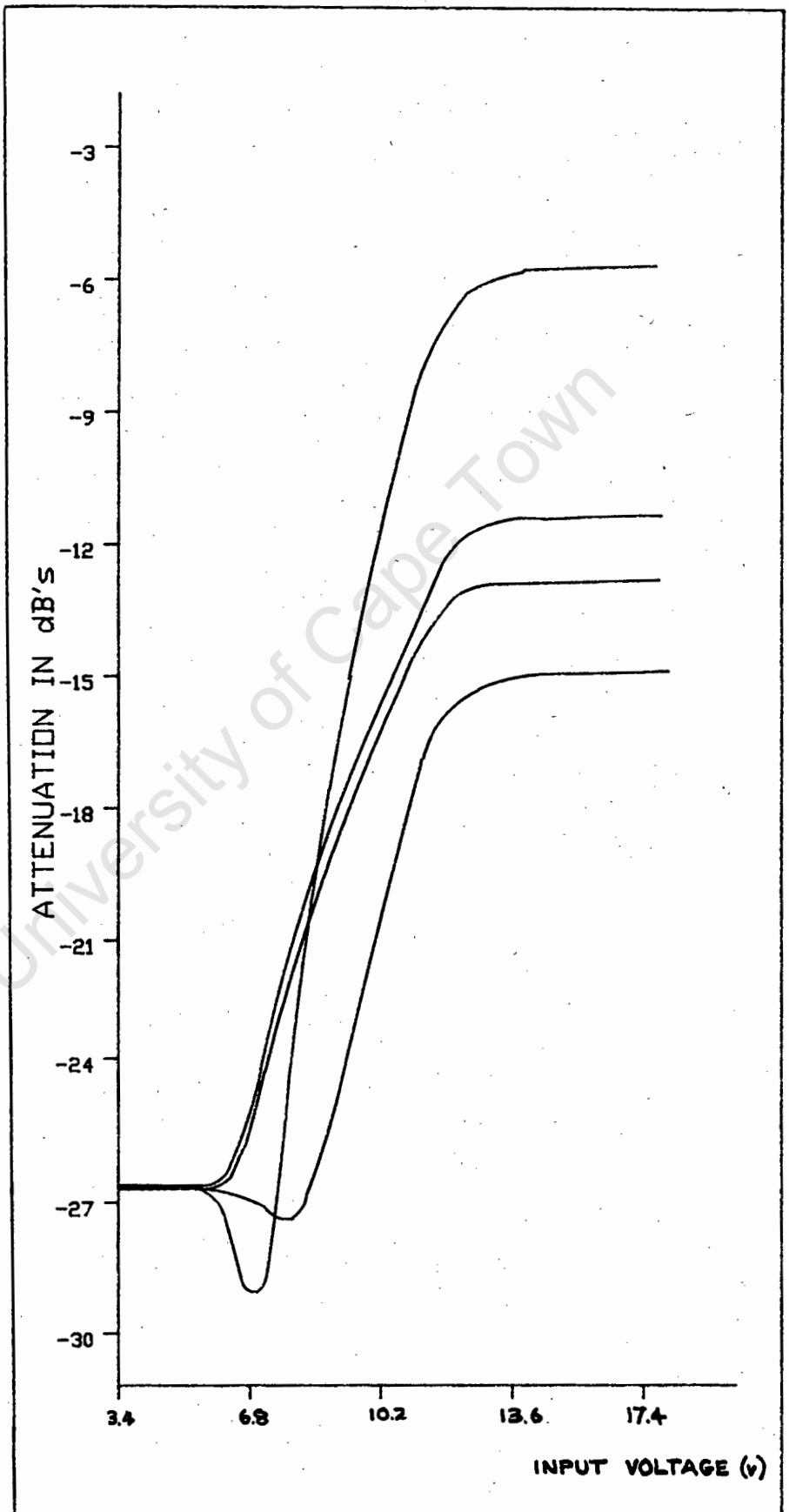

FIG 6.6 Voltage-Attenuation Relationship

6.2 GPIO INTERFACE

GPIO stands for General Purpose Input Output and is one of the I/O buses available for the HP85 computer. The hardware configuration and installation of the GPIO is not discussed here but can be read in reference [6.5]. However the pin configurations and software configuration codes are discussed in appendix B, and their use can be seen in the computer program in appendix C.

The handshaking which is used in this application is the Strobe handshake, the timing of which is shown in figure 6.7. This method assumes that the peripheral device is always ready and the flag line is not used. The cycle begins with the output of data (t1). After a programmable delay (td), the interface sets CTL to the true state (t2). This state is held for the delay time, then CTL is returned to the false state (t3). In other words the interface supplies data, followed by a strobe pulse to indicate that the data is valid. This is done for 4 eight bit data buses.

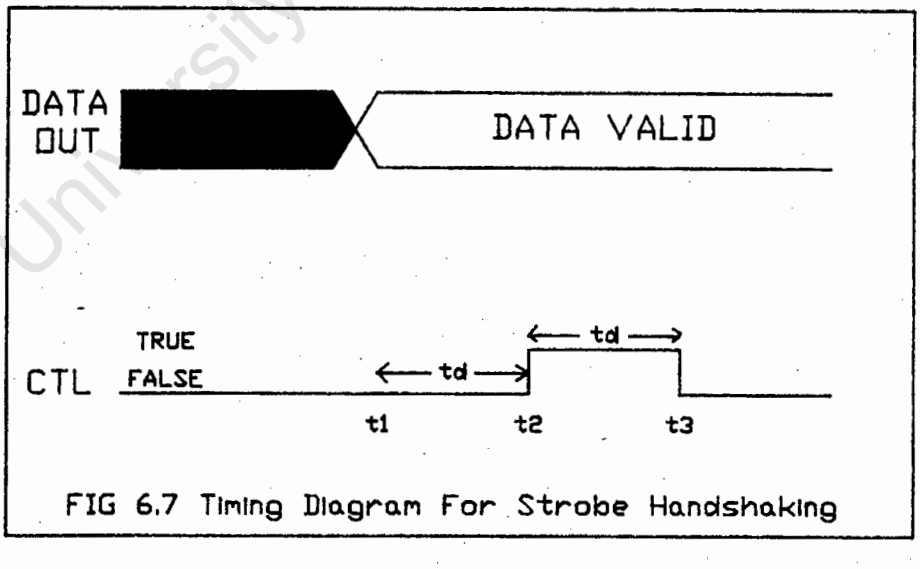

FIG 6.7 Timing Diagram For Strobe Handshaking

6.3 CONTROL VOLTAGE INTERFACE

Because of the simplicity of the handshaking with the GPIO, the control voltage interface requires very little

logic and timing (unless one needs to vary all four quadrants as well as the delayed signal, in which case a more complicated interface is required).

Figure 6.8 shows the block diagram of the interface. Each of the 8 data bits is latched using the associated control lines, to ensure the data is always valid. The latched data is applied to the DAC's which also have a constant current reference applied. The analogue output voltage is then amplified to cover the required range of the voltage controlled attenuators.

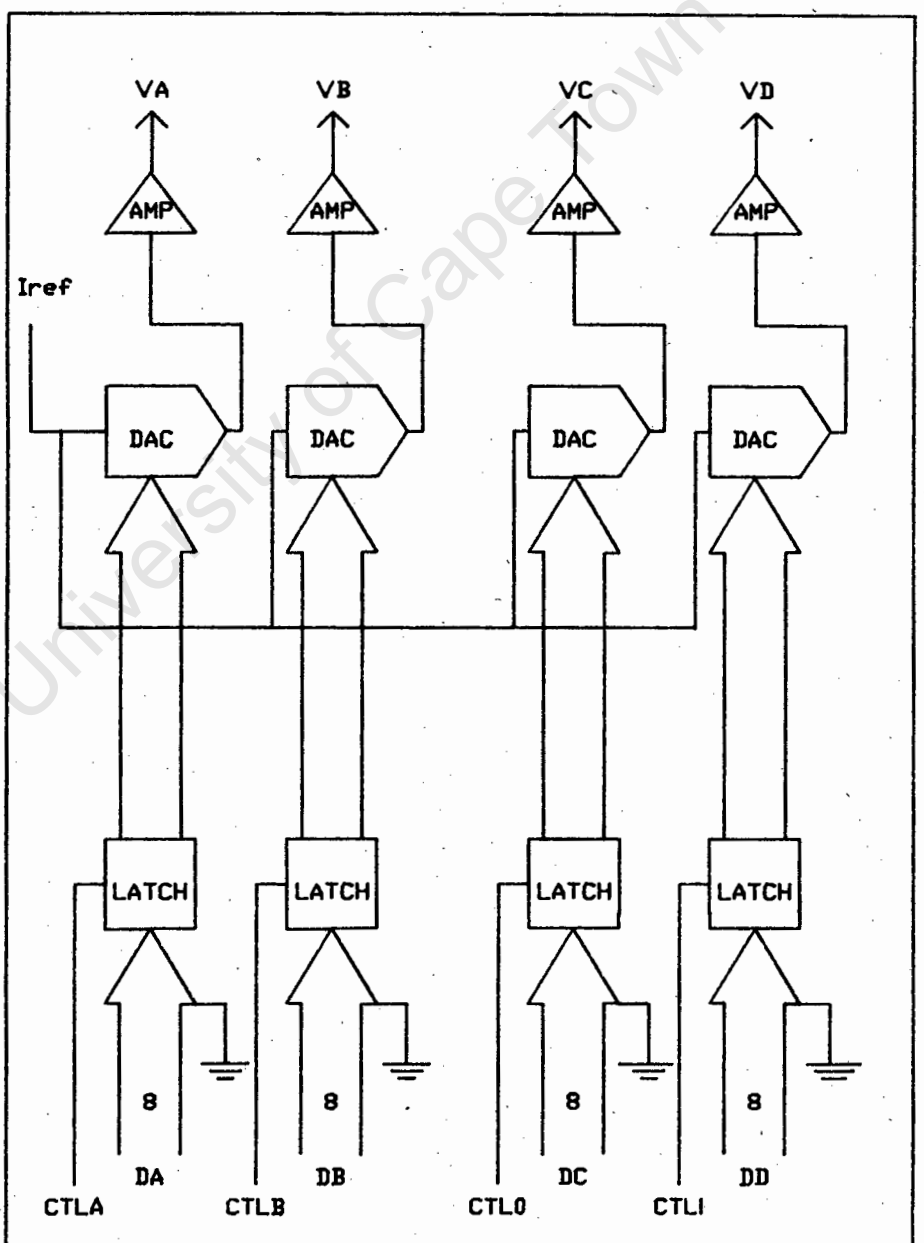

FIG 6.8 Block Diagram Of GPIO Interface

Figure 6.9 shows the final circuitry of the control voltage interface and should be studied with reference to the GPIO interface discussed in Appendix B. The latching is done by the 74373's which have the respective control line (CTLA, CTLB, CTL0, or CTL1) connected to the latch enable pin. This latching configuration is the method recommended in the 74373 data sheet. The 32 data lines are then connected to the four DAC0800 IC's which have a current reference provided by the 12 volt supply using the 8k2 resistors . Pin 1 of the DAC is grounded to set the input logic level TTL compatible. This digital to analogue converter application is given as a typical application on the DAC0800 data sheet.

The output current (= $-V_{ref}/R_{ref}*255/256$) is converted to a voltage and amplified using 741's in the inverting mode configuration. The output voltage from the amplifiers is 0.00 volts DC for logic 00000000, up to 17.4 volts for logic 11111111. It should be noted that figure 6.3 shows five attenuators which are necessary to provide a four quadrant positioning of the offset frequency, but the hardware simulator prototype only has four attenuators and can thus only provide 2 quadrant positioning at any specific time. This was due to the fact that the HP85 computer can only provide four digital outputs.

6.4 LABORATORY GENERATION OF MULTIPATHS

Figure 6.10 shows the hardware simulator prototype, which was completed in June of 1987. However it was only in the middle of 1988 that it was possible to test the system on a MSK modulator, the specifications of which are discussed in reference [2.8].

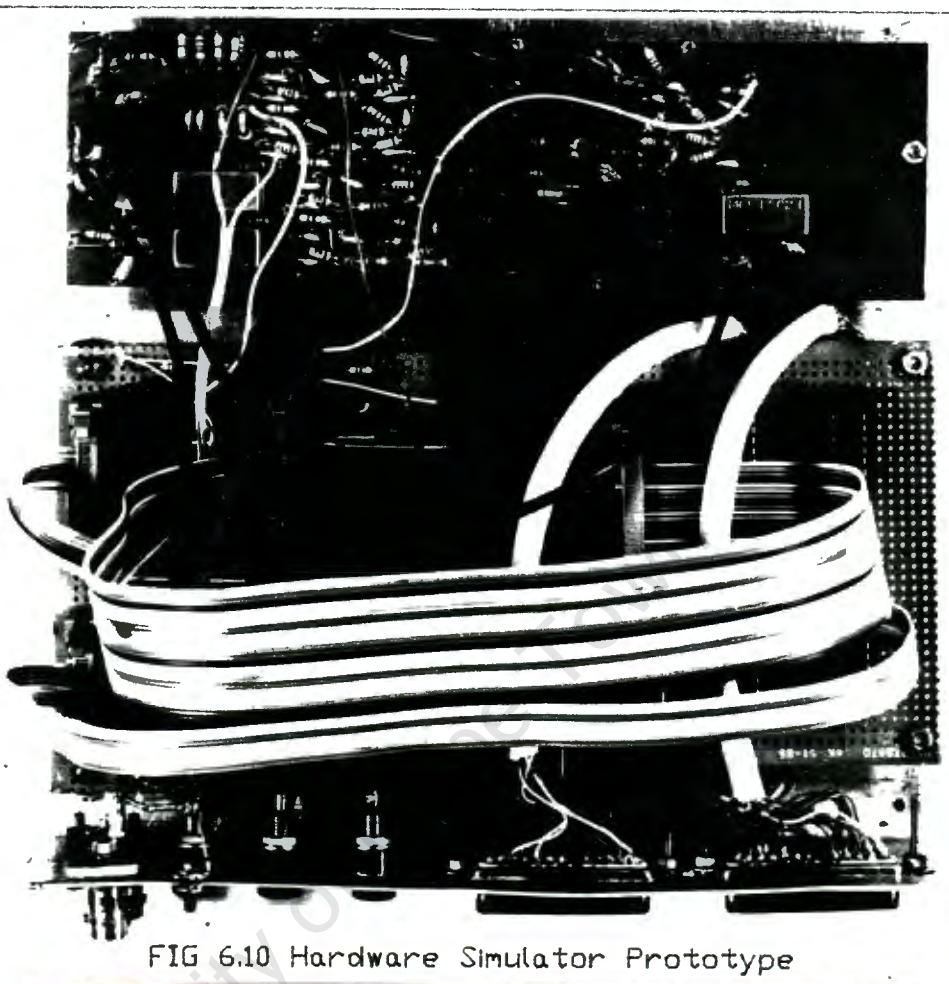

FIG 6.10 Hardware Simulator Prototype

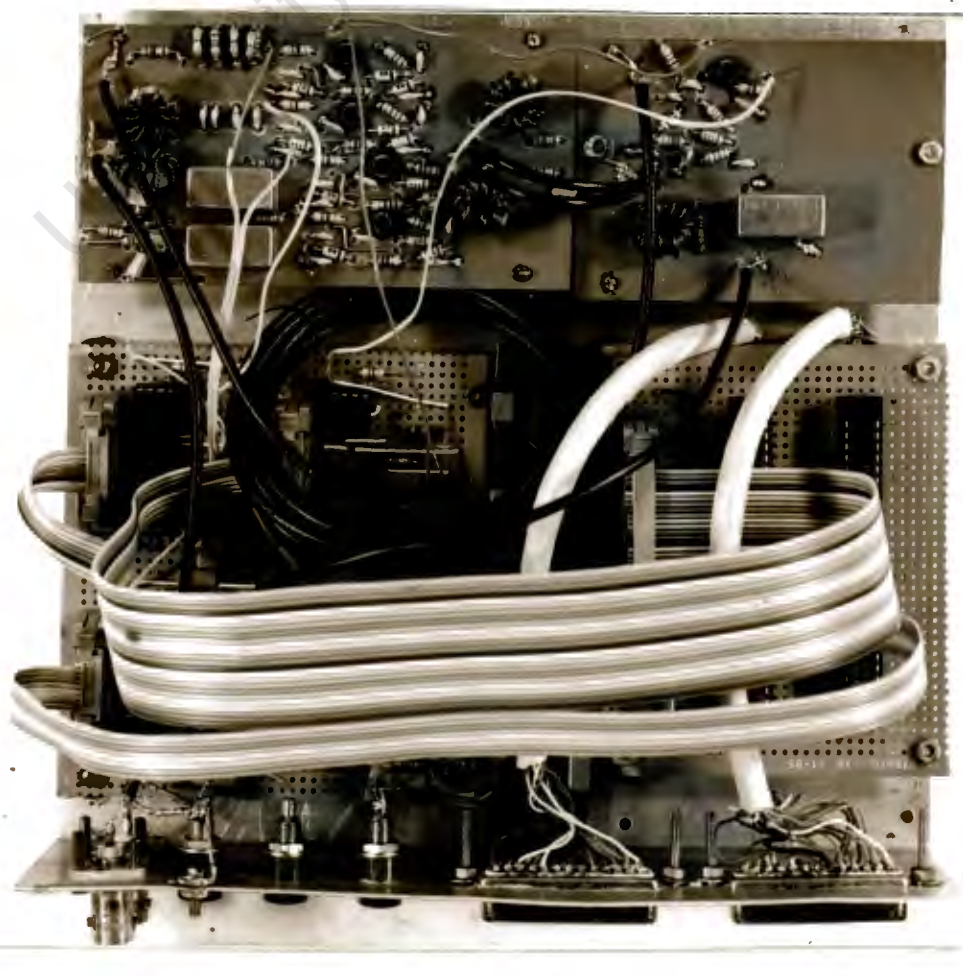

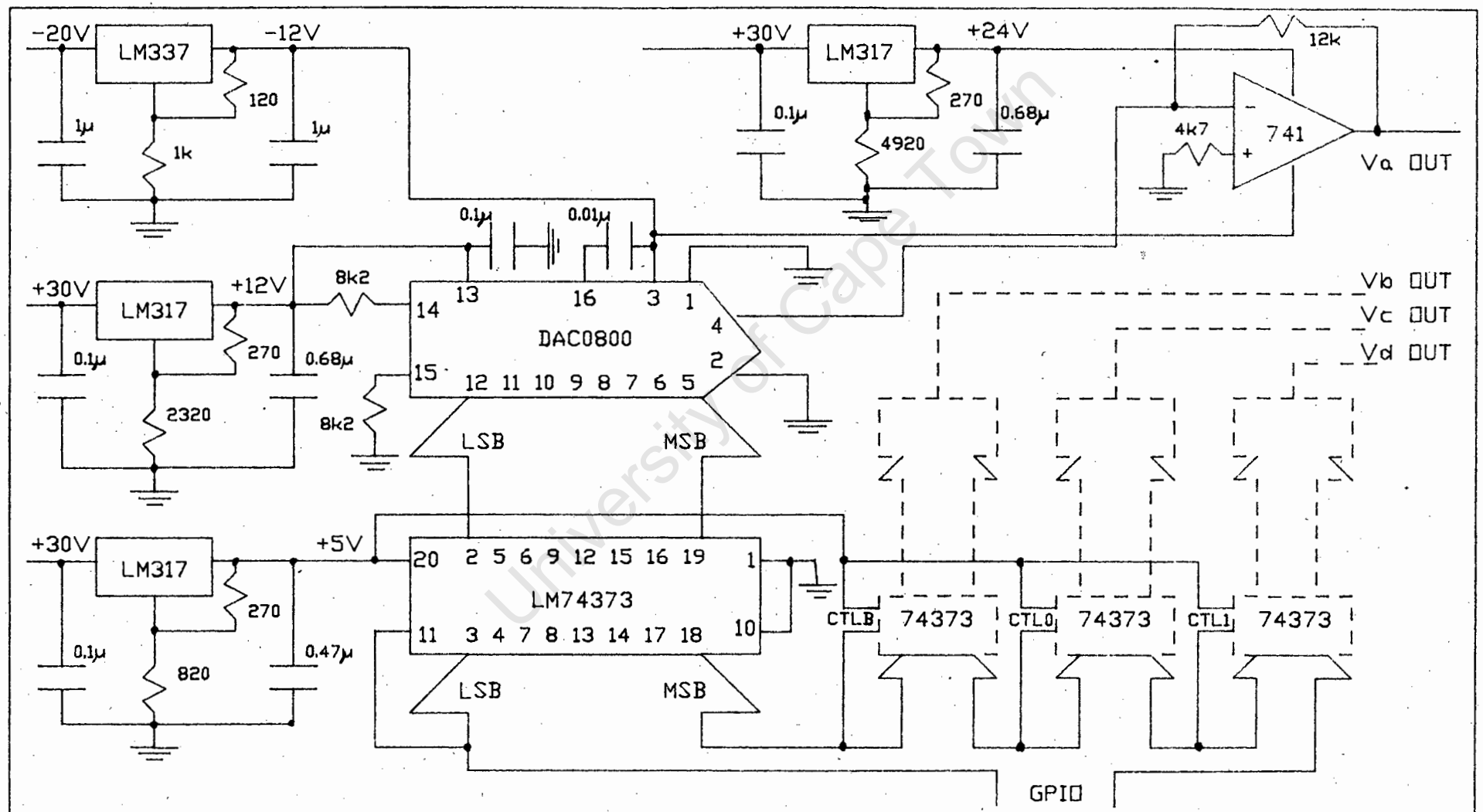

FIG 6.9 Circuitry For The Control Voltage Interface

During the final simulations with a MSK modulator in July of 1988, it was discovered that the channel isolation problems mentioned earlier are such that it was not possible to generate deep notches but only flat fading and slope fading. Figure 6.11 shows the unaffected MSK signal and figure 6.12 shows the MSK signal affected by heavy rainfall.

In order to simulate deep fading it is necessary to replace the **MINICIRCUIT** phase combiners with matched input impedance summing amplifiers which are now available at the required operating frequency and are used in the construction of the adaptive equalizer.

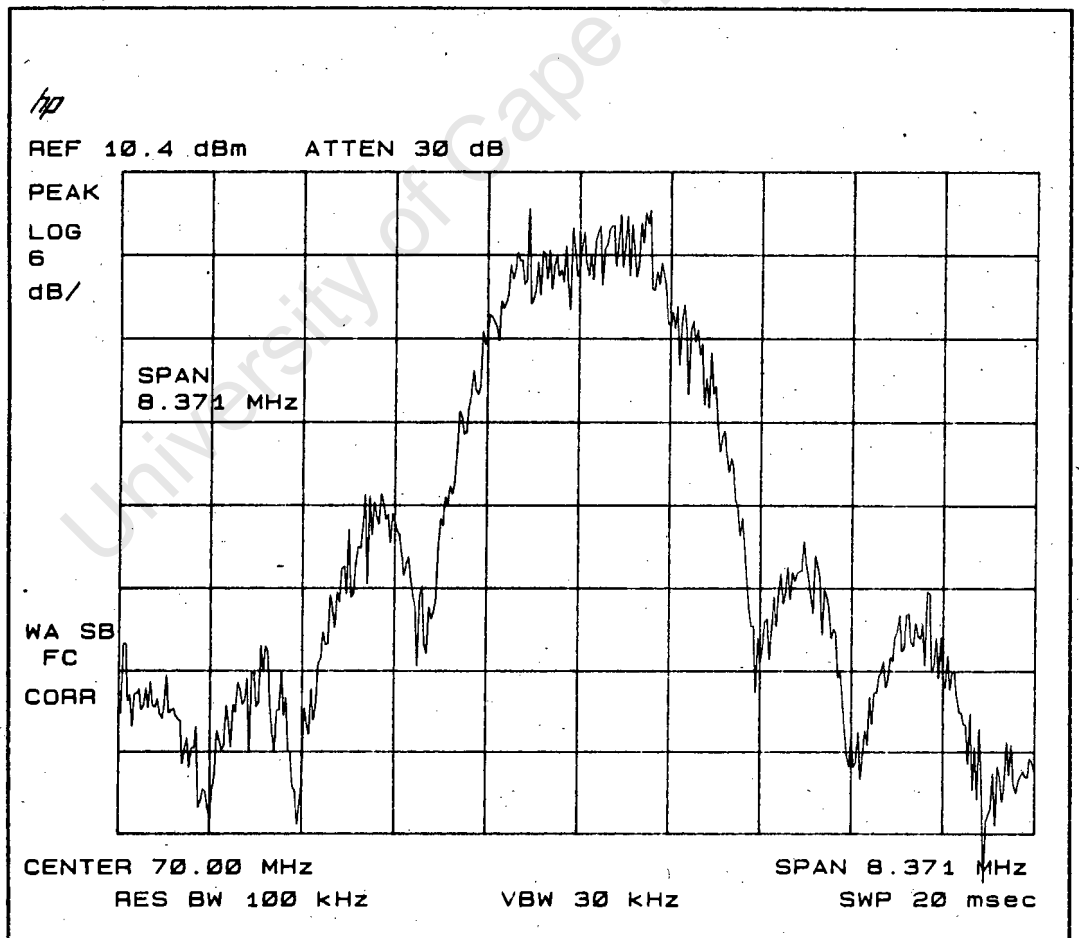

FIG 6.11 Unaffected MSK Spectrum

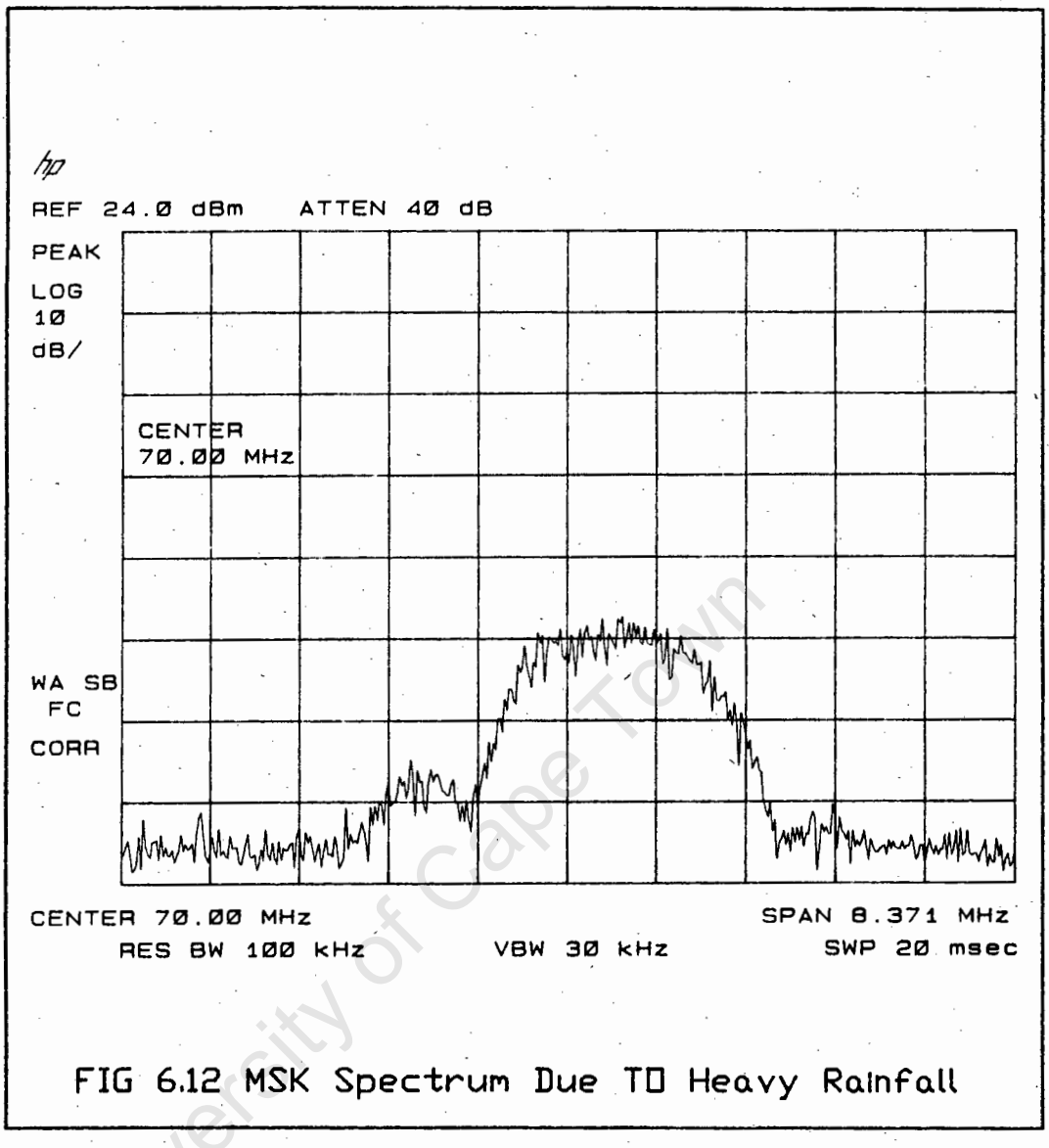

FIG 6.12 MSK Spectrum Due TO Heavy Rainfall

CHAPTER 7

COMPUTER SIMULATION OF MSK COMMUNICATION LINK

A program to simulate a MSK modulator and demodulator, as well as the multipath propagation affects over a hop has been written to run on the HP9000 computer in Pascal. The purpose of the program is to study the BER as a function of the signal/noise ratio and the parameters of the multipath model. From the results it is hoped to obtain some insight into the affects of multipath propagation.

The flow diagram for the computer program is shown below in figure 7.1.

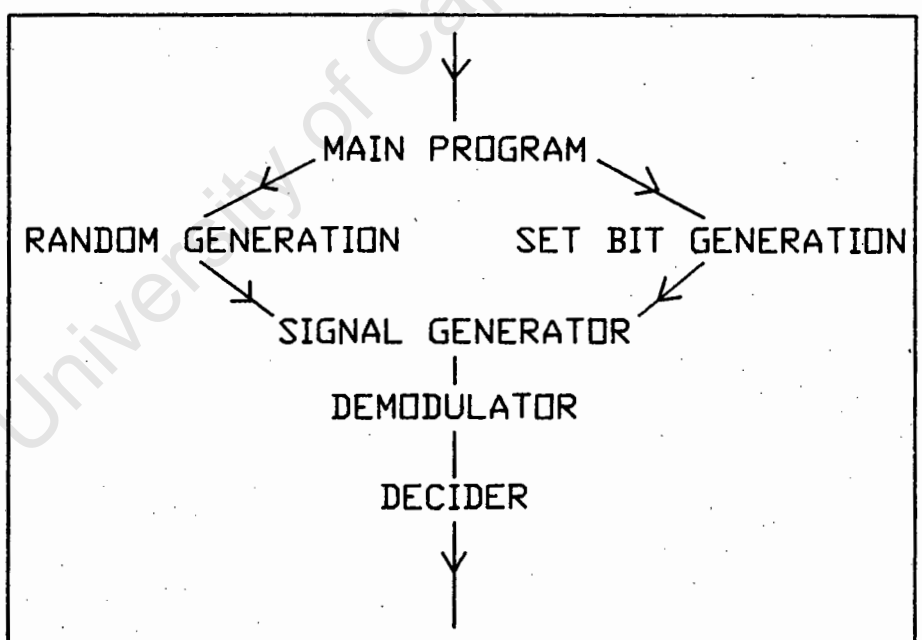

FIG 7.1 Flow Diagram For Computer Simulator

Before discussing the purpose of each of the procedures the parameters used in the program will be defined. The BER is simply the number of bits that were in error

divided by the total number of bits generated. E_b is the energy per bit which is equal to the power level of that bit or
$E_b = E_s^2/(zB_r)$ where E_s is the RMS voltage of the signal, B_r is the bit rate and z is the impedance across which E_s is measured. Similarly $N_o=E_n^2/(zENB)$ where E_n is the RMS voltage of the noise and ENB is the effective noise bandwidth. Thus in log notation
$E_b/N_o = 20\log(E_s/E_n)+10\log(ENB/B_r)$.

To obtain E_s and E_n, the value of the signal and the value of the random generator at each iteration are squared, separately summed throughout the program, divided by the total number and then squarerooted*.

7.1 MAIN PROGRAM

The main program defines all constants and global variables. It generates an array of sine and cosine values to be used in the demodulator (this is purely a program time saving step). The main program also calls the INPUTPAGE procedure which sets up the consul screen and instructs the operator what options he has and what information is required to be entered. Finally the main program prints out the results of the simulation, such as the errors that occurred, BER, and E_b/N_o value.

7.2 SET BIT GENERATION

The procedure SETBITGEN uses the 8 bit sequence entered by the operator (eg 10111010) and produces a 10000 bit sequence of the repetitive 8 bits. This 10000 bit sequence is used in the signal generator.

---

* The derivation of Eb/No is explained in reference [1.4]

7.3 RANDOM BIT GENERATION

The procedure RANDOMGENERATION generates a pseudo random bit sequence using the function RANDOM. RANDOM is a repetitive mathematical equation initialized by a seed entered by the operator.

7.4 SIGNAL GENERATOR

If the generated bit is a 1 the phase value is reduced linearly by 90 degrees over the bit duration. If the generated bit is a 0 the phase value is increased linearly by 90 degrees over the bit duration. This varying phase is included in the mathematical expression $\cos(2\pi ft + \text{phase})$ to produce the IF modulated signal. The procedure SIGNALGENERATOR also includes the multipath propagation model and noise generation.

The multipath model simply varies the amplitude of the above expression and adds this value to a second expression which is generated by delaying the above expression by a fixed number of iterations (as well as varying the amplitude).

The noise is simply achieved by adding the output of the random generator to the multipath signal. The signal to noise ratio is varied by varying the amplitude of the multipath signal. The RMS values of the original signal (as stated above), and the RMS of the noise is also calculated in this procedure and these values are used in the main program to calculate the E_b/N_o value.

7.5 DEMODULATOR

The first part of the DEMODULATOR procedure is a digital bandpass filter. This is necessary in order to measure the effective bandwidth which is used in the E_b/N_o calculation.

7.5.1 DIGITAL BANDPASS FILTER

Reference [6.6] discusses the theory of digital filtering.The specifications required in this application are a passband from 60 MHz to 80 MHz. The reason for such a wide bandwidth is to have the second bandpass filter (associated with digital filters) as far away from the centre frequency as possible. The sampling frequency is 280 MHZ (set by the number of iterations per cycle). Using the equations stated in reference [6.6]

$\alpha = \cos[(f2+f1)/fs]\pi/\cos[(f2-f1)/fs]\pi = 0$

$\beta = \Omega\cot[(f2-f1)/fs]\pi = 4.38129\Omega$

For a third order butterworth filter

$$H(s)=\frac{1}{s^3 + 2s^2 + 2s + 1}.$$

where $s=4.38129(1+z^{-2})/(1-z^{-2})$. Substituting into the above formula gives :-

K1=0.007561
K2=-0.022683
K3=0.022683
K4=-0.007561
K5=-2.109052
K6=-1.573856
K7=-0.40436

The frequency response of the bandpass filter is shown in figure 7.2 and the effective bandwidth was measured graphically. Note though that a digital filter is cyclic but the calculations used in the computer program have only included one of the bandpasses in the E_b/N_o calculation and this makes it difficult to quantitatively compare the results with results measured by actual systems.

The structure of the bandpass filter is shown in the figure 7.3 and it is this delay line configuration with constants taken from the above expression that is included in the computer program.

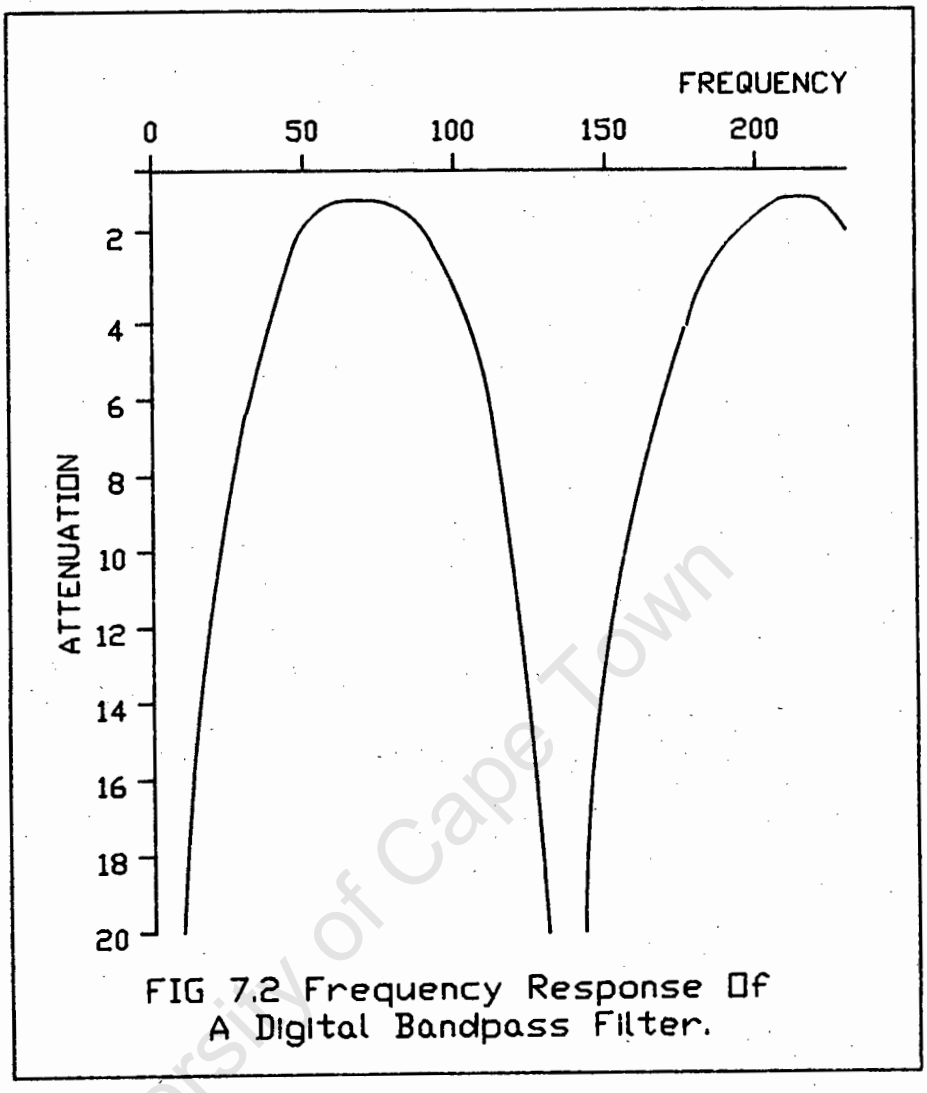

FIG 7.2 Frequency Response Of A Digital Bandpass Filter.

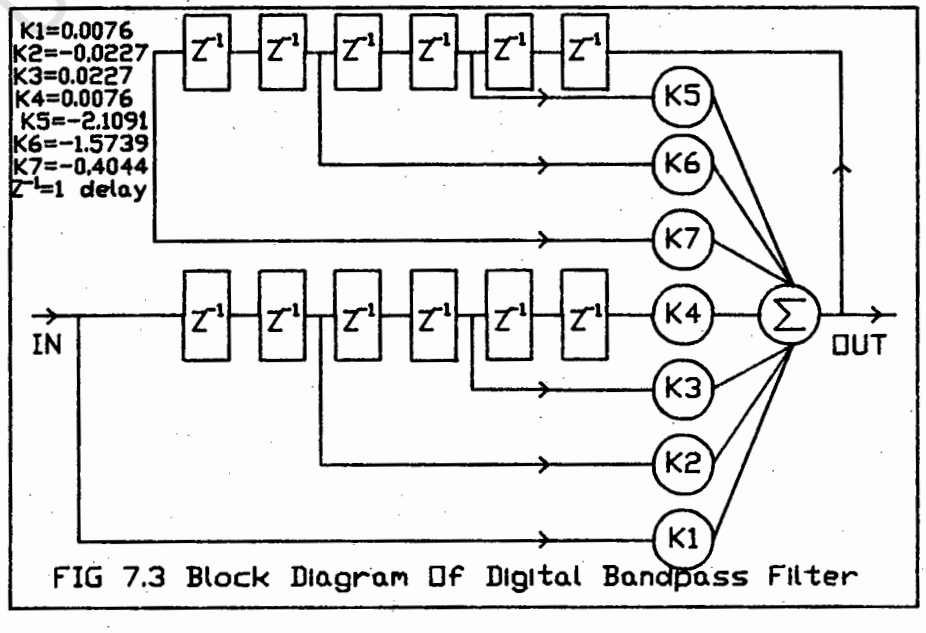

FIG 7.3 Block Diagram Of Digital Bandpass Filter

The output of the bandpass filter is multiplied by the expressions $\sin(2\pi ft).\sin(\pi t/(2T))$ to form the Q channel, and $\cos(2\pi ft).\cos(\pi t/(2T))$ to form the I channel. The two channel signals are then digitally low pass filtered.

7.5.2 DIGITAL LOW PASS FILTER

The specifications for the low pass filter are that it must be flat to 3dB from 0 to 75 MHz and more than 10 dB's at 130 MHz. As with the bandpass filter the sampling frequency is 280 MHz.

Using the formulae from reference [6.6],

wd1t=0.5357
wd2t=0.9643
wa1= 1.1189
wa2=17.814
n=2
wc=1.1189

The form of the second order butterworth filter is

$$H(s)=\frac{1.252}{s^2 + 1.5824s + 1.252}.$$

Substituting in $s = (1-z^{-1})/(1=z^{-1})$ gives

$$H(z) =\frac{0.3266(1+2z^{-1}+z^{-2})}{1+0.1315z^{-1}+0.1748z^{-2}}.$$

Using the delay line diagram of figure 7.4 with the constants of the above equation gives the form of the digital filter which is used in the computer program.

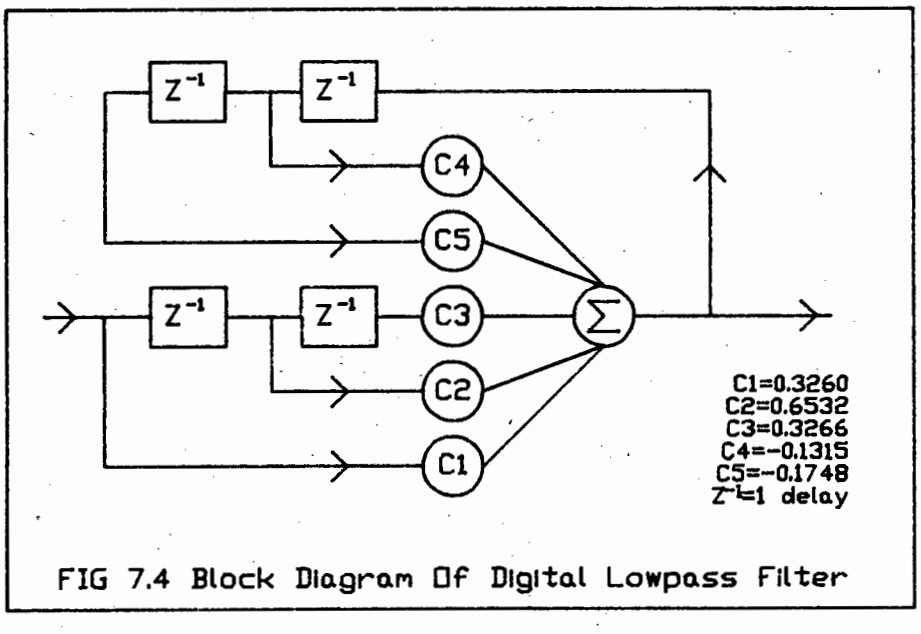

FIG 7.4 Block Diagram Of Digital Lowpass Filter

The output of the Q filter is integrated from 0 to 2T and then the integrator is dumped and the integration begins again, the dumping being repeated at multiples of 2T. The output from the I filter is integrated from T to 3T and then the integrator is dumped and the integration begins again, the dumping also being repeated at multiples of 2T.

The decision as to whether the values of the integrator correspond to 1's or 0's is done in the DECIDER procedure but the 1's and 0's from the DECIDER are differentially decoded in the DEMODULATOR procedure.

7.6 DECIDER

The DECIDER procedure first decides whether the values of the integrators are greater than 0 (corresponding to a 1) or whether they are less than 0 (corresponding to a 0). It also compares the output of the differential decoder with the transmitted bitstream and if they differ prints that an error has occurred. The DECIDER also calculates the BER value.

The final computer program that was used is shown in appendix D and the results discussed in chapter 8.

CHAPTER 8

RESULTS OF COMPUTER SIMULATIONS

The first simulations run on the computer were with no multipath propagation but simply involved changing the signal level and recording the BER vs E_b/N_o values. The results are plotted for a=1.0 b=0.0 on figure 8.1 curve 1. Comparing the results with reference 2.1 figure 7 it can be seen that the general shape fits in well with the different modulation techniques, although it is shifted to the left by 4 dB's. This error is due to the ENB value used in the calculation of E_b/N_o. The ENB should be a constant 20MHz as discussed in section 7.5.1. but the digital bandpass filter is periodic in nature and so any noise appearing in shadow areas will alter the ENB value.

Also shown in figure 8.1 are the effects of multipaths with different A and B values. As is expected a decrease in A or an increase in B produces a shift to the right from the ideal position ie the signal power would need to be increased to maintain a fixed BER.

It is also interesting to note that except at very high BER's the errors occur in pairs, as is to be expected due to the information being differentially decoded from the I and Q channels.

The effects of centre frequency offset, as shown in figure 8.2, are different from those due to Rummlers model. The reason is that the recovered carrier signal has been phase shifted due to the multipath affect and so the f_0 value needs to be resolved. Normalising the curves with respect

to the a=1,b=0 curve will produce similar curves to Rummlers.

It was difficult to see whether there is a relationship between the bit sequence and the BER as the program takes 25 minutes to obtain one result and numerous results would be necessary to determine the relationship. Secondly, the program only generates 10000 bits and there is still a detectable quantization between the error pairs. However the BER does seem to depend on the bit sequence. In practical systems the BER increases as the sequence of just 1's or just 0's increases.

With regard to the constellation diagrams (which were generated for 1000 bits) it can be seen from figures 8.3, 8.4, and 8.5 that increasing the noise value produced a random scattering of the points around the ideal position*. The BER is calculated by the simulator. Further study of constellation diagrams have shown that a reduction of value a causes the ideal position to move closer to the intersection of the axes. Variations of b and f_0 also cause a repositioning of the ideal position relative to the origin but do not produce any "scattering" of the points.

*Figures 8.3, 8.4, and 8.5, have been drawn for simplicity with the axis realigned and normalised, so, although the constellation diagram looks like QPSK they are in fact for MSK.

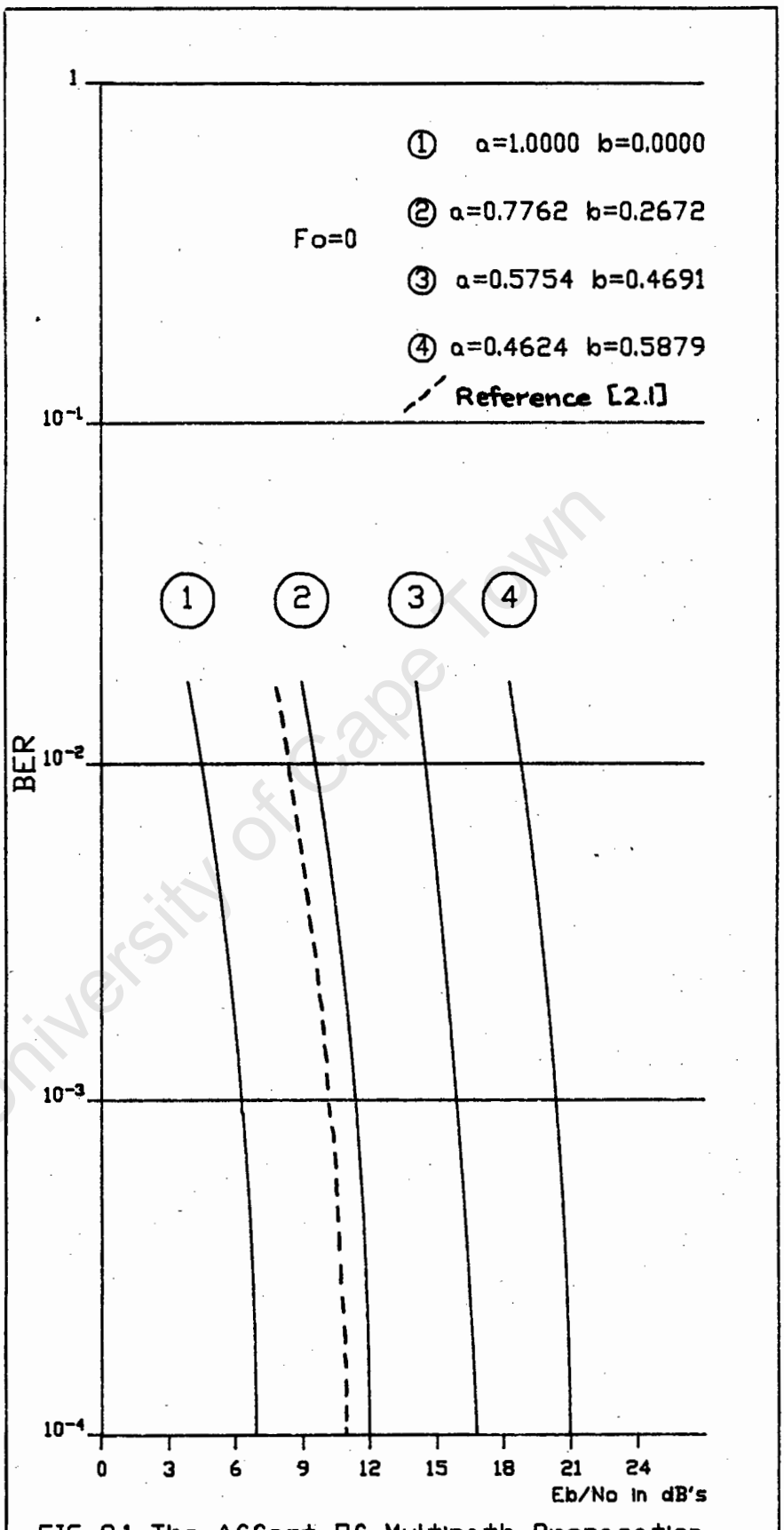

FIG 8.1 The Affect Of Multipath Propagation On The BER-Eb/No Relationship.

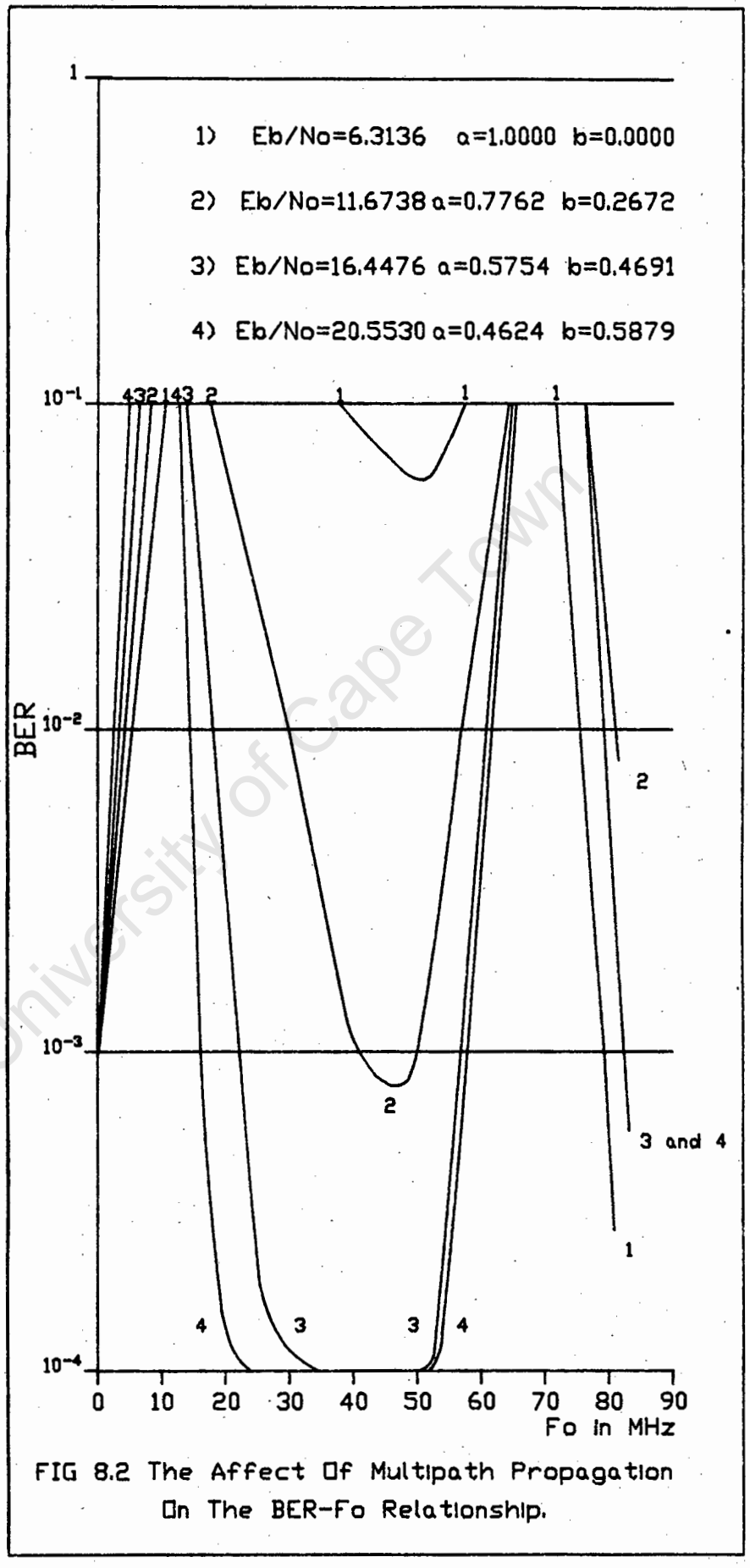

FIG 8.2 The Affect Of Multipath Propagation On The BER-Fo Relationship.

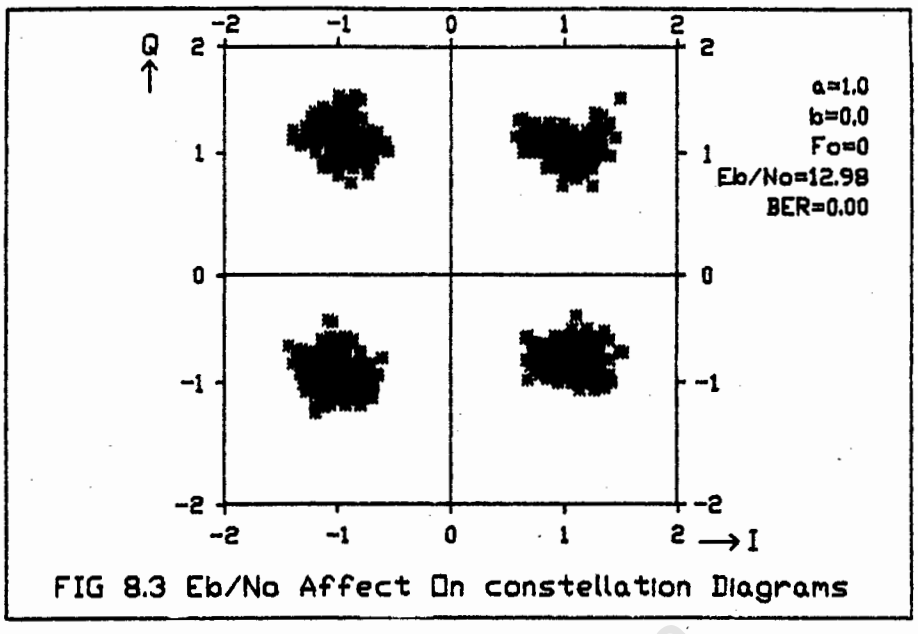

FIG 8.3 Eb/No Affect On constellation Diagrams

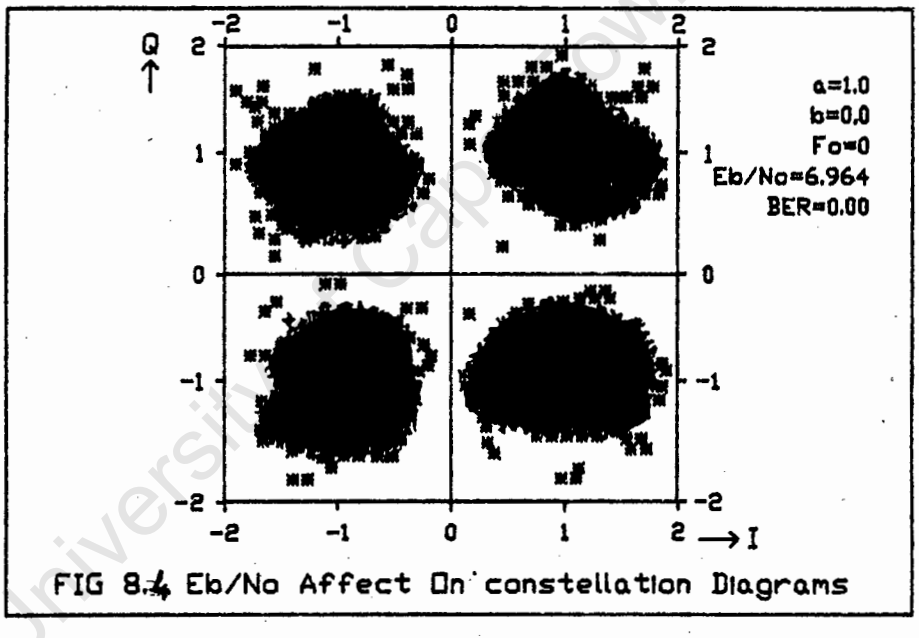

FIG 8.4 Eb/No Affect On constellation Diagrams

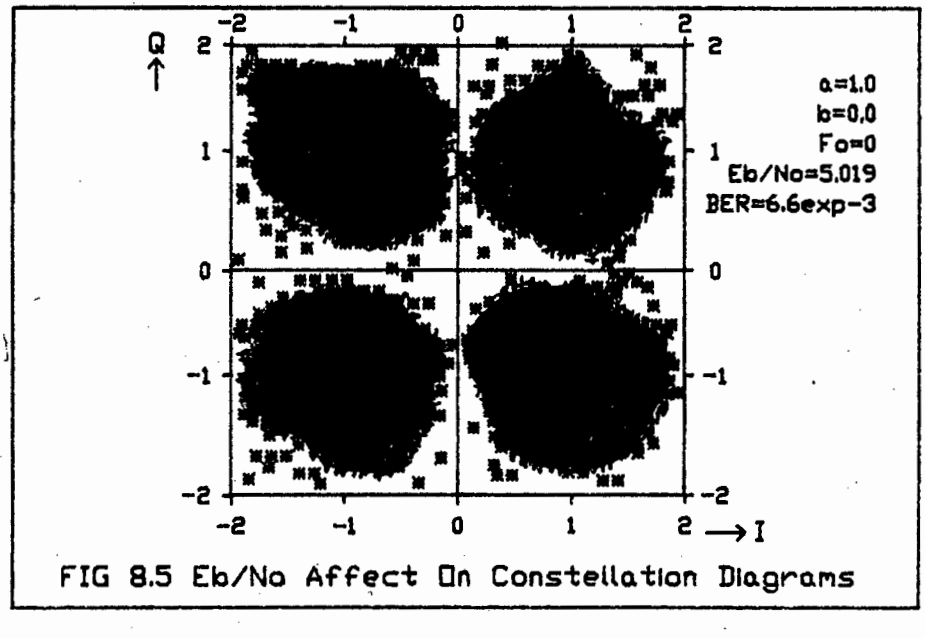

FIG 8.5 Eb/No Affect On Constellation Diagrams

CHAPTER 9

ADAPTIVE EQUALIZERS

The nature and effects of multipath propagation have been discussed in previous chapters. There it was mentioned that the linear channel distortions vary slowly in time. In order to compensate for them it is necessary to use devices which ideally produce "complementary" distortions and that these too vary in time; in other words to employ adaptive equalizers.

Some of the variations of adaptive equalizers that can be designed, as well as their control algorithms, will be discussed later in this chapter. First the phenomena of inter-symbol interference (and crosstalk in quadrature carrier modulation systems) is discussed.

9.1 INTERSYMBOL INTERFERENCE

In bandwidth efficient digital communication systems the effect of each symbol transmitted over a time dispersive channel extends beyond the time interval used to represent that symbol. The distortion caused by the resulting overlap of received symbols is called intersymbol interference (ISI).

ISI arises in all pulse modulation systems, including FSK, PSK, and QAM. However its effect can be most easily described for a baseband pulse amplitude modulation (PAM) system. Figure 9.1, taken from reference [5.7], shows a generalized PAM system with the "channel" including the effects of the transmitter filter, the modulator, the transmission medium and the demodulator.

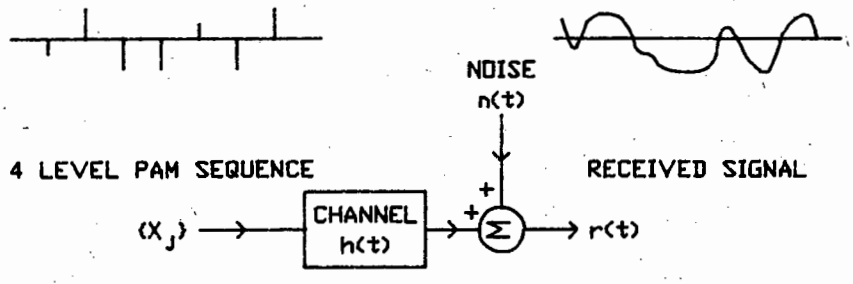

FIG 9.1 Baseband PAM System Model.

A symbol x_n, one of L discrete amplitude levels, is transmitted at instant mT through the channel where T seconds is the signaling interval. The channel impulse response is shown in figure 9.2. The received signal r(t) is the supersition of the impulse responses of the channel to each transmitted symbol and additive white Gaussian noise, n(t).

$r(t)=\sum_j [x_j h(t-jT)+n(t)]$.

If the received signal is sampled at instant $kT+t_0$, where t_0 accounts for the channel delay and sampler phase, the formula becomes :-

$r(t_0+kT)=x_k h(t_0)+\sum_{j=k} x_j h(t_0+kT-jT)+n(t_0+kT)$.

The first term on the right is the desired signal since it can be used to identify the transmitted amplitude level. The last term is the additive noise, while the middle sum is the interference from neighbouring symbols. Each interfering term is proportional to a sample of the channel impulse response $h(t_0+iT)$ spaced a multiple iT of symbol intervals T away from t_0. The ISI is zero if and only if $h(t_0+iT)=0 \quad i\neq 0$, that is if the channel impulse response has zero crossings at T spaced intervals.

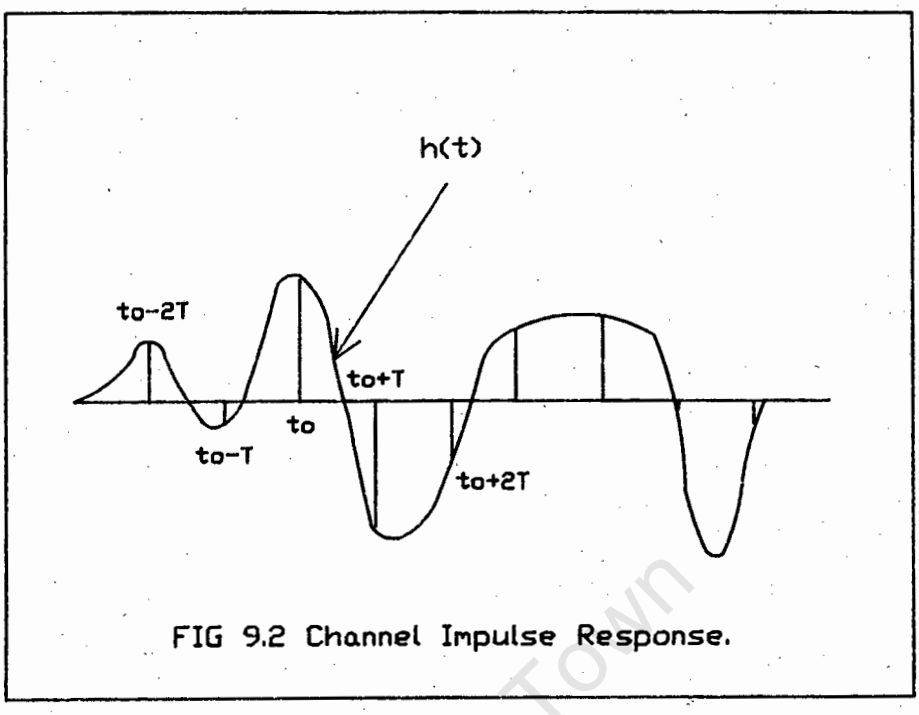

FIG 9.2 Channel Impulse Response.

In practice, the effect of ISI can be seen from the eye pattern as shown in figure 9.3. If the channel satisfies the zero ISI condition there are only two distinct levels at the sampling time t_0. The eye is then fully open and the peak distortion is zero. Peak distortion is the ISI that occurs when the data pattern is such that all intersymbol interference terms add to produce the maximum deviation from the desired signal at the sampling time.

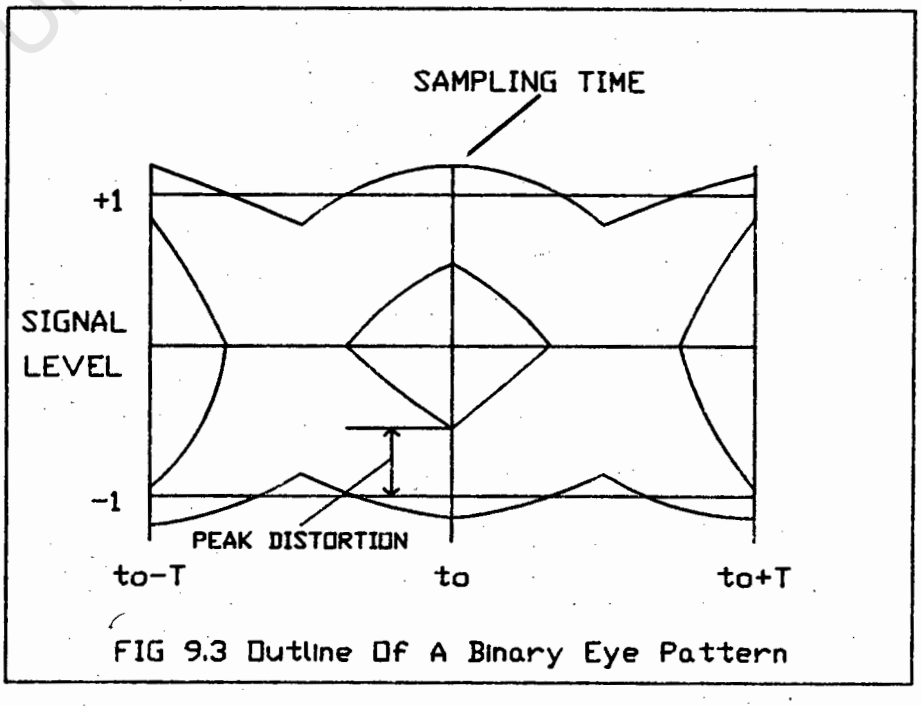

FIG 9.3 Outline Of A Binary Eye Pattern

9.2 CROSSTALK

MSK can be viewed as consisting of two quadrature carrier signals of the same frequency, each one modulated by an independent series of positive and negative half sine wave pulses of width 2T seconds, and the pulses on each carrier are T seconds out of phase with each other.

Since adjacent time slots are associated with different channels the term crosstalk is more appropriate than ISI. Reference [2.7] develops a formula for calculating the mean-square crosstalk in quadrature carrier modulation systems, which is helpful in comparing the sensitivity with respect to ISI and crosstalk, of MSK with other systems. However it is of limited help in the design of adaptive equalizers and so is not discussed further.

9.3 HARDWARE IMPLEMENTATION OPTIONS FOR ADAPTIVE EQUALIZERS

The different types of adaptive equalizers can be divided into three main classes:-

1) Bandpass adaptive equalizers (working in the frequency domain).
2) Adaptive baseband equalizers (working in the time domain).
3) Space diversity systems.

Only the first two classes will be discussed here as this study is only interested in equalizers that can be easily incorporated into the receiver, whereas class 3 equalizers, although very effective, require a major restructuring of the receiver hardware. Reference [5.3] gives a detailed discussion of all three classes.

9.3.1 BANDPASS ADAPTIVE EQUALIZERS

This class of equalizer works in the frequency domain to produce a distortion complementary to that occurring in

the channel so as to bring the overall characteristics back to an ideally flat amplitude versus frequency response (with linear phase).

As a rule, for reasons of practical implementation, equalization takes place at intermediate frequency and is limited to correcting the amplitude versus frequency response only, with the transfer function only depending on a few parameters. Although it is a simple method to implement it will not be discussed in any greater detail here as frequency domain equalization of digital radio is not as affective as time domain equalization of digital radio.

9.3.2 SLOPE EQUALIZERS

Control is achieved by monitoring the output power spectrum at two or three frequencies, using a set of narrow band filters, and comparing the measured powers with each other or with predetermined undistorted levels. A general block diagram is shown in figure 9.4.

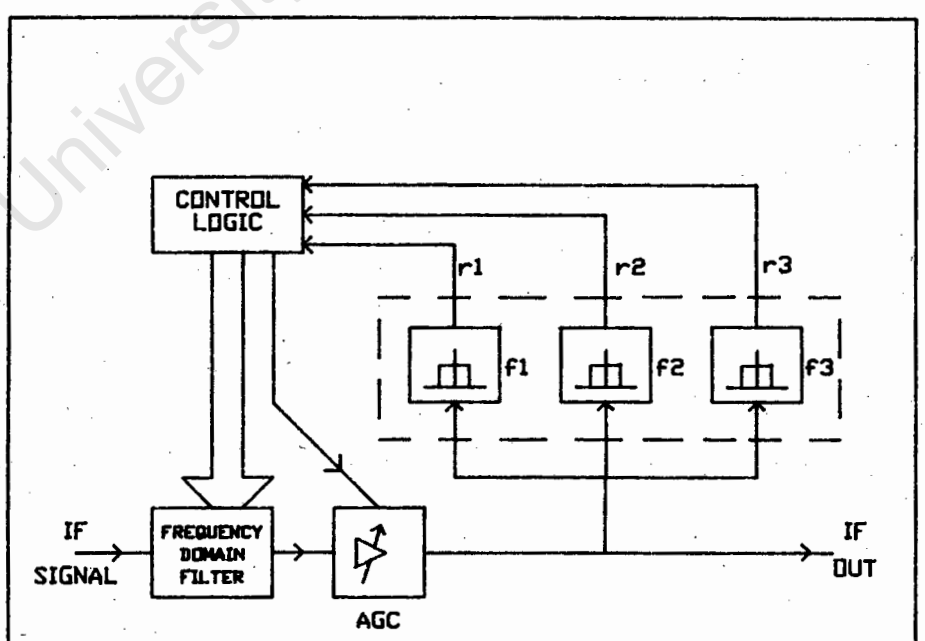

FIG 9.4 Block Diagram Of A Slope Equalizer

The general nature of anomalous propagation is such that, in the frequency domain, multipath distortion most often appears as slope asymmetries in the radio channel response. The compensating circuit consists of a variable slope block and a variable Q bandpass resonator (with fixed resonance frequency corresponding to the midband frequency) capable of producing various distortion shapes of its amplitude versus frequency characteristic (usually linear and quadratic components) to restore equality to the spectral density measured at the passband edges as shown in figure 9.5.

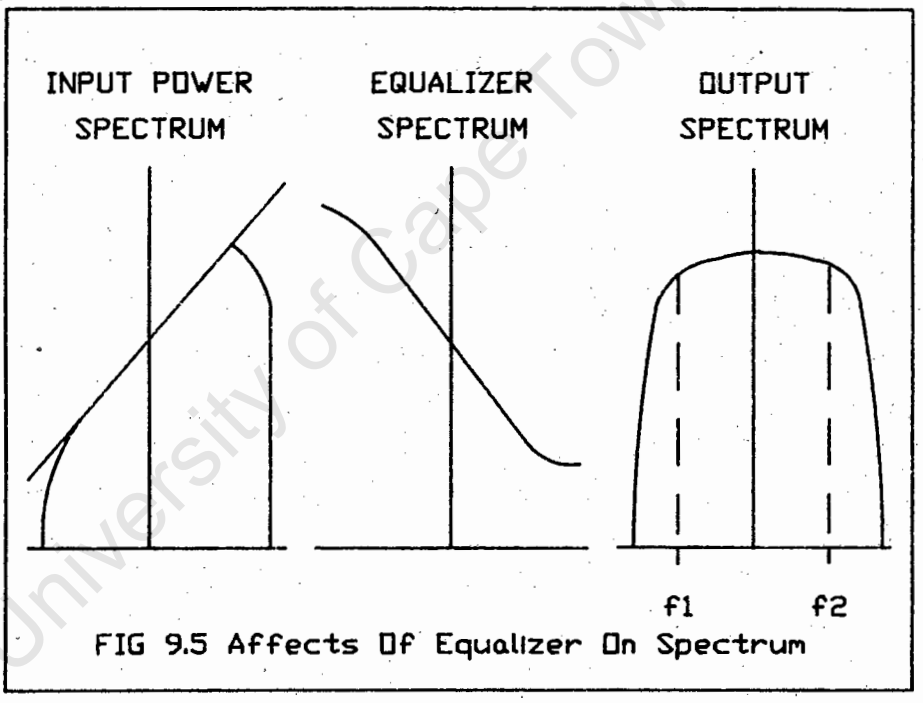

FIG 9.5 Affects Of Equalizer On Spectrum

A slope equalizer is primarily able to compensate for frequency selective fades where any attenuation notch lies outside the passband. It can match the amplitude characteristics that these produce: uncompensated group delay distortions, being more concentrated around the notch frequency, are small and contribute only weakly to system performance degradation. Note that since

9.3.3 NOTCH EQUALIZERS

Very high equalization efficiencies can be achieved if the compensation circuit is realized with a resonator in which both the Q and the resonant frequency can be varied continuously. In fact, assuming the control system to be capable of setting the resonance frequency exactly in coincidence with the notch of the channel transfer function, by choosing a suitable Q value, the resonator amplitude response may quite accurately reproduce a distortion complementary to that of the channel.

Even in this case the group delay behavior of the equalizer is related to the amplitude response so that, while in the case of minimum phase fading there is also a compensation of the channel group delay distortion, in the case of non minimum-phase fading ($\tau<0$) an impairment of such distortion occurs, causing the overall group delay to be roughly doubled.

Since the control system has to perform rather complex operations in order to correctly position the resonator frequency and to optimize the Q value, microprocessor systems are normally employed. The functional diagram of this type of equalizer is shown in figure 9.6. The resonator is normally realized using lumped elements and variations in f_r and Q are generally obtained with varicaps and pin diodes.

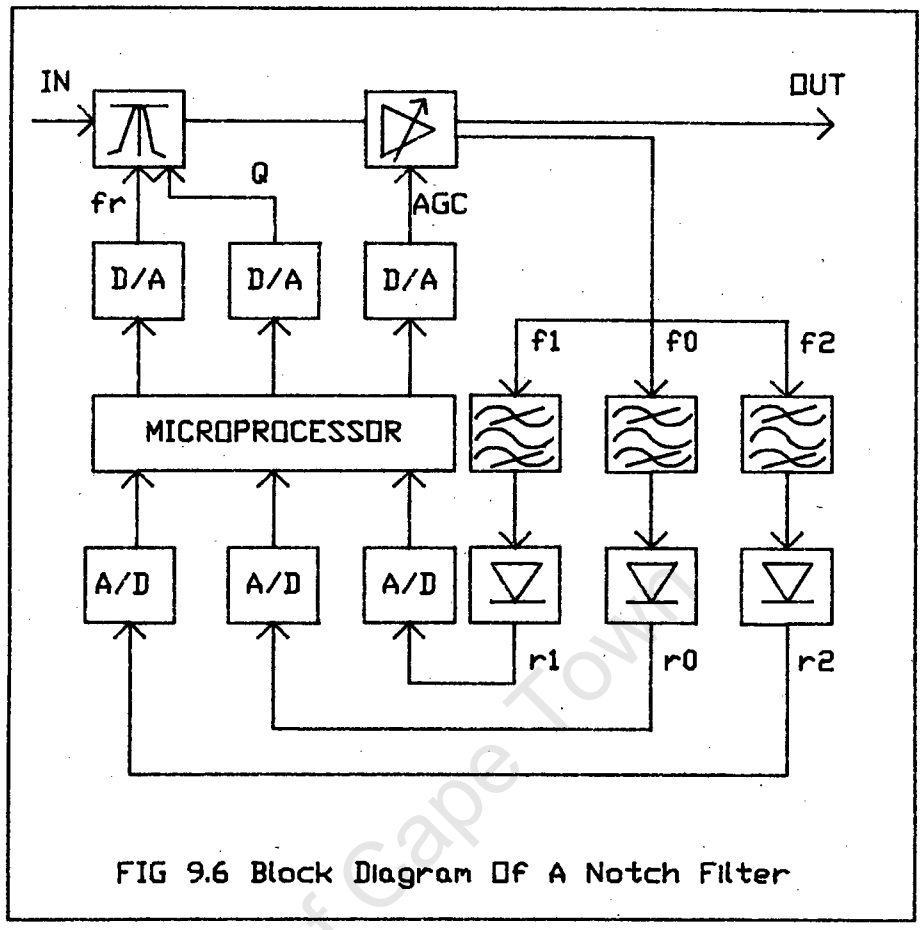

FIG 9.6 Block Diagram Of A Notch Filter

9.3.4 OTHER FORMS OF EQUALIZERS

Although it was stated earlier that this dissertation would not discuss space diversity systems, reference [5.6] describes an equalizer which is a combination of space diversity and frequency domain equalization. The principle involves trying to separate the outputs of a small number of discrete paths, not only for freeing the output of at least one usable path, but also possibly for combining the various path outputs in constructive ways to take advantage of the additional signal energy. In principle this is possible by converting directional and propagation differences into very distinct frequency differences by synthetic Doppler methods. Reference [3.6]

agrees that the group delay and angle of arrival are sufficient to make this method possible.

Reference [5.4] uses a method of discrete fourier transformation (DFT) to perform a frequency domain adaptive digital filter. Figure 9.7 shows the implementation procedure. The input signal data x_n and desired response d_n (used during the set up procedure) are transformed to the frequency domain by the N point DFT.

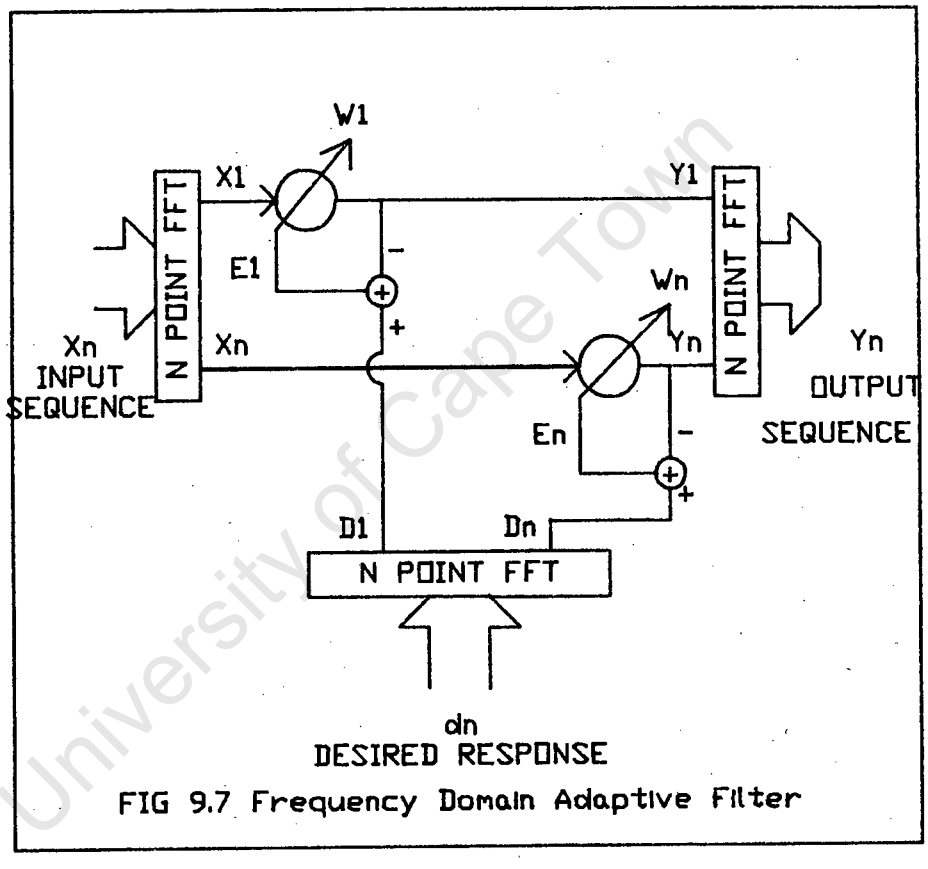

FIG 9.7 Frequency Domain Adaptive Filter

Let $X_k(m)$ and $D_k(m)$ be the kth frequency bin in the mth data block of the input signal and desired response respectively. There are N complex weights $W_k(m)$, one corresponding to each frequency bin. The weighted outputs given by

$Y_k(m)=W_k(m).X_k(m)$ are fed to the inverse FFT operator to produce N point output signals. If the input signals are wide sense stationary over the observation time, then

the frequency components become orthoganal and each of the N complex weights may be updated independently.

Another frequency domain adaptive filter using FFT's is given in reference [5.5]. This filter employs a cascade of analogue forward and inverse Fourier transform processors interconnected via a digital interface. The interface multiplies the transformed input, sample by sample by a set of weights stored in RAM and compares the products against a desired complex spectrum. The resulting error is used to update the RAM weights via a feedback loop, which forces the multiplied output to converge towards the desired complex spectrum.

9.4 ADAPTIVE BASEBAND EQUALIZERS

This class of equalizer works in the time domain to reduce intersymbol interference at the decision instants by making a distinction between leading elements (precursors) and lagging elements (postcursors) of the intersymbol interference in the impulse response of the system. Reference [5.3] discusses this class of equalizer in detail. Adaptive baseband equalizers (operating in the time domain) can be further divided into two others classes :-

-linear forward equalizers (LFE) using transversal filter structures

-non linear equalizers through the use of estimated symbols in retroaction (DFE:decision feedback equalizer).

In both cases equalization adaptivity is achieved by varying the multiplier coefficients (weights) of the taps of a transversal filter configuration. The conceptual advantage over the previous class of equalizers is the ability to compensate for both amplitude and phase distortions simultaneously by acting in a more synthetic way directly on the intersymbol interference.

Explaining the terms precursor and postcursor more clearly; the interfering contributions are called postcursor when they follow the symbols which precedes the useful symbol (in other words, interference is due to their right hand tails); and they are called precursors when they precede the symbols that follows (in other words the interference is due to the left hand tails).

If a_k represents the transmitted symbol, owing to the effects of distortion, the received value will in general have the following representation:

$x_k = \sum_i \lambda_i a_{k-i}$

Coefficients λi represent, for $i<0$, the precursor levels; for $i>0$ the postcursor levels; while $i=0$ will be the amplitude of the useful symbol. The purpose of the equalizer is to eliminate the terms with $i \neq 0$ that appear in the x_k summation.

The above expression is expanded for orthoganal systems to describe the in-phase distortion and quadrature distortion that occurs. In-phase distortion results from the perturbations of the amplitude and group delay responses that have even symmetry about the channel centre frequency and produce pulse distortions within each data stream separately. Quadrature distortion results from asymmetries in the channel responses producing crosstalk between the two streams.

9.4.1 LINEAR TRANSVERSAL EQUALIZERS

Among the many structures used for equalization the simplest is the transversal (tapped delay line or non recursive) equalizer shown in figure 9.8., and discussed in reference [5.7]. In such an equalizer, the current and past values r(t-nT) of the received signal are linearly weighted by equalizing coefficients (tap gains) C_n, and

summed to produce the output. If the delays and tap gain multipliers are analogue, the continuous output of the equalizer, z(t), is sampled at the symbol rate and the samples go to the decision device. In the commonly used digital implementation, samples of the received signal at the symbol rate are stored in a digital shift register (or memory), and the equalizer output samples are computed digitally, once per symbol according to
$z_k = \sum_{n=0}^{N-1} C_n r(t_0+kT-nt)$ where N is the number of equalizer coefficients, and t_0 denotes sample timing.

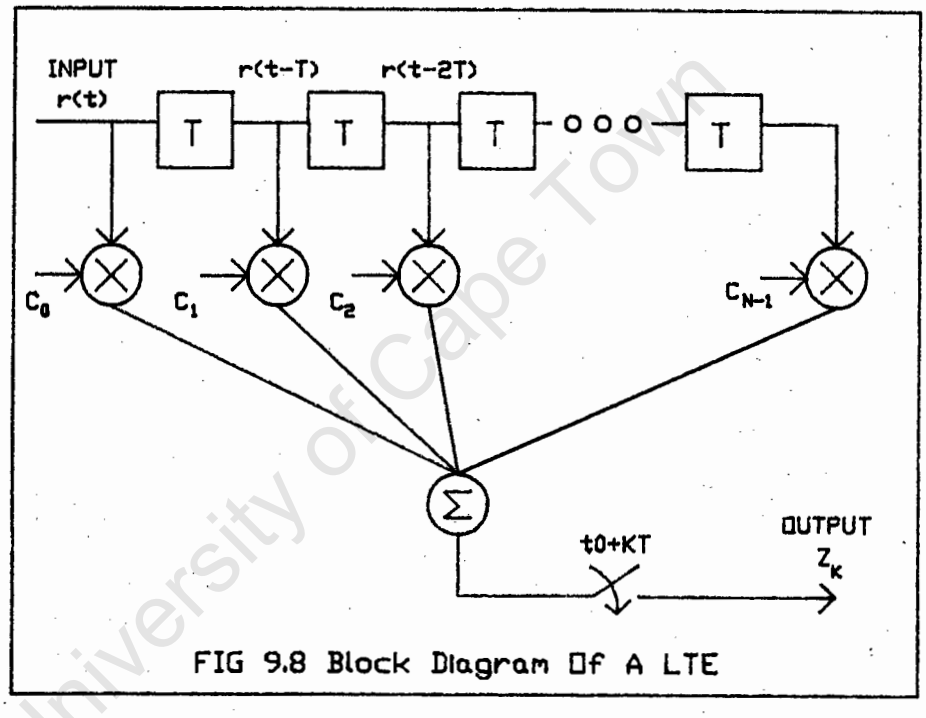

FIG 9.8 Block Diagram Of A LTE

The equalizer coefficients C_n, n=0,1,....,N-1 may be chosen to force the samples of the combined channel and equalizer impulse response to zero at all but one of the N T-spaced instants in the span of the equalizer. This is shown graphically in figure 9.9 and an equalizer based on this principle is known as a zero forcing (ZF) equalizer.

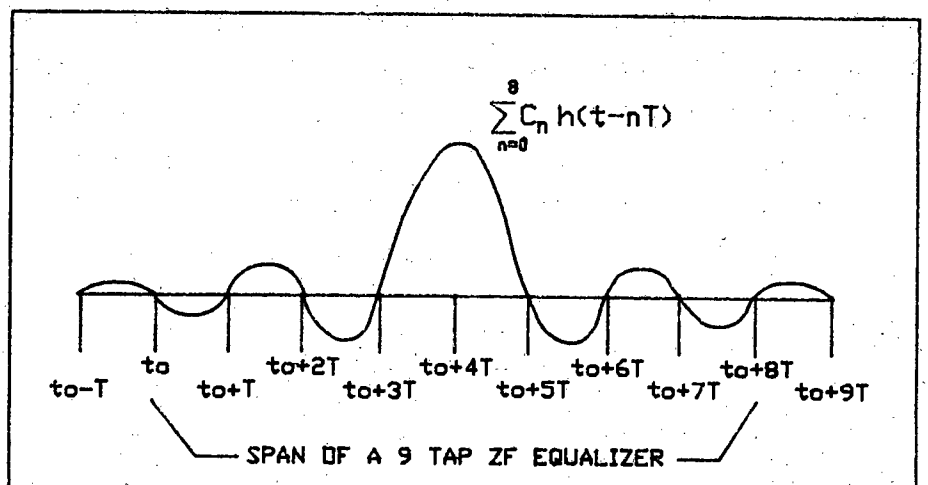

FIG 9.9 Channel Impulse Response With ZF Equalizer

If the number of coefficients of a ZF equalizer is increased without bound, an infinite length equalizer, with zero ISI at its output, would be obtained since it can be shown that an infinite length zero ISI equalizer is simply an inverse filter which inverts the folded frequency response of the channel. A finite length ZF equalizer approximates the inverse.

However the ZF criteria neglects the effects of noise, and also a finite length ZF equalizer is guaranteed to minimize the peak distortion or worst case ISI only if the peak distortion before equalization is less than 100%. In practice finite length LFE's have typically 5 or 7 taps and the ZF algorithm is used due to its simplicity of implementation. The ZF algorithm will be discussed again in more detail under DFE's.

The LFE can easily be extended to the bi-dimensional case (2 in the case of QAM or MSK) as shown in figure 9.10. The bi-dimensional equalizer is generally referred to as a complex equalizer as it is most easily explained

$e(k)=e_r(k)=je_i(k)$, where e_r and e_i are are the differences between Z_r and Z_i and their desired values. The update method is similar to the simple LFE except that all variables are complex valued $C_n(k+1)=C_n(k).\Delta e_k Y^*(t_0+kT-nT)$ where Y^* is the complex conjugate of Y.

The structure of the equalizer linear section affects the receiver noise band. For an equalizer with forward taps only the received noise can be split into two components, the inphase n_x and the quadrature n_y (ie a bi-dimensional LFE). Figure 9.12 shows the situation.

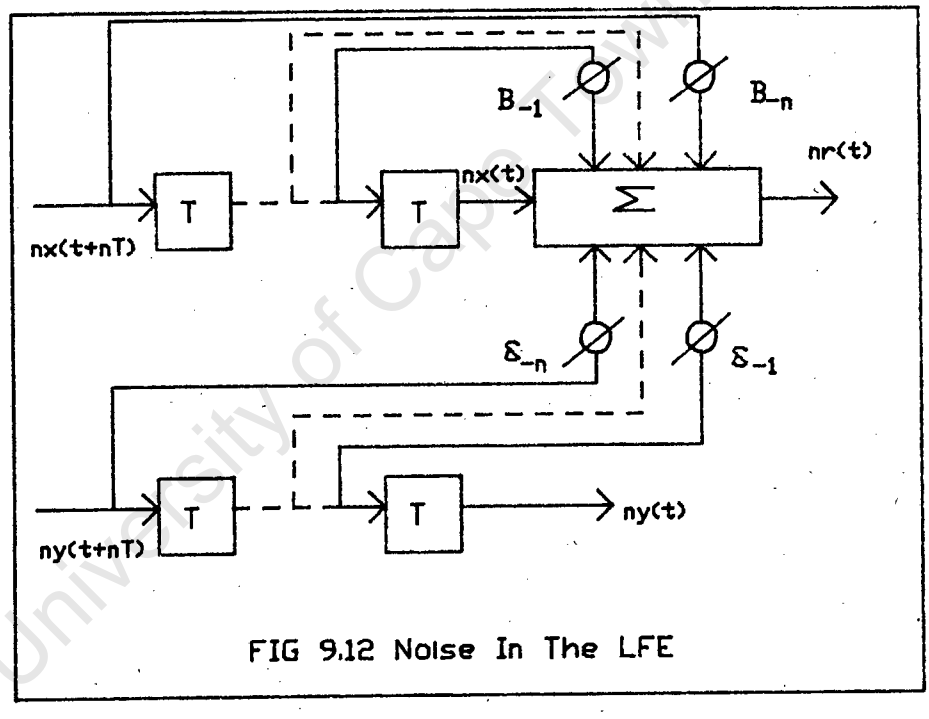

FIG 9.12 Noise In The LFE

Reference [5.3] goes on to show that the degradation introduced by the forward cells in terms of N is given by

$\Delta|N|_{dB}=10\log_{10}[1+\sum_{j=1}^{n}(B^2_{-j}+\delta^2_{-j})]$

Thus there exists a trade off between approximation of the inverse channel transfer function and the noise degradation.

9.4.2 DECISION FEEDBACK EQUALIZERS

This non-linear equalization technique is based on direct cancellation of the intersymbol interference from previously detected symbols and is particularly useful for channels with severe amplitude distortion. References [5.1], [5.3], [5.7], [5.10], [5.13], and [5.15] discuss theoretical and practical considerations of this type of equalizer. Figure 9.13 shows an example of a one-dimensional decision feedback equalizer (DFE) with a single input, x_{k-n}. The equalized signal, r_k, is the sum of the outputs of the forward and feedback parts of the equalizer. The forward part is like the linear transversal equalizer discussed in section 9.4.1.

Decisions made on the equalized signal are fed back via a second transversal filter (the bottom part of figure 9.13). The forward coefficients, the B's, and the feedback coefficients, the Y's, may be adjusted simultaneously to minimize the mean square error (MSE). The update equation for the forward coefficients is the same as for the linear equalizer. The feedback coefficients are adjusted according to

$$Y_m(k+1)=Y_m(k)+\Delta e_k \hat{a}_{k-m} \qquad m=1,.....,M$$

where $\hat{a}_k$ is the kth symbol decision, $Y_m(k)$ is the mth feedback coefficient at time k, and there are M feedback coefficients in all.

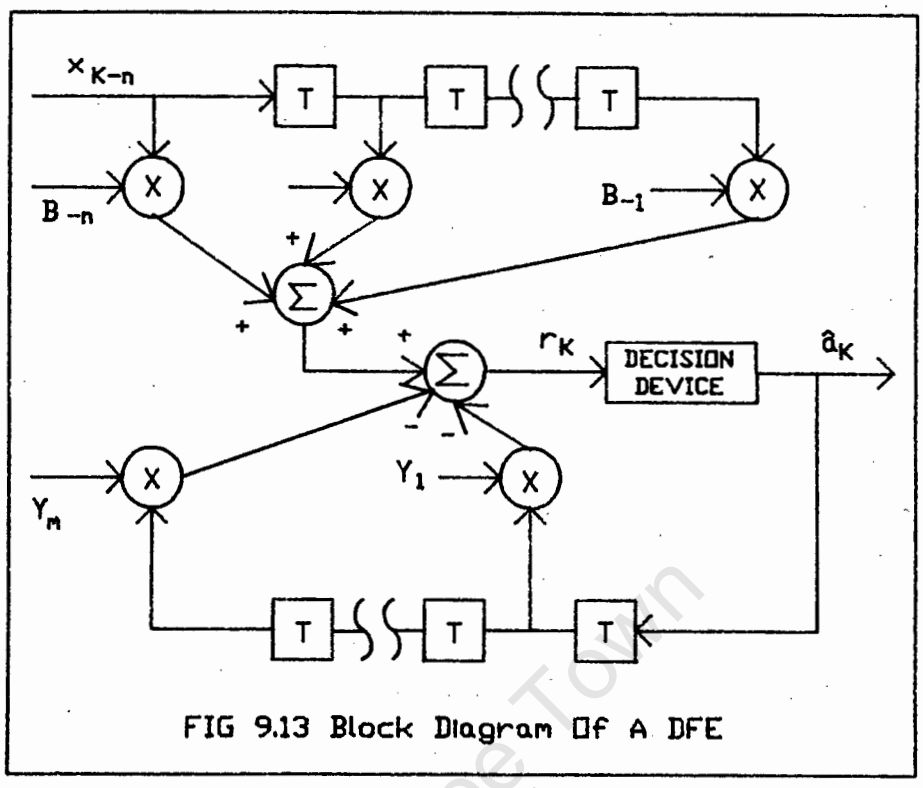

FIG 9.13 Block Diagram Of A DFE

In practice DFE's used in digital radio systems typically comprise one or two feedback taps and two or three forward taps. This combination gives good performance against minimum phase fades, but in non-minimum phase fades its behavior is similar to a linear equalizer.

The equalized signal can be written as

$$r_k = x_k - \sum_{j=1}^{n} B_{-j} x_{k+j} - \sum_{j=1}^{m} Y_j a_{k-j}$$

which can be rewritten as

$$r_k = \sum_i \lambda_i a_{k-i} + \sum_{j=1}^{n} B_{-j} \sum_i \lambda_{i+j} a_{k-i} + \sum_{j=1}^{m} Y_j a_{k-j}$$

(with $x_k = \sum_i \lambda_i a_{k-i}$), and finally by reversal of the summation order in the second term of the expression, the coefficient of the ith interfering symbol in the general expression of r_k may be isolated obtaining

$$r_k = \sum_i (\lambda_i + Y_i + \sum_{j=1}^{n} B_{-j} \lambda_{i+j}) a_{k-i}$$

Interpreting the meaning of the last expression it can be seen that

-term λ_i represents the interfering contributions due to the distortion whose index i varies (at least in theory) from $-\infty$ to $+\infty$.
-term Y_i represents the corrective effect of a generic postcursor tap and index i varies from 1 to m.
-the corrective action of precursors is different :the terms $\sum_{j=1}^{n} B_{-j}\lambda_{i+j}$ shows that the action is extended to all interfering symbols (including postcursors). Therefore index i varies from $-\infty$ to $+\infty$.

The zero forcing principle requires the cancellation of n+m interfering symbols, leading to a system of n+m linear equations. By varying index i from -n to +m (i=0)
$\lambda_i+Y_i+\sum_{j=1}^{n} B_{-j}\lambda_{i+j}=0$

Better performance of the equalizer can be achieved if the tap gains are adjusted to minimize the mean square error (MSE) at the output, defined as the sum of the intersymbol interference and noise powers. This forms the basis for the "stochastic gradient" algorithm or "least mean square" algorithm (LMS). The MSE may be envisioned as an N dimensional parabuloid (punch bowl) with a bottom or minimum. The adjustment to each tap gain is in a direction opposite to an estimate of the gradient of the MSE with respect to that tap gain. The idea is to move the set of equalizer coefficients closer to the unique optimum set corresponding to the minimum MSE.

Instead of the true gradient of the MSE $\partial E[e^2_k]/\partial C_n(k)$, a noisy but unbiased estimate $\partial e^2_k/\partial C_n(k)=2e_k r(t_0+kT-nT)$ is used. Thus the tap gains are updated according to
$C_n(k+1)=C_n(k)-\Delta e_k r(t_0+kT-nT) \qquad n=0,1,.....,N-1$

In the case of the complex DFE there are two information signals x(t) and y(t) and the distortion can be written as
$x_k=\sum_i \lambda_i a_{k-i}+\mu_i b_{k-i}$

$$y_k=\xi_i\lambda_i b_{k-i}-\mu_i a_{k-i}$$

where a_k and b_k represent the symbols transmitted on the two channels in quadrature and λ_i and μ_i are the co-channel and quadrature interference coefficients respectively. Hence in addition to extending the basic equalizer structure to both channels, it is necessary to cancel the quadrature intersymbol interference by the addition of cross taps. By so doing the expressions for the equalized signals become

$$r_{x,k}=\xi_i(\lambda_i+Y_i+\xi_{j=1}^{m}B_{-j}\lambda_{i+j})a_{k-i}+\xi(\mu_i+V_i+\xi_{j=1}^{n}\delta_{-j}\mu_{i+j})b_{k-i}$$

$$r_{y,k}=\xi_i(\lambda_i+Y_i+\xi_{j=1}^{m}B_{-j}\lambda_{i+j})b_{k-i}+\xi(\mu_i+V_i+\xi_{j=1}^{n}\delta_{-j}\mu_{i+j})a_{k-i}$$

9.4.3 FRACTIONALLY SPACED EQUALIZERS

A fractionally spaced transversal equalizer (FSE) is shown in figure 9.14. The delay line taps of such an equalizer are spaced at an interval τ which is less than, or a fraction of, the symbol interval T. This type of equalizer is discussed in references [5.7], [5.13], and [5.18].

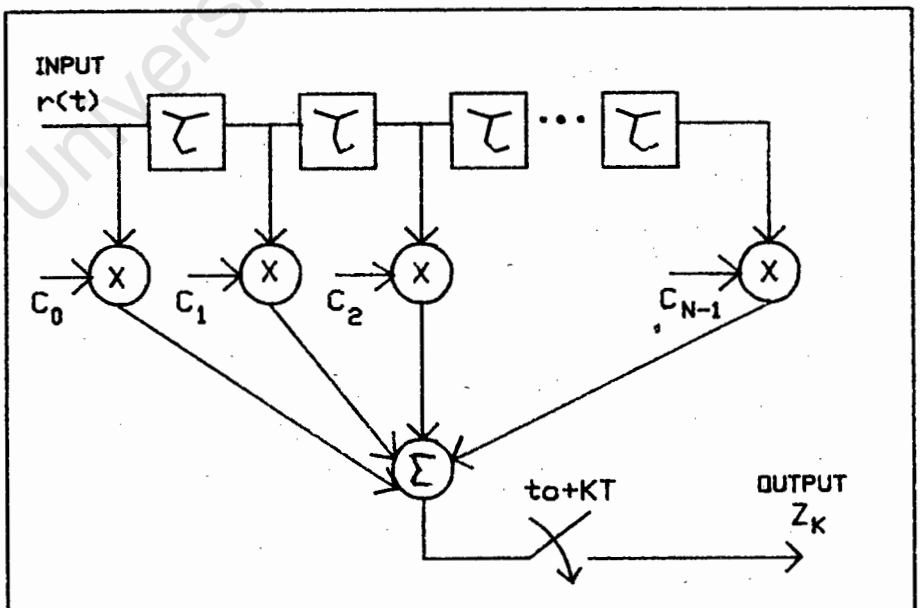

FIG 9.14 Block Diagram Of A FSE

The tap spacing τ is typically selected such that the bandwidth occupied by the signal at the equalizer input is $|f| < 1/2\tau$ *ie* τ spaced sampling satisfies the sampling theorem. In a analogue implementation, there is no other restriction on τ, and the output of the equalizer can be sampled at the symbol rate. In a digital implementation must be KT/M, where K and M are integers and M>K (in practice it is convenient to choose τ=T/M where M is a small integer *eg* 2). The received signal is sampled and shifted into the equalizer delay line at a rate M/T and one output is produced each symbol interval.

In general the equalizer output is given by

$$z_k = \sum_{n=0}^{N-1} c_n r(t_0 + kT - nKT/M)$$

The coefficients of a KT/M equalizer may be updated once per symbol based on the error computed for that symbol, according to

$$c_n(k+1) = c_n(k) - \Delta e_k r(t_0 + kT - nKT/M)$$

Because of the increased sampling rate fractionally spaced equalizers can synthesize a combination of the characteristics of adaptive matched filters and T spaced equalizers. This results in greater efficiency, within the constraints of the length of the equalizer and the associated delay. A T spaced equalizer with symbol rate sampling at its input cannot perform matched filtering. An FSE can effectively compensate for more severe delay distortion and deal with amplitude distortion with less noise enhancement than a T equalizer , as explained in reference [5.7].

9.4.4 VARIATIONS OF TIME DOMAIN EQUALIZERS

The types of time domain equalizers discussed so far are a base for numerous perturbations, both with regard to hardware considerations and software considerations. The

theory and construction of these various equalizers cannot be mentioned here but some references are given below.However the performance of some of these systems will be discussed later when the choice of equalizer for MSK is made.

As far as control algorithms are concerned; reference [5.7] introduces the ZF and LMS algorithms, as well as fast converging algorithms such as the Kalman and Fast Kalman. Reference [5.8] discusses several variations of the Recursive Least Squares algorithm. Reference [5.9] compares the performance characteristics of the differential (DSD) and LMS algorithms, both based on the method of steepest descent, and the linear random search (LRS) algorithm, based on a random search procedure derived from the Darwinian concept of "natural selection".

Reference [5.10] discusses the implementation of a DFE using a fractionally spaced forward filter and a T-spaced feedback filter, and applying an estimated-gradient algorithm. Reference [5.11] describes a five tap baseband complex analogue equalizer of the form shown in figure 9.11 and with a ZF control algorithm. Reference [5.12] compares the effectiveness of T-spaced LTE and DFE equalizers on staggered QPSK and QPR modems. Reference [5.13] describes a 1 dimensional fractionally spaced DFE and discusses the advantages of using a fast recursive least squares (FRLS) algorithm over the LMS. Reference [5.14] introduces a slightly modified LTE called a cascaded finite impulse response (FIR) filter, and uses a newly introduced algorithm called the constant modulus algorithm (CMA).

9.5 AUTOMATIC SYNTHESIS AND ADAPTIVE EQUALIZATION

Before regular data transmission begins, automatic synthesis of the ZF or LMS equalizers for unknown

channels, which involves the iterative solution of one of the previously mentioned sets of simultaneous equations, may be carried out during a training period. In some cases the adaptive equalizers are required to bootstrap in a decision directed mode without the help of a training sequence. This type of equalizer is discussed in reference [5.3].

During a training period, a known signal is transmitted and a synchronized version of this signal is generated in the receiver to acquire information about the channel characteristics. The training signal may consist of periodic isolated pulses or a continuous sequence with a broad, uniform spectrum such as the widely used maximum-length shift register or pseudo noise (PN) sequence. The latter has the advantage of much greater average power, and hence a larger received signal to noise ratio for the same peak transmitted power. The training sequence must be at least as long as the length of the equalizer so that the transmitted signal spectrum is adequately dense in the channel bandwidth to be equalized.

Given a synchronized version of the unknown training signal, a sequence of error signals $e_k=Z_k-x_k$ can be computed at the equalizer output and used to adjust the equalizer coefficients to reduce the sum of the squared errors as shown in figure 9.15.

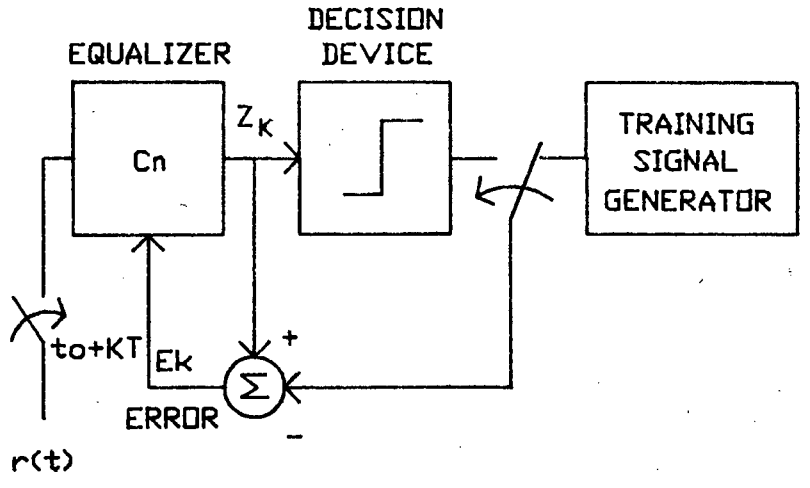

FIG 9.15 Automatic Adaptive Equalization

After the initial training period (if there is one), the coefficients of an adaptive equalizer may be continually adjusted in a decision directed manner. In this mode the error signal $e_k=Z_k-\hat{x}_k$ is derived from the final (not necessary correct) receiver estimate $\hat{x}_k$ of the transmitted sequence x_k. In normal operation, the receiver decisions are correct with high probability so that the error estimates are correct often enough to allow the adaptive equalizer to maintain precise equalization. Moreover a decision directed adaptive equalizer can track slow variations in the channel characteristics or linear perturbations in the receiver front end, such as slow jitter in the sampler phase.

The larger the step size, the faster the equalizer tracking capability. However a compromise must be made between fast tracking and the excess mean square error of the equalizer. This excess MSE, caused by tap gains wandering around the optimum settings, is directly proportional to the number of equalizer coefficients, the

step size, and the channel noise power. In practice, the value of the step size is selected for fast convergence during the training period and then reduced for fine tuning during the steady state operation (or data mode).

CHAPTER 10

CHOICE OF ADAPTIVE EQUALIZER

This chapter investigates various equalizer designs, both from a hardware point of view and from a control algorithm point of view, with the objective of designing an optimum equalizer for a MSK system, optimum meaning the best compromise between criteria such as construction cost, ease of implementation, circuit complexity, and performance improvement. The results of equalizers used in other modulation systems, information regarding MSK and anomalous propagation, as well as proposed system specifications are taken into account when making this choice.

Although the majority of discussions which follow are with specific reference to MSK the same arguments can be used in the choice of an adaptive equalizer for any other system.

It should be remembered that the potential performance theoretically available with various equalization structures is difficult to achieve in practice due to numerous factors which limit the efficiency. In general the difference between theory and practice increases in proportion with the equalization complexity. This consideration (together with considerations such as circuit complexity and cost) is very important in the choice of an optimal equalizer structure to be employed in an actual system, in relation to the performance objectives envisaged.

Assuming a linear channel the following subdivision of limiting factors of equalization gain are suggested :-

a) Disturbances that are not correlated with the signal (thermal noise and ACI).

b) Residual ISI (channel shaping imperfections, and residual equipment mis-alignment).

c) Imperfections in the mo-demodulation process.

d) Insufficient adaptivity (imperfections or excessive simplification in the equalizer design algorithms and control procedures).

The last point is the most difficult to comment on as it involves a great number of examples strongly connected with factors of a practical nature, but it is discussed in connection with practical system results.

10.1 THERMAL NOISE AND ACI

The overall performance depends both on the outage probability due to selectivity, P_s, and on the outage probability due to the thermal noise threshold, P_t, so that the relative overall probability of outage, P_{or}, may be approximately expressed by

$P_{or}=[P_t^{\alpha/2}+P_s^{\alpha/2}]^{2/\alpha}$ (with reference [5.3] quoting $\alpha=1.5$)

It is assumed that uncorrelated disturbances are represented only by thermal noise and adjacent channel interference. It is shown in the reference that for single reception

$P_t=1/m_0^2+\alpha_0/K_0$ where m_0= flat fade and α_0= threshold S/N of the system for a BER=10^{-3}.

Regardless of the growing complexity of the equalizer, the overall relative outage probability P_{or} cannot get any lower than value P_t which is a function of the fade margin and the discrimination with respect to adjacent interference (K_0/α_0) available in the system.

Using the fade margin formula stated in chapter 3, with A=1, B=0.5, d=10km and a 99.99% service reliability gives a fade margin of 15.38 dB's. It appears from the graph that P_t is indeed the limiting factor, and so little benefit will be obtained in producing too complicated an equalizer. The affects of thermal noise on the system will be discussed again later.

As far as ACI is concerned, 23 GHz is a new allocation for South Africa and so the effects of ACI will be minimal at this point in time.

10.2 RESIDUAL ISI

Reference [5.3] introduces various distortions into its computer simulations to cover ISI due to improper shaping of the transmission channel, and from residual lack of alignment and equalization in the equipment. This interference, collectively labelled D(x), is of the form

$D(x)=(1+2kx).\exp[-j\pi x^2(T_1-8/3T_2x)]$ with

T=symbol duration

L=linear amplitude difference=20log((1+k)/(1-k))

x=normalized frequency shift from midband ($x=\Delta ft$)

k=constant associated with climatic conditions

T_1=linear component of the group delay in the band $\pm 1/2T$

T_2=parabolic component of the group delay in the band $\pm 1/2T$

The figures in the reference demonstrate the amount of acceptable residual mis-alignment or mis-equalization for the various modulation methods and relate the values L,T1,and T2 in coincidence with an impairment of P_s equal to 20 %. Table 10.1 summarizes the results.

TABLE 10.1 Linear Distortion Components
For A Ps Increment Of 20%

SYSTEM	L (dB)	T1	T2
4 PSK	4	0.36	0.4
QPRS	5	0.45	0.22
8 PSK	1.8	0.25	0.18
16 QAM	1.3	0.2	0.11

The effect of linear distortion in limiting the equalizer performance increases as the equalization gain increases. Figure 10.2 shows the equalization gain, $G=P_{so}/P_s$, for 16 QAM modulation as a function of the linear component of the amplitude distortion with DFE type equalizers having no feedback cells (IPOST=0), one feedback cell (IPOST=1), and two feedback cells (IPOST=2). It can be seen from figure 10.2 that the variation of efficiency increases with equalizer complexity.

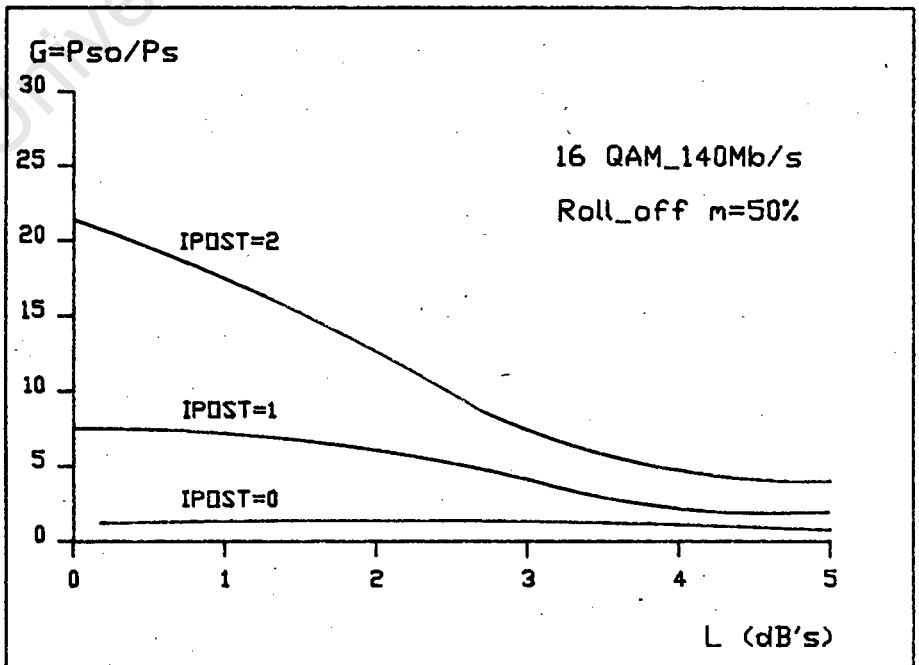

FIG 10.2 Equalization Gain As A Function Of The Linear Amplitude Distortion L

10.3 MODEM IMPERFECTIONS

Imperfections in the mo-demodulation process may include modulation errors, decision threshold errors, and imperfections in carrier and timing extraction circuitry. Obviously modulation errors and decision errors become worse with growing modulation complexity.

Reference [5.3] shows graphs of how the imperfections in carrier and timing extraction deteriorates as the modulation complexity grows. The cumulative effect on the error rate due to the various imperfections being present simultaneously (k=1 ie 4% modulation error, 2.5% decision threshold error, 10% error on symbol estimates, and 1% carrier synchronizer noise bandwidth) is presented in table 10.2 which shows the BER multiplying factor, for the various modulation methods, with respect to the theoretical performance.

TABLE 10.2 Error Rate Multipling Factor, BER(K=1)/BER(K=0), Due To Modemodulation Imperfections (Mo=3.5dB's)

4 PSK	8 PSK	QPRS	16 QAM
3	8.5	9.5	22.5

With a newly designed MSK system it must be expected that design imperfections will be present and a BER multiplying factor of 6 is not unreasonable.

10.4 OUTAGE PROBABILITY CONSIDERATIONS

The absolute outage probability is required to be known in order to decide what performance improvement is necessary from the adaptive equalizer. The absolute outage probability may be directly calculated once the relative probability P_{or}, mentioned earlier, has been determined, since the occurrence statistics of the propagation phenomenon are known. Such statistics are influenced by various parameters related to the hop.

The absolute outage probability is given by the product of P_{or} and the multipath occurrence probability ie $P_{out}=\mu P_{or}$. For the occurrence coefficient, μ, one can refer to the known semi-empirical formula provided by CCIR Rep-3393 valid for the multipath occurrence probability in the worst month ie $\mu=kQf^{B}D^{C}$ with

k=climatic factor
Q=geographic factor
f=link frequency in GHz
D=hop length in km

Factor k and exponents B and C depend on the location of the link; they are classified in terms of the most representative geographic and climatic areas as shown in table 10.3.

TABLE 10.3 Regional Variation Of k,B And C

CLIMATE ZONE	k	B	C
JAPAN	0.97exp-9	1.2	3.5
EUROPE (N-W)	1.4exp-8	1	3.5
UNITED STATES			
-equatorial	1.2exp-6	1	3
-subtropical	9exp-7	1	3
-continental	6exp-7	1	3
-polar	3exp-7	1	3

Coefficient Q, generally comprised in the interval $1/4 \leqslant Q \leqslant 4$, depends on the geometrical characteristics of the terrain and reaches its maximum value for links in proximity of the coastline or over the sea.

The value μ can be generally confidently determined experimentally, not by using outage measurements (which generally involve extremely low time percentages and therefore are easily lacking in precision) but on measurements of the received signal strength. Figure 10.3 provides the μ values as a function of the hop length D for North West Europe at 4,7 and 11 GHz.

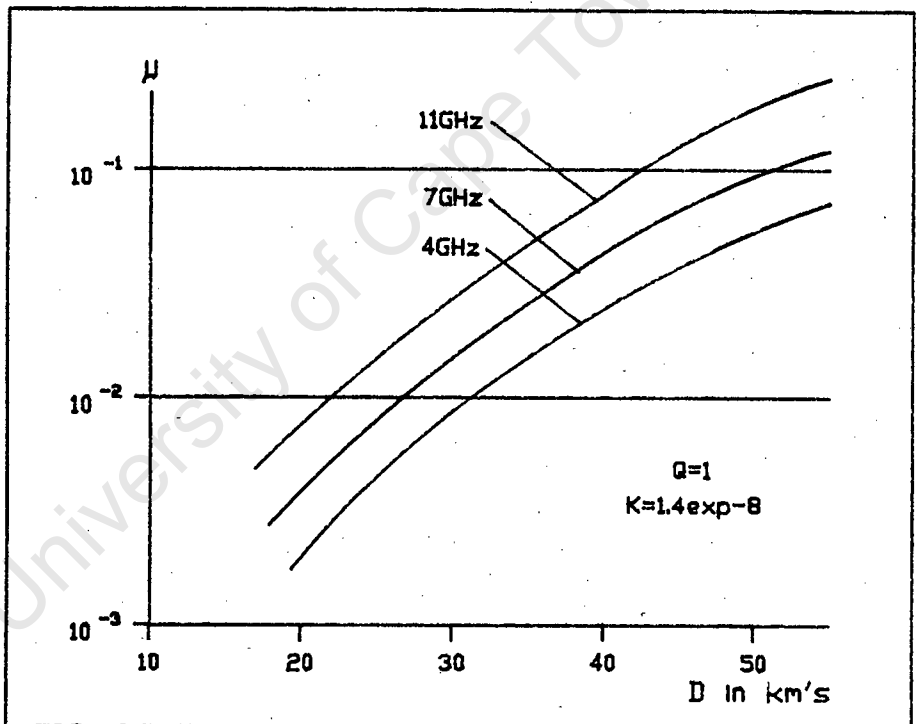

FIG 10.3 Occurance Coefficient μ For N-W Europe

It may not be possible to determine the chances of minimum phase dispersion or non minimum phase dispersion, but the procedure for the determination of the relative probability can also be applied to the case of non-minimum phase dispersions, assuming the statistics

utilized for the various parameters are retained in the case where τ is negative.

A more general equation for outage, taken from reference [5.3], is

$P_{out} = \mu[\eta P_{or}(+) + (1-\eta)P_{or}(-)]$

where η represents the probability of the events with $\tau>0$. Conflicting data exists in the literature for the value of η . While η =50% could be pessimistically assumed for single reception most recent experiences seem to confirm values of η =95%, especially in the case of diversity systems.

Not enough information about the proposed system is available to use the previously mentioned formulae , and although a rough outage value was obtained using Rummlers model statistics (approximately 1612 seconds), it is easiest to use the simplified formula for predicting the multipath fading outage introduced in reference [4.6]. It is proposed that in band amplitude dispersion probability on a radio path is a product of the multipath fade occurrence factor and the joint probability of Raleigh distributed random variables which are located at both ends of the radio transmission band. The final expression is

$P_{out}=(2.5*10^{-3})C(\Delta f D^2/f)[r_0^2/(r_0^2-1)^2]$ with

D=path length in miles

f=radio frequency in GHz

Δf=transmission bandwidth in GHz

C=terrain factor (1=average, 4=over water, 1/4=mountains and dry regions)

r_0=maximum ratio of R1 to R2 where R1 and R2 indicate the amplitude of two signals separated by Δf.

Reference [3.2] gives the maximum change of inband amplitude as $2.85\Delta f/f$

$=2.85*1.024*10^6/23*10^9$

=1.0127

If we consider average terrain a value of C=1 can be substituted into the above formula. The proposed system is to operate over an approximate distance of 10 km's (D=6.25 miles), have a trasmission bandwidth of 1.026MHz ($f=1.026*10^{-6}$), have a transmission frequency of 23GHz ($f=23*10^{9}$), and r_0 has been calculated above as 1.0129. Thus P_{out} will be $6.82*10^{-4}$, which works out as 1769 seconds in a heavily fading month, and renders the system unacceptable for a performance reliability of 99.99%.

Reference [3.2] gives some further insight into how multipath propagation may affect the link. It analyses LOS microwave links with the aid of a piece-wise linear approximation of the atmospheric index of refraction. As explained in an earlier chapter, no deep fading will occur if the path is short enough. From graph 3.4 (which is computed for several frequencies on a 22.8 mile hop in New Jersey) it can be seen that at 23 GHz Lo is 5.24 km, meaning that no deep fading will occur on links shorter than this and there will rarely be deep fading on links less than 10 km's. The maximum echo delay on a 5 km hop is $1.63*10^{-11}$ seconds which is 0.114% of the propagation time for a 70 MHz IF signal.

The above results seem to indicate that the system degradation on the proposed link is such that an adaptive equalizer is necessary but that it may not be necessary to resort to complex configurations to obtain the desired performance specifications.

10.5 HARDWARE CONSIDERATIONS

The next choice to be made is the class of equalizer. Space diversity systems (and frequency diversity systems) can be very effective but they are generally too expensive, and cannot easily be incorporated into existing

systems. It is also impractical in this case involving a 60 cm antenna which is to be roof mounted. Thus this dissertation will only discuss time domain and frequency domain equalizers.

The main disadvantage of bandpass equalization is that it is limited to correcting the amplitude versus frequency response only and has little effect if the distortion is not of the minimum phase type ($\tau<0$). Figure 10.4, taken from reference [5.3], shows the signatures for $\tau>0$ and $\tau<0$ for a 16 QAM 140 Mb/s system using a 5 frequency spectrum analyzer notch equalizer. Observe the very modest gain with respect to the unequalized performance that can be obtained in the case of non-minimum phase distortions. With slope equalizers the improvement may only range from 3 to 4 times , depending on the type of modulation and again is even less in the case of non-minimum phase distortions. Figure 10.5, taken from reference [5.3], shows typical signatures for $\tau>0$ and $\tau<0$ for 70 Mb/s 8 PSK modulation.

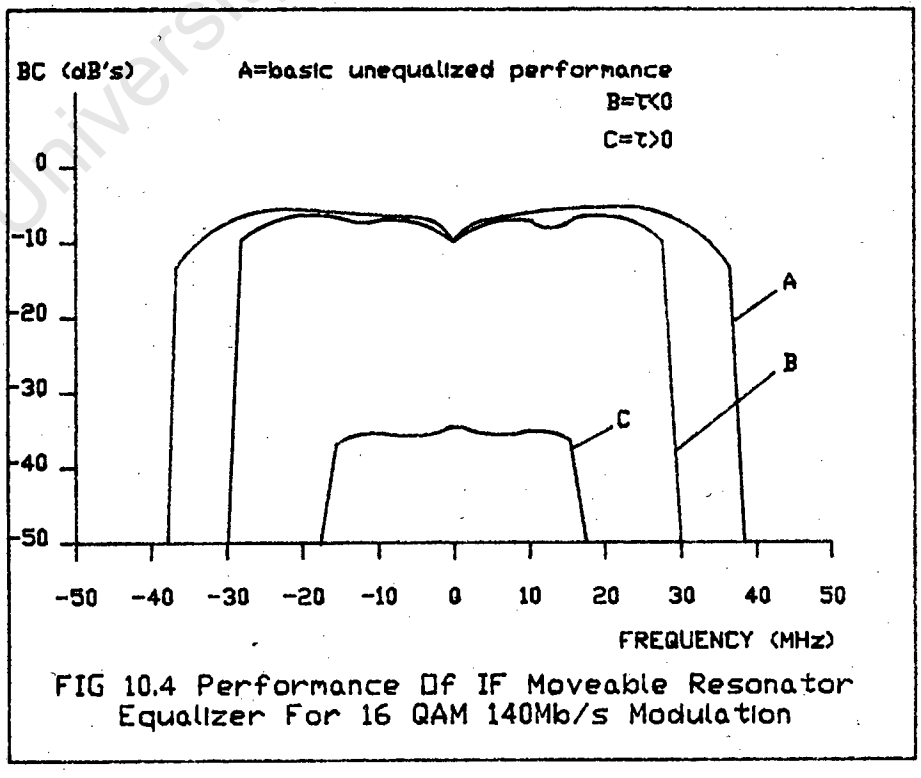

FIG 10.4 Performance Of IF Moveable Resonator Equalizer For 16 QAM 140Mb/s Modulation

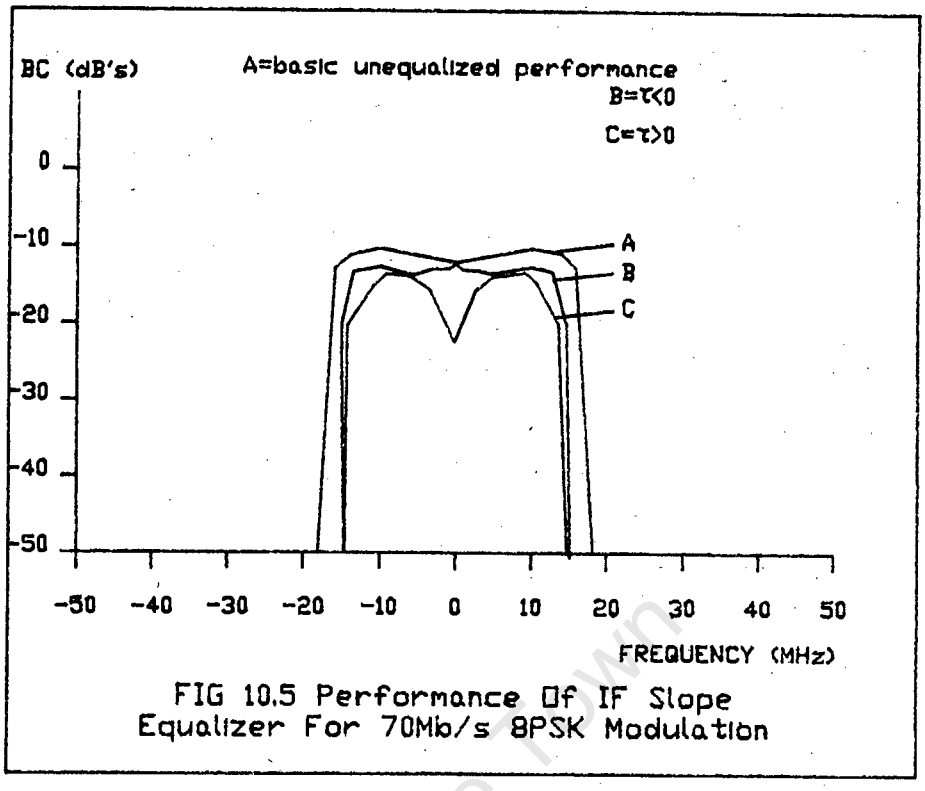

FIG 10.5 Performance Of IF Slope Equalizer For 70Mb/s 8PSK Modulation

The main advantage of operating in the frequency domain is circuit simplicity. The control system will only have to be capable of performing simple analogue addition and subtraction operations, and in such cases it will include only operational amplifiers. In other cases the control strategy might require a more complex elaboration, requiring a microprocessor system.

The advantage of time domain equalizers over frequency domain equalizers is the ability to compensate for both amplitude and phase distortions simultaneously by acting in a more synthetic way directly on the ISI. Reference [2.7] shows that MSK suffers less from crosstalk than other constant envelope modulation schemes but since this system in unlikely to suffer from deep fading it appears as if time domain equalization is the natural choice (and intuitively to do complex time domain equalization since MSK is a quadrature modulation scheme).

Having decided on time domain equalization the next topic of discussion is the choice of LTE's, DFE's, FSE's, and variations thereof. Obviously LTE's are the most simple form of equalizers as the others are merely extensions thereof which operate with postcursors as well as precursors. LTE's cannot however be extended infinitely (to provide an inverse channel characteristic) first because of practical reasons, and secondly because of the noise degradation introduced by the forward cells.

Better performance will be achieved, as far as non-minimum phase distortions are concerned, if the overall equalizer includes some forward stages since distortions with $\tau<0$ tend to cause ISI with a prevalence of precursors. Figure 10.6, taken from reference [5.3], shows the behavior of P_s (dispersive outage probability) for $\tau>0$ and $\tau<0$, for structures which have backward cells only ie with IPRE=0. As expected the gain obtained for $\tau<0$ (with respect to the basic performance corresponding to IPRE=IPOST=0) is very modest. On the other hand with balanced structures it is possible to obtain good equalization even for $\tau<0$, as depicted in figure 10.7, taken from reference [5.3]. These structures clearly provide better performance but have higher circuit complexity especially when expanded to the complex form.

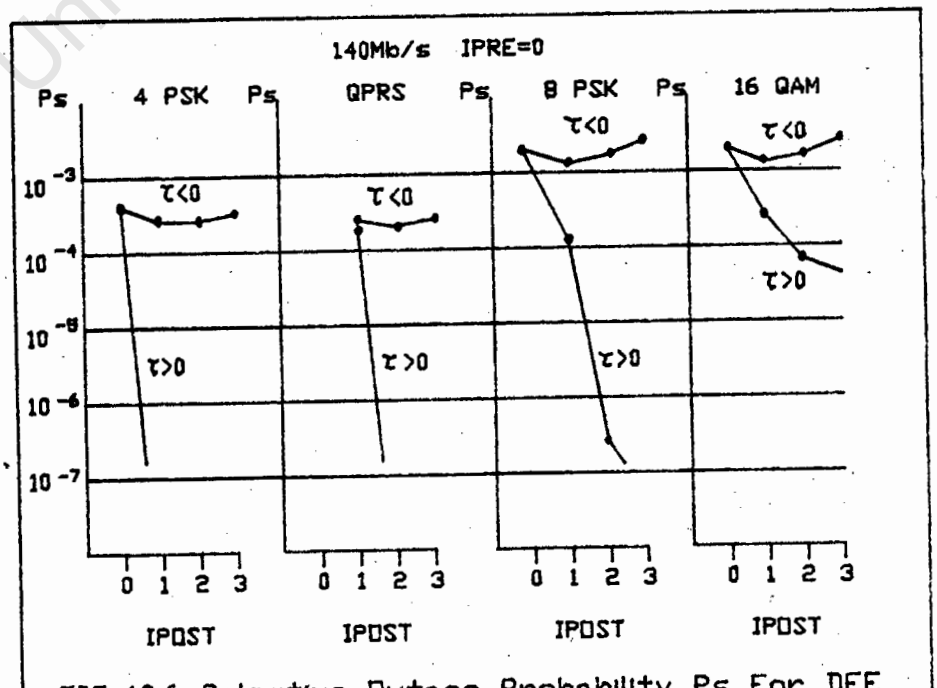

FIG 10.6 Selective Outage Probability Ps For DFE Equalizers As A Function Of The Cell Number (IPOST)

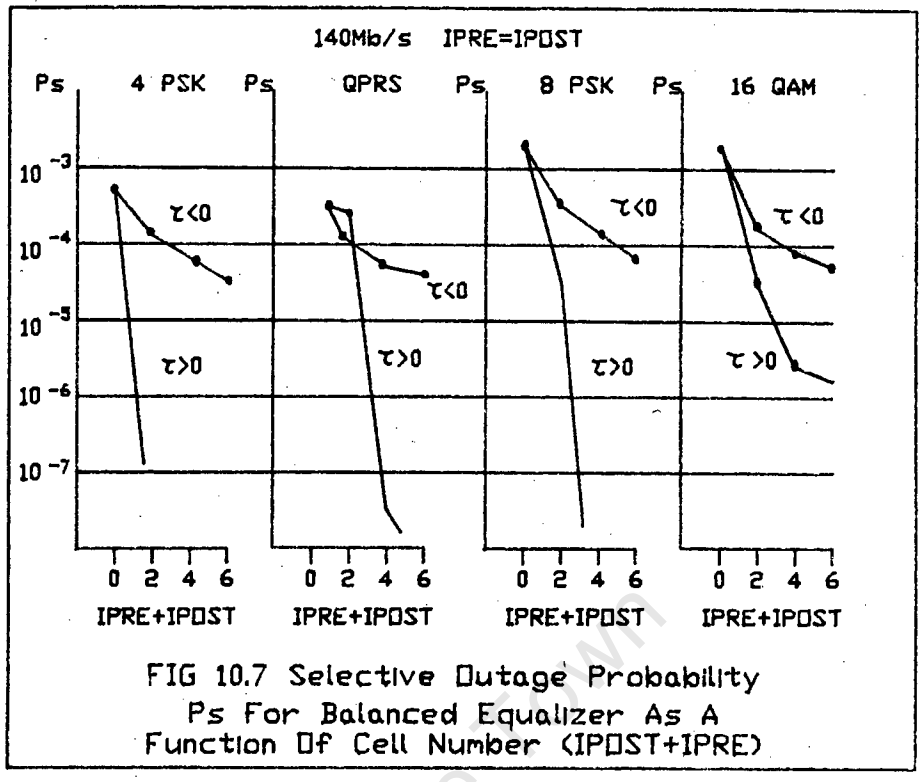

FIG 10.7 Selective Outage Probability Ps For Balanced Equalizer As A Function Of Cell Number (IPOST+IPRE)

With a DFE the ability of the feedback section to cancel the ISI, because of a number of past symbols, allows more freedom in the choice of coefficients of the forward section. The combined impulse response of the channel and the forward section may have non zero samples following the main pulse. In other words the forward section of a DFE need not approximate the inverse of the channel characteristics, so avoiding excessive noise enhancement and sensitivity to sampler phase.

A disadvantage of DFE's is error propagation. When a particular incorrect decision is fed back, the DFE output reflects this error during the next few symbols as the incorrect decision traverses the feedback delay line. Thus there is a greater likelihood of more incorrect decisions following the first one.

The calculation of the effect of error propagation in the DFE becomes very complex as the number of taps and the number of possible modulation states grows, so that it is

generally considered sufficient to determine an upper limit to the error probability in the presence of error propagation. The simplified formula which is derived in reference [5.3] is stated below.

$P(E) < pL^m/[1+pL(L^m-1)/(L-1)]$

where L represents the number of states, p is the symbol error probability in the absence of feedback errors, and m the number of DFE taps. Consider the case of a two tap structure on a MSK system, then

$P(E) < p4^2/[1+p^4(4^2-1)/3]$

$P(E) < 16p$

Clearly it becomes advantageous as far as error propagation is concerned to keep the tap number as low as is tolerable (to obtain satisfactory performance improvement).

Fortunately the error propagation in a DFE is not catastrophic. Errors occur in short bursts which degrade performance only slightly.

Reference [5.12] contains computer simulations of a SQPR system with a DFE. It shows that choosing 3 forward taps provides a large range of sample time variations over which the S/MSE is near its maximum, although this maximum is only slightly higher than with two forward taps. As the number of forward taps gets smaller the sensitivity to synchronization error increases. The reference also suggests 5 or 6 feedback taps as the optimum value.

Equalization gains (P_{SO}/P_S), calculated in the two cases of minimum and non-minimum phase distortions, are summarized in tables 10.4, 10.5, and 10.6, for different system capacities and modulation schemes.

From the discussions and results presented to date it appears as if a complex DFE with 2 forward stages and 2

feedback stages will offer the necessary performance improvement necessary for the proposed system and have the advantage of relatively simple circuit complexity*.

With regard to FSE's, it would involve very little extra circuit complexity to have fractionally spaced forward delays, and as has been shown in reference [5.7], a FSE does not require a fixed receiver shaping filter before it which, although not too critical for MSK, will make implementation to receiver circuitry that much easier.

* Reference [5.15] shows graphically that increasing the number of feedback taps from 2 to 6 may only produce a 2 dB improvement. The average error burst length versus tap number relationship is also represented.

TABLE 10.4 Equalizer Gains For 35Mb/s System

G=Pso/Ps

35Mb/s bit rate 0.5 Roll off factor

Raised cosine shaping for total response system

COS(πfT) shaping for partial response systems

CONFIG. IPOST IPRE NTEQ-DIV	4 PSK		QPRS		8 PSK		16 QAM	
BASIC CONFIG.	(0,0,0-0)		(1,0,0-0)		(0,0,0-0)		(0,0,0-0)	
Sign of	+	−	+	−	+	−	+	−
Pso (10^{-6})	10.7		8	7.7	36		35	
(1,0,0-0) (1)	(∞)	1.3	1	1	14	1.3	7	1.3
(2,0,0-0) (1)	(∞)	1.4	(∞)	1.4	(900)	1.4	22	1.4
(1,1,0-0) (2)	(∞)	4	1.2	2.5	70	6	30	8
(2,2,0-0) (2)	(∞)	7	(1200)	5.2	(∞)	13	(400)	16
(0,0,11-0)(3)	4.2	0.9	3.5	0.7	3.8	2.3	4.7	2.7
(0,0,22-0)(3)	(∞)	0.4	(130)	0.3	(300)	1.1	(230)	1.5
(0,0,0-1) (4)	800		900		250		350	
(0,0,0-2) (4)	1000		1000		320		400	
(1,1,22-0)(5)	(∞)	1.2	(130)	0.4	(450)	4.6	(320)	7.7
(0,0,11-1)(5)	9000		11000		2500		4000	
(0,0,11-2)(5)	10000		12000		3000		5000	

(1) Baseband equalizer (only DFE)

(2) Baseband equalizer (DFE+LFE)

(3) IF equalizer

(4) Space diversity (ρs=0.8; Mo=35dB)

(5) Mixed configurations

TABLE 10.5 Equalization Gains For 140Mb/s Systems

G=Pso/Ps

140Mb/s bit rate 0.5 Roll off factor

Raised cosine shaping for total response system

COS(πfT) shaping for partial response systems

CONFIG. IPOST IPRE NTEQ-DIV	4 PSK		QPRS		8 PSK		16 QAM	
BASIC CONFIG.	(0,0,0-0)		(1,0,0-0)		(0,0,0-0)		(0,0,0-0)	
Sign of	+	−	+	−	+	−	+	−
Pso (10^{-6})	449		327	338	1470		1450	
(1,0,0-0) (1)	(∞)	1.3	1	1	14	1.3	7	1.3
(2,0,0-0) (1)	(∞)	1.4	(∞)	1.4	(900)	1.4	22	1.4
(1,1,0-0) (2)	(∞)	4	1.2	2.5	70	6	30	8
(2,2,0-0) (2)	(∞)	7	(1200)	5.2	(∞)	13	(400)	16
(0,0,11-0)(3)	3.8	1.2	1.8	0.4	5.3	2.3	6	3
(0,0,22-0)(3)	(∞)	0.4	(1800)	0.3	(2500)	1.1	(1000)	1.4
(0,0,0-1) (4)	95		100		40		27	
(0,0,0-2) (4)	140		140		95		100	
(1,1,22-0)(5)	(∞)	1.3	(1800)	0.4	(2800)	4.8	(1200)	6.6
(0,0,11-1)(5)	9000		900		350		100	
(0,0,11-2)(5)	1200		1200		900		170	

(1) Baseband equalizer (only DFE)
(2) Baseband equalizer (DFE+LFE)
(3) IF equalizer
(4) Space diversity (Qs=0.8; Mo=35dB)
(5) Mixed configurations

TABLE 10.6 Equalization Gains For 70Mb/s Systems
G=Pso/Ps

70 Mb/s bit rate 0.5 Roll off factor
Raised cosine shaping for total response system
COS(πfT) shaping for partial response systems

CONFIG. IPOST IPRE NTEQ-DIV	4 PSK		QPRS		8 PSK		16 QAM	
BASIC CONFIG.	(0,0,0-0)		(1,0,0-0)		(0,0,0-0)		(0,0,0-0)	
Sign of	+	−	+	−	+	−	+	−
Pso (10^{-6})	79		57	51	226		218	
(1,0,0-0) (1)	(∞)	1.3	1	1	14	1.3	7	1.3
(2,0,0-0) (1)	(∞)	1.4	(∞)	1.4	(900)	1.4	22	1.4
(1,1,0-0) (2)	(∞)	4	1.2	2.5	70	6	30	8
(2,2,0-0) (2)	(∞)	7	(1200)	5.2	(∞)	13	(400)	16
(0,0,11-0)(3)	3.4	1.2	3.2	0.8	4	2.1	6	2.2
(0,0,22-0)(3)	(∞)	0.4	(1000)	0.3	(1500)	1.1	(700)	1.4
(0,0,0-1) (4)	300		300		90		100	
(0,0,0-2) (4)	400		400		140		150	
(1,1,22-0)(5)	(∞)	1.2	(1000)	0.4	(1600)	4.7	(800)	7
(0,0,11-1)(5)	2000		2800		1600		1800	
(0,0,11-2)(5)	2400		3300		2000		2400	

(1) Baseband equalizer (only DFE)
(2) Baseband equalizer (DFE+LFE)
(3) IF equalizer
(4) Space diversity (Qs=0.8; Mo=35dB)
(5) Mixed configurations

10.6 CONTROL ALGORITHM CONSIDERATIONS

The next choice to be made is the choice of control algorithm. The ZF algorithm is the simplest to implement (particularly in high speed systems) even if in general not the best one, with the circuitry consisting mainly of logic gates and integrators. The ZF criterion does however neglect the effects of noise and so performance may degrade below acceptable limits in the presence of receiver noise. In addition a finite length ZF equalizer is guaranteed to minimize the peak distortion or worst case ISI only if the peak distortion is less than 100%.

The LMS algorithm is more robust in the presence of noise and large amounts of ISI, and superior to ZF in its convergence properties.

The LMS algorithm itself is not perfect and a severely distorted channel will cause the rate of convergence to be slower. There are algorithms which use a prefixed weighting matrix to transform the input signals to the equalizer tap gains so that they are approximately orthonormal resulting in all eigenvalues of the transformed equalizer covariance matrix being approximately equal and so lead to faster equalizer convergence. Reference [5.7] also explains bi-periodic and cyclic equalization algorithms which can be used to speed up equalizer convergence in the case where a PN training sequence which is equal to the time span of the equalizer is used.

Recursive least squares (RLS) algorithms are useful for rapidly tracking adaptive equalizers when neither the reference signal nor the input signal characteristics can be controlled. The Kalman algorithm on the other hand is one of the fastest algorithms available but has the disadvantage in that it requires an order of N^2 operations

per iteration for an equalizer with N coefficients. The Fast Kalman algorithm only requires N operations per iteration.

Simulation studies have reported the tendency of RLS algorithms implemented with finite precision to become unstable and adaptive filter coefficients to diverge. This appears to be due to the long term accumulation of finite precision errors. The Fast Kalman is the most prone to instability out of the RLS algorithms. Reference [5.13] does however show that a fast RLS algorithm with periodic restart yields superior performance to LMS in rapidly fading conditions, for a fractionally spaced DFE.

Table 10.7 compares the number of operations (multiplications and divisions) required per iteration, for T and T/2 spaced transversal equalizers of span NT seconds.

TABLE 10.7 Comparison Of Operations Per Iteration For Different Control Algorithms

ALGORITHM	No. of ops. per iteration	
	T Equalizer	$\frac{T}{2}$ Equalizer
LMS GRADIENT	2N	4N
KALMAN	$2N^2+5N$	$8N^2+10N$
FAST KALMAN	7N+14	24N+45
RLS LATTICE	15N-11	46N

The Fast Kalman is the most efficient type of RLS algorithms because of its speed of convergence and because of its tracking capability. However, compared to the LMS gradient algorithm the Fast Kalman algorithm is still about 4 times as complex for T equalizers and about 6 times for T/2 equalizers. The RLS lattice algorithm is still in contention due to its better numerical stability

and order-recursive structure, despite a two fold increase in computational complexity over the Fast Kalman. Since the proposed system has a low channel capacity severe channel distortion is unlikely and it would appear that the LMS algorithm is able to provide adequate stability and convergence whilst providing a large advantage as far as circuit complexity and computational complexity are concerned.

Due to the enormous advantage in circuit simplicity that the ZF algorithm has over the other algorithms it was decided to use a ZF algorithm on the proposed system and try to minimize the excess receiver noise which is the main disadvantage of the ZF algorithm.

For low BER's it can be assumed that the estimated signal of the equalizer, âk, is equal to the transmitted signal, ak, so it will not be necessary to have a training period. This makes the integration of the equalizer and existing receiver circuitry very much simpler.

CHAPTER 11

CONCLUSIONS AND RECOMMENDATIONS

The first eight chapters of this dissertation have given a background to digital microwave radio and to the MSK modulation technique, and have investigated the effects of non-linear propagation on the proposed microwave link. Chapter 9 has given a detailed breakdown of adaptive equalization and of the possible types of equalizers that could be implemented in the system in order to improve on performance and reliability. Finally chapter 10 has discussed the choice of adaptive equalizer based on criteria such as performance improvement, construction cost, ease of implementation, and circuit complexity. The recommendations for the proposed system are summarized below.

A space diversity system is not recommended as, although it is a very effective method, the cost and circuit complexity required compared to the performance improvement required is not justifiable. Secondly time domain equalization is advised since it is much more affective at correcting intersymbol interference (ie it corrects both amplitude and phase distortions) than frequency domain equalization, although the later is a simpler and cheaper method.

Since MSK is a quadrature modulation scheme complex time domain equalization is recommended to enable the correction of intersymbol interference on both the I and Q channels, as well as correction of crosstalk between the I and Q channels.

Chapter 10 has also shown that a decision feedback equalizer is advisable so that both minimum phase

It must be remembered however that the proposed construction techniques would only be applicable for data rates of the order of 2Mb/s and that systems with higher data rates would involve alterations such as the monolithic IC's being replaced with hybrid integrated circuits and this would significantly increase the construction cost.

REFERENCES

1. DIGITAL RADIO AND GENERAL.

[1.1] D.P. Taylor and P.R. Hartmann, Telecommunications by Microwave Digital Radio, IEEE Comm., Vol. 24, No. 8, Aug. 1986, pg 11-16.

[1.2] K. Feher, Digital Communications: Microwave Applications, Prentice Hall Inc., New Jersey, 1983.

[1.3] Telecommunications symposium South Africa, Hewlett Packard, 1986.

[1.4] S.J. Erst, Receiving Systems Design, Artech House Inc., pg 87-88.

2. MSK MODULATION.

[2.1] J.D. Oetting, A Comparison of Modulation Techniques for Digital Radio, IEEE Trans. on Comm., Vol. 27, No. 12, Dec. 1979, Pg 1752-1762.

[2.2] M. Borgne, Comparison of High Level Modulation Schemes for High Capacity Digital Radio, IEEE Trans. on Comm., Vol. 33, No. 5, May 1985, pg 442-449.

[2.3] D.H. Morais, The Effects of Filtering And Limiting on the Performance of QPSK, Offset QPSK, and MSK Systems, IEEE Trans. on Comm., Vol. 28, No. 12, Dec. 1980, pg 1999-2009.

[2.4] D.H. Morais and K. Feher, Bandwidth Efficiency and Probability of Error Performance of MSK and Offset Qpsk

Systems, IEEE Trans. on Comm., Vol. 27, No. 12, Dec. 1979, pg 1794-1801.

[2.5] R. de Buda, Coherent Demodulation of Frequency Shift Keying With Low Deviation Ratio, IEEE Trans. on Comm., Vol. 20, No. 3, June 1972, pg 429-435.

[2.6] W.A. Sullivan, High Capacity Microwave Systems for Digital Data Transmission, IEEE Trans. on Comm., Vol. 20, No. 3, June 1972, pg 466-470.

[2.7] I. Kalet, A Look at Crosstalk in Quadrature Modulation Systems, IEEE Trans. on Comm., Vol. 25, No. 9, Sep. 1977, pg 884-892.

[2.8] M. Aldera, Study Of The MSK And FSK Modulation Schemes Under Non Linear Conditions, MSc Dissertation, University Of Cape Town, South Africa, 1988.

3. MULTIPATH PROPAGATION.

[3.1] W.D. Rummler et al, Multipath Fading Channel Models for Microwave Digital Radio, IEEE Comm., Vol. 24, No. 11, Nov. 1986, pg 30-42.

[3.2] C.L. Ruthroff, Multiple Path Fading on Line of Sight Microwave Radio Systems as a Function of Path Length and Frequency, BSTJ, Vol. 50, No. 10, Dec. 1971, p 3211.

[3.3] S. Komaki et al, Characteristics of a High Capacity 16 QAM Digital Radio System in Multipath Fading, IEEE Trans. on Comm., Vol. 27, No. 12, Dec. 1979, pg 1854-1861.

[3.4] R.A. Semplak and R.H. Turrin, Some Measurements of Attenuation by Rainfall at 18.5 GHz, BSTJ, Vol. 48, 1969, pg 1767-1787.

[3.5] C.L. Ruthroff, Rain Attenuation and Radio Path Design, BSTJ, Vol. 49, 1970, pg 121-135.

[3.6] A.R. Webster, Angles of Arrival and Delay Times on Terrestrial Line of Sight Microwave Links, IEEE Trans. on Ant. and Prop., Vol. 31, No. 1, Jan. 1983, pg 12-17.

[3.7] Handbook of Digital Communications, Microwave Systems News, Vol. 9, No. 11, Sep. 1979.

4. MULTIPATH MODELING AND STATISTICAL ANALYSIS.

[4.1] L.J. Greenstein, Outage Calculation Methods for Microwave Digital Radio, IEEE Comm., Vol. 25, No. 2, Feb. 1987, pg 30-39.

[4.2] L.J. Greenstein, Polynomial Model for Multipath Fading Channel Responses, BSTJ, Vol. 59, No. 7, Sep. 1980, pg 1197-1226.

[4.3] W.D. Rummler, A New Selective Fading Model, BSTJ, Vol. 58, No. 5, June 1979, pg 1037-1071.

[4.4] W.D. Rummler, More on the Multipath Fading Channel Model, IEEE Trans. on Comm., Vol. 29, No. 3, March 1981, pg 346-352.

[4.5] C.W. Lundgren, Digital Outage Due to Selective Fading- Observations Versus Prediction from Laboratory Simulations, BSTJ, vol. 58, No. 5, May 1979, pg 1073-1100.

[4.6] Y. Serizawa, A Simplified Method for Prediction of Multipath Fading Outage of Digital Radio, IEEE Trans. on Comm., Vol. 31, No. 8, Aug. 1983, pg 1017-1021.

5. ADAPTIVE EQUALIZERS.

[5.1] J.K. Chamberlain, Receive Techniques for Microwave Digital Radio, IEEE Comm., Vol. 24, No. 11, Nov. 1986, pg 43-54.

[5.2] P. Hartman, Adaptive Equalizer for 6 GHz Digital Radio, Proc. IEEE Int. Conf. on Comm., ICC-79, Boston, June 1979.

[5.3] B. Baccetti and G. Tartaso, Equalization and Quality Prediction in Digital Radio Systems, GTE Telecomunicazioni-Spa.

[5.4] J.C Ogue et al, A Fast Convergence Frequency Domain Adaptive Filter, IEEE Trans. on Acous., Speech and Sig. Proc.,Vol. 31, No. 5, Oct. 1983, pg 1312-1314.

[5.5] A. Morgul et al, Wide-Band Analogue/Digital Frequency Domain Adaptive Filter, IEEE Trans. on Acous., Speech and Sig. Proc., Vol. 32, No. 4, Aug. 1984, pg 762-769.

[5.6] E.J. Baghdady, Novel Techniques for Counteracting Multipath Interference Effects in Receiving Systems, IEEE Journal on Selec. Areas in Comm., Vol. 5, No. 2, Feb. 1987, pg 274-285.

[5.7] S. Qureshi, Adaptive Equalization, IEEE Proceedings, Vol. 73, No. 9, Sep. 1985, pg 1349-1387.

[5.8] B. Friedlader and M. Morf, Least Squares Algorithms for Adaptive Linear-Phase Filtering, IEEE Trans. on Acous., Speech and Sig. Proc., Vol. 30, No. 3, June 1982, pg 381-389.

[5.9] B. Widrow and J. M. McCool, A Comparison of Adaptive Algorithms Based on the Methods of Steepest Descent and Random Search, IEEE Trans. on Ant. and Prop., Sep. 1976, pg 615-637.

[5.10] P. Monsen, Feedback Equalization, IEEE Trans. on Inform. Theory, Vol. 17, Jan. 1971, pg 56-64.

[5.11] G.L. Fenderson et al, Adaptive Transversal Equalization Of Multipath Propagation, AT&T Bell Lab. Tech. Journal, Vol. 63, Oct. 1984, pg 1447.

[5.12] P.A. Bello, Performance of Adaptive Equalization for Staggered QPSK over Frequency Selective Channels, Int. Conf. on Comm., Vol. 2, 1982, pg 3HI 1-6.

[5.13] E. Eleftheriou and D. Falconer, Adaptive Equalizer Techniques for HF Channels, IEEE Journal on Selec. Areas in Comm., Vol. 5, No. 2, Feb. 1987, pg 238-247.

[5.14] K.D. Kammeyer et al, A Modified Adaptive FIR Equalizer for Multipath Echo Cancellation in FM Transmission, IEEE Journal on Selec. Areas in Comm., Vol. 5, No. 2, Feb. 1987, pg 226-237.

[5.15] C.A. Belfiore and J.H. Park Jnr., Decision Feedback Equalization, Proc. IEEE, Vol. 67, Aug. 1979, pg 1143-1156.

[5.16] D.D. Falconer and G.J. Foschini, Theory Of Minimum Mean-Square-Error QAM Systems Employing Decision Feedback Equalization, BSTJ, Vol. 53, Nov. 1973, pg 1821-1849.

[5.17] P.J. von Gerwer et al, Design Consideration For a 144 kbits/s Digital Unit For The Local Telephone Network,

IEEE J. Select. Areas in Comm., Vol. 2, March 1984, pg 314-323.

[5.18] G. Ungerboeck, Fractional Tap Spacing Equalizer and Consequences For Clock Recovery In Data Modems, IEEE Trans. on Comm., Vol. 24, Aug. 1976, pg 856-864.

6. HARDWARE AND SOFTWARE.

[6.1] S.M. Bozic, Digital And Kalman Filtering, Dept. of Electronic And Electrical Engineering, University of Birmingham, Edward Arnold Pub.

[6.2] J. Sevick, Broadband Matching Transformers Can Handle Many Kilowatts, Electronics, Vol. 49, No. 25, 1976, pg 123-128.

[6.3] Krauss and Allen, Electronics, Aug. 1973, pg 113-116.

[6.4] Pin Diode Designers' Guide, M/A.COM Silicon Products Inc., U.S.A., 1983.

[6.5] HP-85 Owner's Manual, Hewlett Packard, U.S.A., 1979.

[6.6] S.M. Bozk, Digital And Kalman Filtering, Dept. of Electronic and Engineering, University of Birmingham, Edward Arnold Press.

[6.7] K. Henney, Radio Engineering Handbook, McGraw Hill Publishers, 5th Ed., 1959.

[6.8] Williams, Electronic Filter Design Handbook, McGraw Hill Publishers, 1981.

[6.9] D.A. Evans, Designing With Field Effect Transistors, Siliconix Inc., McGraw Hill Pub., 1981.

BIBLIOGRAPHY

[i] Anderson C.W. et al. The Effect Of Selective Fading On Digital Radio. IEEE Trans. on Comm.. Dec. 1979. pg 1870-1875.

[ii] Babler G.M.. A Study Of Frequency Selective Fading For A Microwave Line Of Sight Narrowband Radio Channel. BSTJ. Vol. 51. March 1972. pg 731.

[iii] Babler G.M.. Selectively Fading Non Diversity And Space Diversity Narrowband Microwave Radio Channels. BSTJ. Vol. 52. Feb. 1973. pg 239.

[iv] Barnett W.T.. Multipath Fading Effects On Digital Radio. IEEE Trans. on Comm.. Vol. 27. No. 12. Dec. 1979. pg 1842-1848.

[v] Horowitz P. and Hill W.. The Art Of Electronics. Cambridge University Press. 1983.

[vi] Journal Selec. Areas in Comm.. Vol. 5. No. 2. Feb. 1987 (Special Edition)

[vii] Kalet I.. A Look At Crosstalk In Quadrature Modulation Systems. IEEE Trans. on Comm.. Vol. 25. No. 9. Sept. 1977. pg 884-892.

[viii] Komaki S.. Characteristics Of A High Capacity 16 QAM Digital Radio System In Multipath Fading. IEEE Trans. on Comm.. Vol. 27. No. 12. Dec. 1979. pg 1854-1861.

[ix] Lavergnat J. and Sylvain M.. Selective Fading, Modeling And Prediction. IEEE Journal on Selec. Areas in Comm.. Vol. 5 No. 3. Apr. 1987. pg 378.

[x] Lin S.H.. Statistical Behavior Of A Fading Signal. BSTJ. Vol. 50. No. 10. Dec. 1971. pg 3211.

[xi] Lucky R.W.. Functional Analysis Relating Delay Variation And Intersymbol Interference In Data Transmission. BSTJ. Vol. 42. Sept. 1963.

[xii] Morais D.H. and Feher K.. Bandwidth Efficiency And Probability Of Error Performance Of MSK And Offset QPSK Systems. IEEE Trans. on Comm.. Vol. 27. No. 12. Dec. 1979. pg 1794-1801.

[xiii] Murase T. et al. 200 MB/s 16 QAM Digital Radio System With Countermeasure Techniques For Multipath Fading. Int. Conf. on Comm.. 1981. pg 46.1.1.

[xiv] Qureshi S.. Adaptive Equalization In Communications. IEEE Comm.. Vol. 20. No. 2. March 1982. pg 9-17.

[xv] Rummler W.D.. A Simplified Method For The Laboratory Determination Of Multipath Outage. IEEE Trans. On Comm.. Vol. 30. No. 3. March 1982. pg 487.

[xvi] Rummler W.D.. More On The Multipath Fading Channel Model. IEEE Trans on Comm.. Vol. 29. no. 3. March 1981. pg 346-352.

[xvii] Rummler W.D.. A Simplified Method For The Laboratory Determination Of Multipath Outage. IEEE Trans. on Comm.. Vol 30. No. 3. March 1982. pg 487-494.

[xviii] Sakagami S.. Method Of Estimating In Band Linear Amplitude Dispersion. IEEE Trans. on Comm.. Vol. 30. No. 8. Aug. 1982. pg 1875-1888.

[xix] Sandberg J.. Extraction Of Multipath Parameters From Swept Measurements. IEEE Trans. on Ant. and Prop.. Vol. 28. No. 6. Nov. 1980. pg 743-750.

[xx] Shafi M.. Statistical Analysis/Simulation Of Multipaths. IEEE Journal on Selec. Areas in Comm.. Vol. 5. No. 3. Apr. 1987. pg 389.

[xxi] Shafi M. and Taylor D.P.. Influence Of Terrain Induced Reflections On The Performance Of High Capacity Digital Radio Systems. Int. Conf. Comm.. 1986.

[xxii] Taub H. and Schilling D.L.. Principles Of Communication Systems. McGraw Hill Publ. 1981.

[xxiii] Watermeyer I.R.. A Development Study For A Short Range Low Capacity Digital Microwave Link. MSc Dissertation. University of Cape Town. South Africa. 1986.

[xxiv] Ziemer R.E. and Ryan C.R.. MSK Modem Implementation. IEEE Comm.. Vol. 21. No. 7. pg 28-38.

APPENDIX A

TOROIDAL POWER SPLITTERS AND COMBINERS

This appendix discusses some of the practical aspects which must be taken into account when designing and building toroidal power splitters and combiners.

Reference [6.1] discusses the basic principals of transformer power splitters. A basic power splitter is shown in figure A.1 . Ideally the power into the primary of the transformer is split evenly between amplifier 1 and amplifier 2. However, due to input impedance variations between the two amplifiers, this is rarely the case. Instead one amplifier is usually provided with a bit more drive power than the other. To aid in equalizing the power split, resistor R at the centre tap of the secondary is often left out of the circuit. The small dots are used to indicate polarity.

A typical power combiner is shown in figure A.2. Here the power output of each amplifier is combined in transformer T1 to provide an output power of P1+P2.

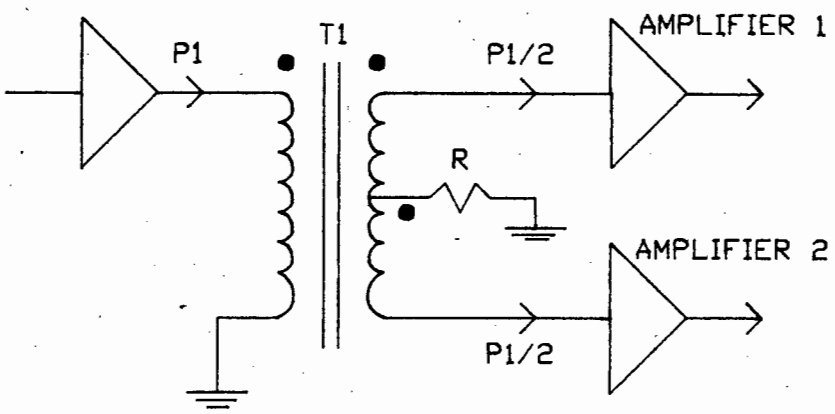

FIG A.1 Typical Power Splitter

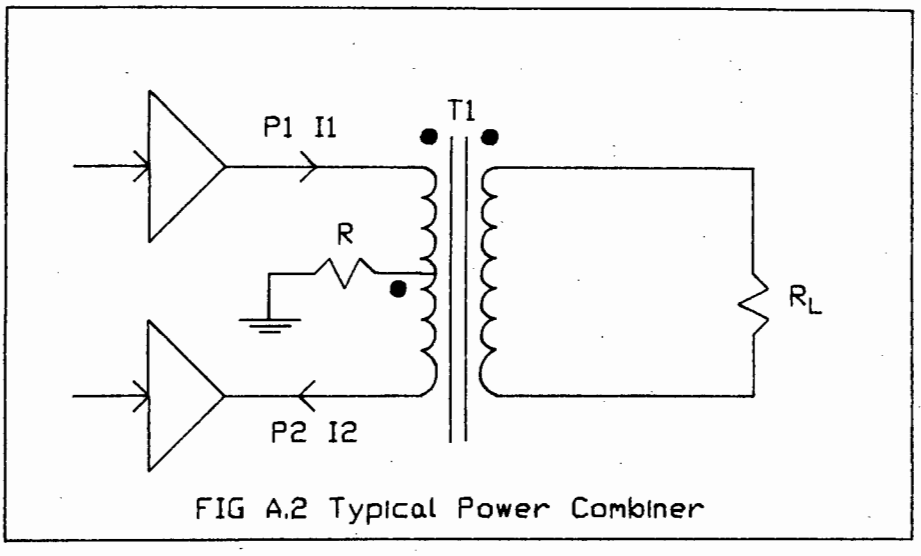

FIG A.2 Typical Power Combiner

Broadband transformers are often called transmission line transformers because they make use of the transmission line properties of the windings. This is done by using bifilar or trifilar type windings rather than conventional types of windings.

A conventional transformer usually has two entirely seperate windings. That is, one of the windings is usually wound onto the core, and then the other winding is wound on top of the first winding. Transmission line transformers use an entirely different technique for the windings. The primary and secondary windings are twisted together producing a certain characteristic impedance.

The use of toroidal power splitters and combiners without amplifiers or buffers led to very poor isolation between the quadrature channels, and this forced us to try and improve the isolation problem by trying to match the impedances better or to use hybrid devices.

The toroidal core power splitters have characteristics of both conventional transformers and transmission line transformers. The transmission line mode seems to be in effect throughout the frequency range except at the very

lowest end of the range. The equal and opposite currents that flow in the transmission line windings essentially cancel core flux and so minimize core loss. The shortness of the transmission line (in relation to the highest operating frequency) minimizes ohmic losses, keeping output voltage nearly equal to input voltage over a wide frequency range. This is discussed further in reference [6.2].

Coiling the line around a magnetic core provides the inductance needed to prevent unwanted currents from flowing, except at very low frequencies. Figure A.3 shows the frequency response.

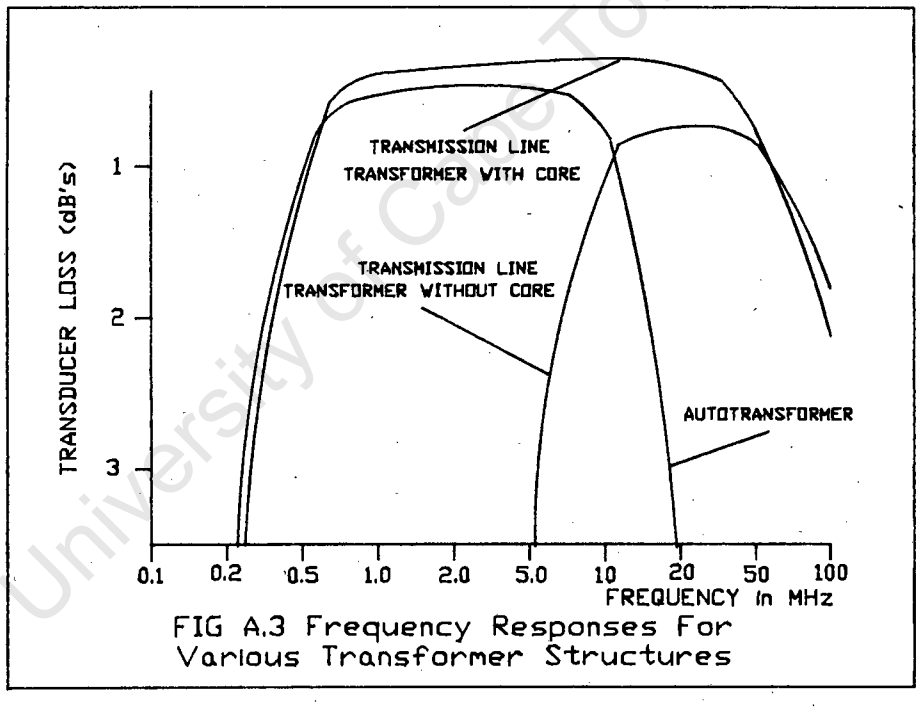

FIG A.3 Frequency Responses For Various Transformer Structures

The transmission line transformer with a core acts just like a conventional autotransformer at very low frequencies. At about 400 kHz transmission line operation starts contributing to its efficiency and through to 40 MHz it suffers much less than the autotransformer from transducer loss. But without a magnetic core to choke off shunting currents, not only is its efficiency much less,

but its frequency response also falls off rapidly below 1.5 MHz.

The efficiency of such a transformer depends on different factors at high and low frequencies. The voltage standing wave ratio is critical at the high end, and the reactance of the windings becomes critical at the low end. Three parameters are needed to design broadband transformers. They are; characteristic impedance Z_0, which depends on the number of turns and the shape and spacing of the windings; the shunting inductance that affects low frequency rolloff, and itself depends on the size and type of core material; and the effective phase constant of the coiled transmission line which determines the transformer high frequency response and depends on the dielectric of the wire insulation and coupling between windings. The optimum characteristic impedance is set by the formula $Z_0 = \sqrt{(R_s R_l)}$ where R_s is the source impedance and R_l is the load impedance.

The characteristic impedance does vary with frequency because the permeability of the core material is frequency sensitive. Usually the optimum value of Z_0 should be determined at the highest frequency of operation.

To lower the characteristic impedance, should that be necessary, transmission lines can be twisted together. Twisting lowers Z_0 by increasing their distributed capacitance (as seen in figure A.4). A more significant change can be made by just tightly coiling the transmission lines and so minimizing spacing between windings.

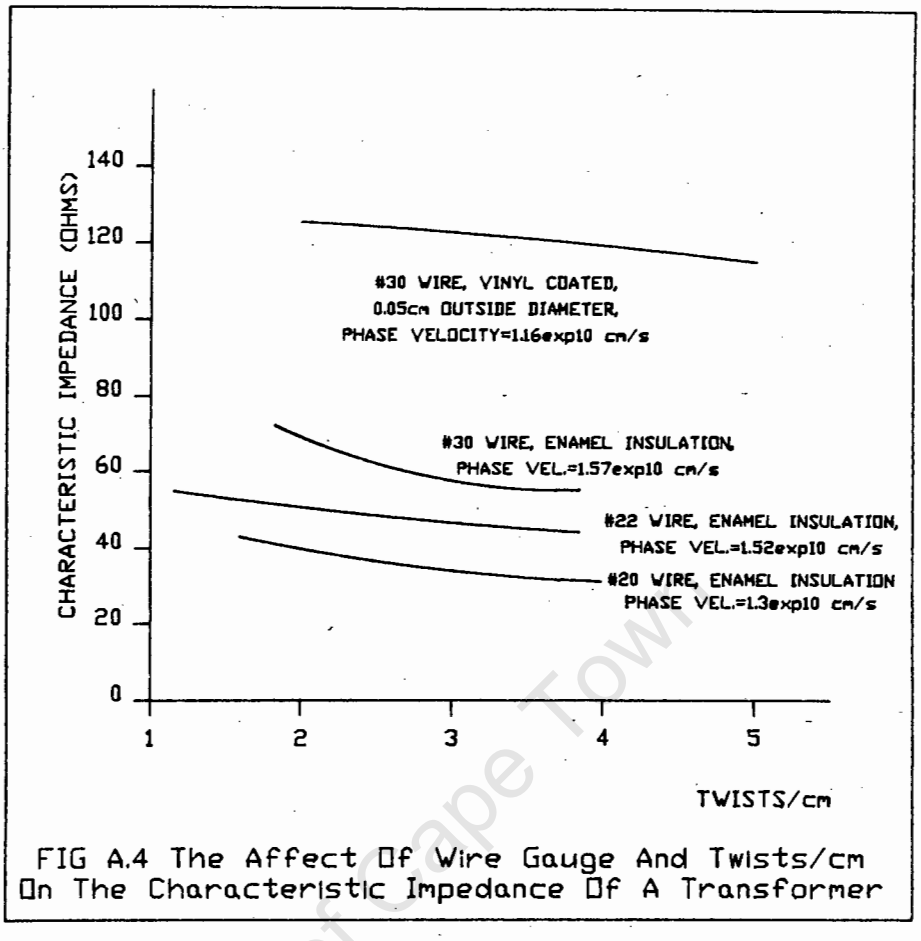

FIG A.4 The Affect Of Wire Gauge And Twists/cm On The Characteristic Impedance Of A Transformer

The lower cutoff frequency f_1 can be determined by the formula $f_1 = (R_s 10^9)(4\pi N_p^2 Al)$ Hz where N_p is the number of twists. The above formula is derived in reference [6.3].

Table A.1 shows some of the ranges of cores available. The combiners and splitters in the hardware simulator were made with T-25-12 cores and used #22 wire with approximately 5 twists/cm.

The upper cutoff frequency for an optimally matched transformer occurs when the line length is approximately 0.3 wavelengths (the phase velocity of the transmission line must therefore be calculated or measured). If possible, to minimize losses due to mismatch, this length should in practice be kept shorter than 0.125 wavelengths.

Even applying all the design techniques described above it was still found that the toroidal power splitters and combiners required equal source and equal load impedances to achieve a suitable isolation. However if the impedances can be matched then the splitting and combining is of a high standard.

TABLE A.1 Selecting Transformer Cores

MIX #	BASIC IRON POWDER	μ_o	TEMP. STABILITY ppm/C	RESONANT FREQ. RANGE MHz	COLOUR CODE
1	CARBONYL C	20	280	0.15-2.0	BLUE
2	CARBONYL E	10	95	0.25-10	RED
3	CARBONYL HP	35	370	0.02-1.0	GREY
6	CARBONYL SF	8.5	35	2.0-30	YELLOW
7	CARBONYL TH	9.0	30	1.0-20	WHITE
8	CARBONYL GQ4	35	255	0.02-1.0	ORANGE
10	CARBONYL W	6.0	150	10-100	BLACK
12	SYNTH. OXIDE	4.0	170	20-200	GREEN/WHITE
15	CARBONYL GS6	25	190	0.1-3.0	RED/WHITE
17	CARBONYL	4.0	50	20-200	BLUE/YELLOW
22	SYNTH. OXIDE	4.0	410	20-200	GREEN/ORANGE
0	PHENOLIC	1	0	50-250	TAN

APPENDIX B

GPIO INTERFACE

As already stated, this dissertation does not discuss the detailed operation of the GPIO interface, but merely the hardware and software configurations necessary to enable output to the control voltage interface.

Firstly the interface default switch S2 must be set, as this determines the configuration at power up. S2(1),S2(2), and S2(3) determine data port configuration and are set for device address 04. S2(4) protects the output drivers. Once the cable has been properly prepared it is set to 1 enabling the interface for data output. S2(5) determines handshake mode and is set for partial handshaking. S2(6) determines data line logic sense and is set for positive-true logic. S2(7) determines FLG and ST logic sense and is set for Busy-High. S2(8) determines CTL logic sense and is st for Set-High.

The pin-configuration layout is unchanged from the factory setting but the colour coding is different and is as shown below in figure B.1.

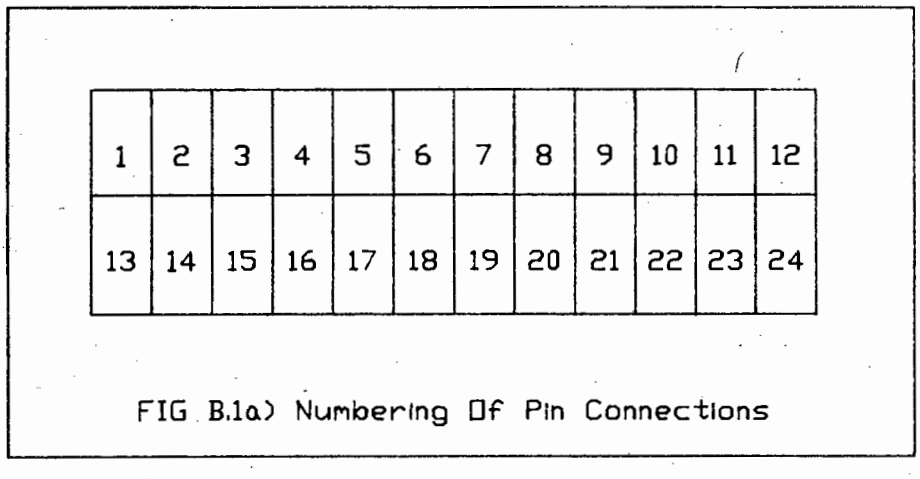

FIG B.1a) Numbering Of Pin Connections

J1 Pin Assignment	J2 Pin Assignment	WIRE COLOUR
1 GND	1 GND	BROWN
2 DC5	2 DD5	RED
3 DC7	3 DD7	WHITE
4 DC2	4 DD2	RED
5 DC0	5 DD0	WHITE/BLUE
8 CTLA	8 CTLB	BLACK
9 DA7	9 DB7	GREY
10 DA5	10 DB5	BLUE
11 DA0	11 DB0	BROWN
12 DA2	12 DB2	ORANGE/BLUE
13 GND	13 GND	WHITE
14 DC4	14 DD4	GREEN
15 DC6	15 DD6	BLUE
16 DC3	16 DD3	WHITE
17 DC1	17 DD1	ORANGE
20 CTL0	20 CTL1	RED
21 DA6	21 DB6	GREY
22 DA4	22 DB4	GREEN
23 DA1	23 DB1	RED
24 DA3	24 DB3	ORANGE

FIG B.1b) Pin Assignments

The strobe handshaking is obtained by configuring the interface by writing to register 4. The **CONTROL 4,4;128** statement on line 10 of the program writes the value 128 to register 4. The value 128 sets the interface for strobe output with input timing Ready-to-Busy, and sets the four ports to Positive-True logic.

The delay time of the strobe handshaking is set for 120 ms and this is controlled by register 6. The **CONTROL 4,6;128+120** statement on line 20 of the program writes this value to the register.

The output inhibit of the interface is set by register 9. The **CONTROL 4,9;0** statement on line 30 allows the output information to be sent to the voltage control interface.

Register 3 determines the logic sense of the handshake lines. Only the handshake lines CTLA,CTLB,CTL0, and CTL1 are used and they require positive true logic. This is achieved by writing the value 0 to register 3 and is done by the statement **CONTROL 4,3;0** on line 40.

The final register that needs to be configured is register 8. Register 8 is for extra protection to ensure that the output drives are not accidentally activated while they are grounded or connected to current-sourcing circuitry. The statement **CONTROL 4,8;3** on line 50 writes the value 3 to register 8 and enables port A and port B for output only.

Port A is at output address 400,B at 401,C at 404, and D at 405. To output an 8 bit binary number to port C the command is **OUTPUT 404 USING "#,B";X** where X is the value to be output such as 79. Thus the output commands on lines 950 to 980 output the values of A3 to port A, A1 to port B, A2 to port C, and A4 to port D.

APPENDIX C

COMPUTER PROGRAM FOR HARDWARE SIMULATOR

The hardware simulator and computer interface have already been discussed, as well as the statistical variation of the channel parameters. This section will discuss the software side of the multipath simulator.

As discussed earlier, the outage time in a heavily fading month is equal to $0.073cfD^3$ which, substituting in worst case values of c=4, D=6 miles, and f=23 GHz, gives an outage time of 1612 seconds. The total computer simulation runs for 1623 seconds, a percentage error of 0.7% which is quite acceptable. The number of iterations within this 1623 second period is 910. It was decided that for f_0 and B, both of which are independent of the other variables, the functions should vary cyclically over the time period. Thus the starting position of f_0 and B are the same as the finishing positions of f_0 and B.

As explained in chapter 5 and shown in figure 5.5, the chance of f_0 being between +20 MHz and -20 MHz is five times greater than between +20 MHz and +40 MHZ or between -20 MHz and -40 MHZ. Since the simulator is only operating in three quadrants (it is not necessary to simulate for minimum and maximum fading simultaneously) the possible variation in frequency offset is from +10 MHz to -30 MHZ. The chance of f_0 being between +10 MHz and -20 MHz is fifteen times greater than between -20 MHz and -30 MHz. Thus for the 910 iterations 853 have f_0 with a value between +10 MHz and -20 MHz, and 57 have f_0 with a value between -20 MHz and -30 MHz.

The time variation of B can either be taken from figure 5.1 or by using the formula $P(B>X) = \exp(-X/3.8)$ the latter of which was used here. Table C.1 shows the range of values of b and the number of iterations necessary for each range.

TABLE C.1 Time Variation Of Parameter b

b>	b<	% TIME	No. OF SECONDS	No. OF ITERATIONS
0.292	0.3	2.57	41.4	23
0.3	0.35	15.27	246.2	139
0.35	0.4	13.81	222.6	126
0.4	0.45	12.41	200.0	113
0.45	0.5	11.00	177.3	100
0.5	0.55	9.67	155.9	88
0.55	0.6	8.37	135.2	76
0.6	0.65	7.10	114.5	65
0.65	0.7	5.91	95.3	54
0.7	0.75	4.76	76.7	43
0.75	0.8	3.65	58.9	33
0.8	0.85	2.66	42.9	24
0.85	0.9	1.70	27.4	15
0.9	0.929	1.10	17.7	11

The time variation of A is more complicated than that of f_0 or B since it is dependent on B. It was decided to use the information of figures 5.2 and 5.3 and produce cyclic variations of A for each of the following possible ranges of B:-

$B<4.5$

$4.5 \leq B<6.5$

$6.5 \leq B<8.5$

$8.5 \leq B$

As B varies the program will alternate between the various cyclic variations, and thus the final value of A will not equal the initial value of A. Tables C.2, C.3, C.4, and C.5 show the ranges of A and the number of iterations within each range.

TABLE C.2 $2.4 \leq \beta < 4.5$			
α BETWEEN VALUES		% TIME	No. ITERATIONS
0.316	0.79	10	91
0.224	0.316	20	182
0.125	0.224	20	182
0.1	0.125	20	182
0.056	0.1	20	182
0.0355	0.056	8	73
	0.0355	2	18

TABLE C.3 $4.5 \leq \beta < 6.5$			
α BETWEEN VALUES		% TIME	No. ITERATIONS
0.708	0.79	2	18
0.282	0.708	10	91
0.141	0.282	19	173
0.089	0.141	19	173
0.063	0.089	20	182
0.0398	0.063	20	182
0.0282	0.0398	8	73
0	0.0282	2	18

TABLE C.4 $6.5 \leq \beta < 8.5$			
α BETWEEN VALUES		% TIME	No. ITERATIONS
0.562	0.79	2	18
0.178	0.562	10	91
0.089	0.178	19	173
0.0708	0.089	19	173
0.0501	0.0708	20	182
0.0316	0.0501	20	182
0.0226	0.0316	8	73
0	0.022	2	18

TABLE C.5 $8.5 \leq \beta$			
α BETWEEN VALUES		% TIME	No. ITERATIONS
0.141	0.251	10	91
0.1	0.141	20	182
0.063	0.1	20	182
0.0398	0.063	20	182
0.0316	0.0398	20	182
0.025	0.0316	8	73
0	0.025	2	18

The final computer program is shown in figure C.1 and is explained below.

Lines 5-50 Initialize the GPIO interface, the control commands of which are explained in appendix B.
Lines 60-160 Initialize the random generator and set up the initial values of the parameters, as well as whether the values should begin increasing or decreasing.
Lines 165-168 Draws the axes of the graph which will plot the variation over the full time period.
Lines 200- Is the start of the iterations.
Lines 210-230 Varies the parameter F0.
Lines 240-380 Varies the parameter B according to the values of table C.1.
Lines 400-430 Determines which of tables C.2, C.3, C.4, or C.5 are used to vary parameter A.
Lines 800-809 Plots the three parameters.
Lines 900-920 Determines which quadrant should be used to position the rotating vector.
Lines 930-940 Converts the values of A and B to an integer value to be outputted to the delay line voltage control.
Lines 950-980 Outputs the integer values to the voltage controls.
Lines 1000-1020 Converts the value of A to the two integer values which must be outputted if the rotating vector is in quadrant two.
Lines 1500-1520 Converts the value of A to the two integer values which must be outputted if the rotating vector is in quadrant three.
Lines 2000-2100 Vary the parameter A according to table C.2.
Lines 3000-3100 Vary the parameter A according to table C.3.
Lines 4000-4110 Vary the parameter A according to table C.4.

Lines 5000-5090 Vary the parameter A according to table C.5.

By running the program several times it is possible to obtain numerous combinations of relative change in the three parameters while still satisfying the statistical behavior. Figure C.2 shows some possible variations of the parameters.

```
 10 ! COMPUTER PROGRAM FOR      !
          HARDWARE SIMULATOR

 20 ! Initialize the interface.!
 30 CONTROL 4,4 ; 128
 40 CONTROL 4,6 ; 128+120
 50 CONTROL 4,9 ; 0
 60 CONTROL 4,3 ; 0
 70 CONTROL 4,8 ; 3
 80 ! Initialize the starting !
 90 ! position of parameters !
100 RANDOMIZE
110 DEG
120 A=.8722*RND+.0178 ! Start A!
130 B=.637*RND+.292 ! Start of B.
    !
140 F0=41*RND-30 ! Start of F0 !
150 S4=RND ! A increasing ? !
160 S5=RND ! B increasing ? !
170 S6=RND ! F0 increasing ? !
180 IF S4<.5 THEN S4=-1 ELSE S4=
    1
190 IF S5<.5 THEN S5=-1 ELSE S5=
    1
200 IF S6<.5 THEN S6=-1 ELSE S6=
    1
210 ! Set up graph !
220 PEN 1 @ GCLEAR
230 SCALE 0,30,0,1
240 XAXIS 0,1
250 YAXIS 0,.1
260 ! Loop for fading time. !
270 FOR L=1 TO 910
280 T=L/910*1623/60
290 ! Variation of frequency !
300 IF F0>-20 THEN F0=F0+S6*2*30
    /853
310 IF F0<=-20 THEN F0=F0+S6*2*1
    0/57
320 IF F0<=-30 OR F0>=10 THEN S6
    =-1*S6
330 ! Variation of parameter B !
340 IF B<=.3 THEN B=B+S5*2*.008/
    23
350 IF B>.3 AND B<=.35 THEN B=B+
    S5*2*.05/139
360 IF B>.35 AND B<=.4 THEN B=B+
    S5*2*.05/126
370 IF B>.4 AND B<=.45 THEN B=B+
    S5*2*.05/113
380 IF B>.45 AND B<=.5 THEN B=B+
    S5*2*.05/100
390 IF B>.5 AND B<=.55 THEN B=B+
    S5*2*.05/88
400 IF B>.55 AND B<=.6 THEN B=B+
    S5*2*.05/76
410 IF B>.6 AND B<=.65 THEN B=B+
    S5*2*.05/65
420 IF B>.65 AND B<=.7 THEN B=B+
    S5*2*.05/54
430 IF B>.7 AND B<=.75 THEN B=B+
    S5*2*.05/43
440 IF B>.75 AND B<=.8 THEN B=B+
    S5*2*.05/33
450 IF B>.8 AND B<=.85 THEN B=B+
    S5*2*.05/24
460 IF B>.85 AND B<=.9 THEN B=B+
    S5*2*.05/15
470 IF B>.9 THEN B=B+S5*2*.029/1
    1
480 IF B>=.929 OR B<=.292 THEN S
    5=-1*S5
490 ! Variation of parameter A !
500 IF B>=.292 AND B<.404 THEN G
    OSUB 850
510 IF B>=.404 AND B<.527 THEN G
    OSUB 950
520 IF B>=.527 AND B<.624 THEN G
    OSUB 1060
530 IF B>=.624 THEN GOSUB 1170
540 ! Plot the variables !
550 PENUP
560 PLOT T,A
570 PENUP
580 PLOT T,B
590 PENUP
600 PLOT T,(F0+30)/41
610 O=360*F0*.0125+45
620 IF O<90 AND O>0 THEN GOSUB 7
    30
630 IF O<0 AND O>-90 THEN GOSUB
    790
640 A4=A*B*48.685+111.747
650 A4=IP(A4)
660 ! Output to interface !
670 OUTPUT 400 USING "#,B" ; A3
680 OUTPUT 401 USING "#,B" ; A1
690 OUTPUT 404 USING "#,B" ; A2
700 OUTPUT 405 USING "#,B" ; A4
710 NEXT L
720 END
730 A1=A*TAN(O)/SQR(1+TAN(O)*TAN
    (O))*64.205+98.857
740 A1=IP(A1)
750 A2=A/SQR(1+TAN(O)*TAN(O))*59
    .619+98.939
760 A2=IP(A2)
770 A3=0
780 RETURN
790 A2=A/SQR(1+TAN(O)*TAN(O))*59
    .619+98.939
800 A2=IP(A2)
810 A3=-A*TAN(O)/SQR(1+TAN(O)*TA
    N(O))*61.912+120.898
820 A3=IP(A3)
830 A1=0
840 RETURN
850 ! !
860 IF A>.316 THEN A=A+S4*2*.474
    /91
```

FIG C.1 Computer Program For Simulator

```
870 IF A<=.316 AND A>.224 THEN A
    =A+S4*2*.092/182
880 IF A<=.224 AND A>.125 THEN A
    =A+S4*2*.099/182
890 IF A<=.125 AND A>.1 THEN A=A
    +S4*2*.025/182
900 IF A<=.1 AND A>.056 THEN A=A
    +S4*2*.044/182
910 IF A<=.056 AND A>.0355 THEN
    A=A+S4*2*.0205/73
920 IF A<=.0355 THEN A=A+S4*2*.0
    355/18
930 IF A>.79 OR A<=.01 THEN S4=-
    1*S4
940 RETURN
950 ! !
960 IF A>.708 THEN A=A+S4*2*.082
    /18
970 IF A<=.708 AND A>.282 THEN A
    =A+S4*2*.426/91
980 IF A<=.282 AND A>.141 THEN A
    =A+S4*2*.0141/182
990 IF A<=.141 AND A>.089 THEN A
    =A+S4*2*.052/182
1000 IF A<=.089 AND A>.063 THEN
     A=A+S4*2*.026/182
1010 IF A<=.063 AND A>.0398 THEN
      A=A+S4*2*.0232/182
1020 IF A<=.0398 AND A>.0282 THE
     N A=A+S4*2*.0116/73
1030 IF A<=.0282 THEN A=A+S4*2*.
     0282/18
1040 IF A>.79 OR A<=.01 THEN S4=
     -1*S4
1050 RETURN
1060 ! !
1070 IF A>.562 THEN A=A+S4*2*.22
     8/18
1080 IF A<=.562 AND A>.178 THEN
     A=A+S4*2*.384/91
1090 IF A<=.178 AND A>.089 THEN
     A=A+S4*2*.089/182
1100 IF A<=.089 AND A>.0708 THEN
      A=A+S4*2*.0182/182
1110 IF A<=.0708 AND A>.0501 THE
     N A=A+S4*.0207/182
1120 IF A<=.0501 AND A>.0316 THE
     N A=A+S4*2*.0185/182
1130 IF A<=.0316 AND A>.022 THEN
      A=A+S4*2*.0096/73
1140 IF A<=.022 THEN A=A+S4*2*.0
     22/18
1150 IF A>.79 OR A<=.01 THEN S4=
     -1*S4
1160 RETURN
1170 ! !
1180 IF A>.251 THEN A=A-.01
1190 IF A>.251 THEN S4=-1
1200 IF A<=.251 AND A>.141 THEN
     A=A+S4*2*.11/91
1210 IF A<=.141 AND A>.1 THEN A=
     A+S4*2*.041/182
1220 IF A<=.1 AND A>.063 THEN A=
     A+S4*2*.037/182
1230 IF A<=.063 AND A>.0398 THEN
      A=A+S4*2*.0232/182
1240 IF A<=.0398 AND A>.0316 THE
     N A=A+S4*2*.0082/182
1250 IF A<=.0316 AND A>.025 THEN
      A=A+S4*2*.006/73
1260 IF A<=.025 THEN A=A+S4*2*.0
     25/18
1270 IF A<=.01 OR A>=.251 THEN S
     4=-1*S4
1280 RETURN
```

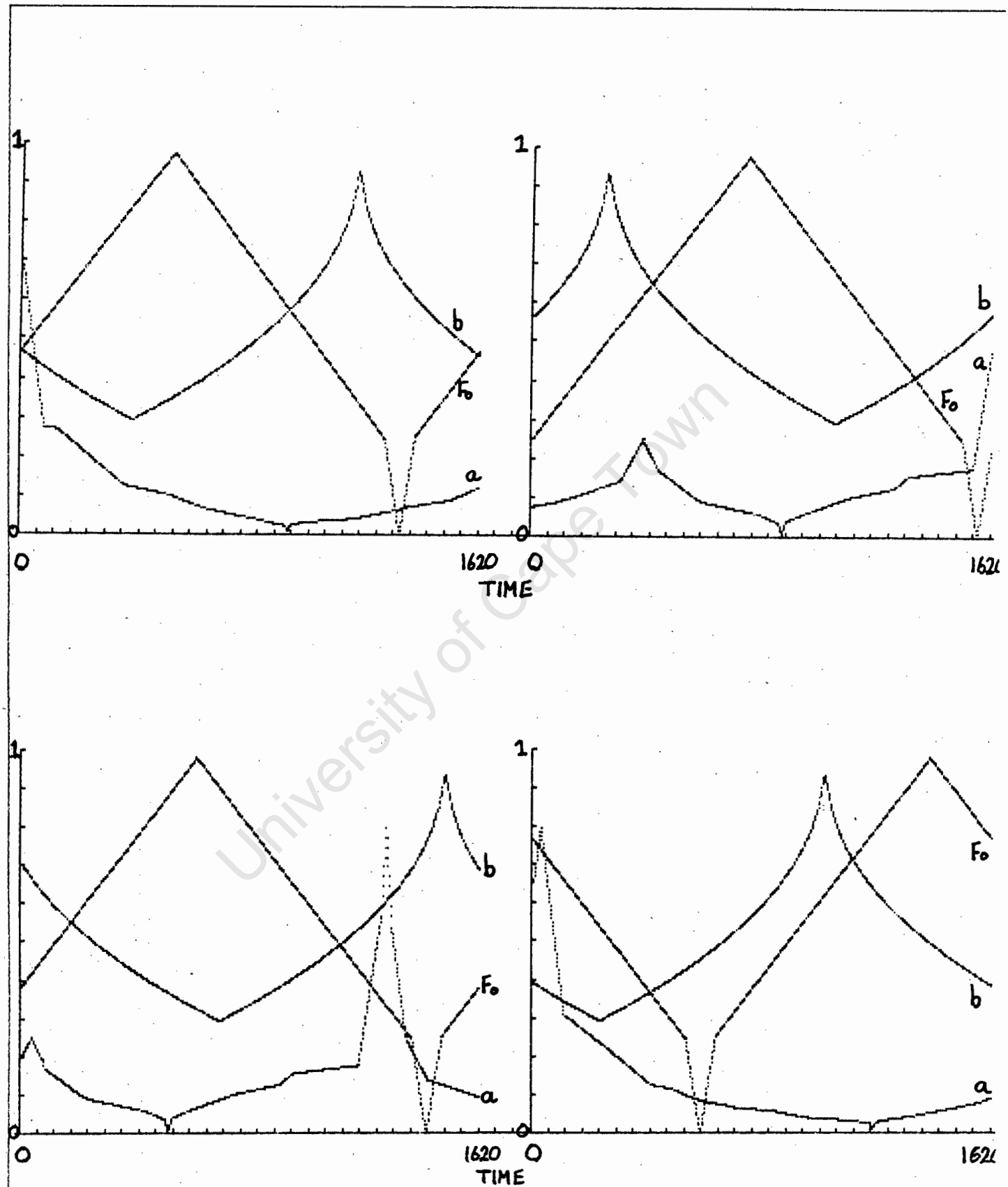

FIG C.2 Possible Variations Of The Parameters

APPENDIX D

COMPUTER SIMULATION OF MSK DIGITAL RADIO LINK

```
PROGRAM MSK(INPUT,OUTPUT);

(* This program will generate the I.F. waveform of a M.S.K.
modulator. The input to the modulator is a bit stream, and
the user has the following options:-
1) Random bit generation
2) Repetition of a user selected 8 bit sequence

The signal to noise ratio can also be adjusted, as can the
parameters of the multipath model.

The output is the BER value.                                  *)


(* Firstly the constants are defined.                         *)
CONST pi=3.141592654;
      c1=0.3266;
      c2=0.6532;
      c3=0.3266;
      c4=-0.1315;
      c5=-0.1748;
      k1=0.007561;
      k2=-0.022683;
      k3=0.022683;
      k4=-0.007561;
      k5=-2.109052;
      k6=-1.573856;
      k7=-0.404316;
      multiplier=25173;
      increment=13849;
      modulus=65536;
      br=2.048;
      ENB=108.44;
      tt=12.5E-9;

(* Secondly the global variables are defined                  *)
VAR a1,bitno,bit1,z,BQ,BI,lastbit,BoutQ,BoutI,Error:integer;
rnd,t1,t2:integer;
point:integer;
datafile: text;
initialphase,initdemodangle,freq1,ran,a2,Fo,It,Qt:real;
time,BER,freq,rmsN:real;
noiseratio,F1,a,b,angl,ang2,ang3:real;
demodangle:array[1..140] of real;
temp:array[1..140] of real;
x1:array[1..3] of real;
```

```
y1:array[1..3] of real;
x2:array[1..3] of real;
y2:array[1..3] of real;
x3:array[1..7] of real;
y3:array[1..7] of real;
Bin:array[1..2] of integer;
sines:array[0..559] of real;
coses:array[0..559] of real;
wave:array[0..2] of real;

(* This function provides the mathematical formula for the
generation of random numbers.                                  *)
FUNCTION random(VAR feed:integer):real;
      VAR rnd:integer;
      BEGIN
      feed:=(multiplier*feed+increment) mod modulus;
      rnd:=(feed mod 1000);
      random:=rnd/500-1;
      END;



(* This procedure instructs the operator to select the type
of bit generation required.                                    *)
PROCEDURE inputpage(VAR a1:integer;VAR a2:real);
      VAR line:integer;
      BEGIN
      for line:=1 to 35 do writeln;
      writeln(' M.S.K. MODULATION SIMULATOR');
      writeln('============================');
      writeln;
      writeln('Do you want random generation (1) or set
bits (2) ?');
      read(a1);
      if (a1<>1) and (a1<>2) then
        BEGIN
        writeln('ERROR! No such option.');
        END;
      writeln('Enter the noise amplitude value .');
      read(a2);
      END;

(* This procedure does differential decoding and error
summation.                                                     *)
PROCEDURE decider;
      BEGIN
      if Bin[1]=-1 then Bin[1]:=0;
      if Bin[2]=-1 then Bin[2]:=0;
      if bitno mod 2 <> 0 then
        BEGIN
        if BoutQ <> Bin[1] then
          BEGIN
          Error:=Error+1;
```

```
          writeln(bitno);
          END;
        END;
      if bitno mod 2 = 0 then
        BEGIN
        if BoutI <> Bin[2] then
          BEGIN
          Error:=Error+1;
          writeln(bitno);
          END;
        END;
      if bitno=lastbit then
        BEGIN
        if BoutI <> Bin[2] then
          BEGIN
          Error:=Error+1;
          writeln(bitno+1);
          END;
        END;
      BER:=Error/(bitno+1);
      END;

(* This procedure is the low pass filter for the I channel*)
PROCEDURE filter1(VAR Iin,I:real);
      BEGIN
      x1[3]:=x1[2];
      x1[2]:=x1[1];
      x1[1]:=Iin;
      y1[3]:=y1[2];
      y1[2]:=y1[1];
      y1[1]:=c1*x1[1]+c2*x1[2]+c3*x1[3]+c4*y1[2]+c5*y1[3];
      I:=y1[1];
      END;

(* This procedure is the low pss filter for the Q channel*)




PROCEDURE filter2(VAR Qin,Q:real);
      BEGIN
      x2[3]:=x2[2];
      x2[2]:=x2[1];
      x2[1]:=Qin;
      y2[3]:=y2[2];
      y2[2]:=y2[1];
      y2[1]:=c1*x2[1]+c2*x2[2]+c3*x2[3]+c4*y2[2]+c5*y2[3];
      Q:=y2[1];
      END;

(* This procedure is the band pass filter for the
demodulator.                                          *)
PROCEDURE filter3(VAR freq1,freq:real);
      BEGIN
      x3[7]:=x3[6];
```

```
      x3[6]:=x3[5];
      x3[5]:=x3[4];
      x3[4]:=x3[3];
      x3[3]:=x3[2];
      x3[2]:=x3[1];
      x3[1]:=freq1;
      y3[7]:=y3[6];
      y3[6]:=y3[5];
      y3[5]:=y3[4];
      y3[4]:=y3[3];
      y3[3]:=y3[2];
      y3[2]:=y3[1];
      y3[1]:=k1*x3[1]+k2*x3[3]+k3*x3[5]+k4*x3[7]+k5*y3[3]+
k6*y3[5]+k7*y3[7];
      freq:=y3[1];
      END;


(* This procedure demodulates the received IF signal.   *)
PROCEDURE demodulator(step:integer);
      VAR Iin,Qin,I,Q:real;
      dumpQ,dumpI:integer;
      BEGIN
      point:=point mod 560;
      filter3(freq1,freq);
      Qin:=freq*sines[point];
      filter2(Qin,Q);
      Qt:=Qt+Q/140;
      dumpQ:=step+140*bitno+1;
      if (dumpQ mod 280=0)then
        BEGIN
        if Qt>=0 then BQ:=1 else BQ:=0;
        Qt:=0;
        if BI=1 then BoutQ:=BQ;
        if BI=0 then
          BEGIN
          if BQ=0 then BoutQ:=1 else BoutQ:=0;
          END;
        END;
      Iin:=freq*coses[point];
      filter1(Iin,I);
      dumpI:=step+140*bitno+1;
      if (dumpI>140) then It:=It+I/140;
      if(((dumpI-140)<>0) and ((dumpI-140) mod 280 = 0)) then
        BEGIN
        if It>=0 then BI:=1 else BI:=0;
        It:=0;
        if BQ=1 then BoutI:=BI;
        if BQ=0 then
          BEGIN




          if BI=0 then BoutI:=1 else BoutI:=0;
```

```
          END;
        END;
      if ((bitno=lastbit) and (step=139)) then
         BEGIN
         if It>=0 then BI:=1 else BI:=0;
         if BQ=1 then BoutI:=BI;
         if BQ=0 then
           BEGIN
           if BI=0 then BoutI:=1 else BoutI:=0;
           END;
         END;
      point:=point+1;
      END;


(* This procedure receives a bit stream and generates the
output signal.                                              *)
PROCEDURE signalgenerater;
      VAR phasevalue,phase,angle,noise,signal:real;
      step,z:integer;
      BEGIN
      for step:=0 to 139 do
         BEGIN
         time:=step/140+bitno;
         phasevalue:=(pi/2*step/139*(-bit1));
         phase:=initialphase+phasevalue;
         angle:=2*pi*Fo*time+phase;
         noise:=random(feed);
         wave[2]:=wave[1];
         wave[1]:=wave[0];
         wave[0]:=cos(angle);
         signal:=a2*(a*b*wave[2]+a*cos(angle-2*pi*F1*tt));
         freq1:=signal+noise;
         rmsS:=(a2*cos(angle)*a2*cos(angle))+rmsS;
         rmsN:=(noise*noise)+rmsN;
         demodulator(step);
         END;
      initialphase:=phase;
      END;

(* This procedure generates a pseudo random bit stream. *)
PROCEDURE randomgeneration;
      VAR loop:integer;
      BEGIN
      writeln('Enter a seed for the generater (any integer
> 0)');
      read(feed);
      lastbit:=9999;
      for loop:=0 to 9999 do
         BEGIN
         ran:=random(feed);
         if ran<0.0 then bit1:=-1 else bit1:=1;
         if bitno mod 2=0 then Bin[1]:=bit1;
         if bitno mod 2<>0 then Bin[2]:=bit1;
         signalgenerater;
         if bitno >=1 then decider;
         bitno:=bitno+1;
```

```
         END;
      END;

(* This procedure generates a repetitive stream of 8 set
bits.                                                    *)
PROCEDURE setbitgen;
      VAR dummy,digit:char;
      bit:array[1..8] of integer;




      loop1,loop2:integer;
      BEGIN
      lastbit:=9999;
      read(dummy);
      for loop1:=1 to 8 do
         BEGIN
         read(digit);
         bit[loop1]:=ord(digit)-48;
         END;
      for loop2:=1 to 1250 do
         BEGIN
         for loop1:=1 to 8 do
           BEGIN
           bit1:=bit[loop1];
           if (bit1=0) then bit1:=-1;
           if bitno mod 2=0 then Bin[1]:=bit1;
           if bitno mod 2<>0 then Bin[2]:=bit1;
           signalgenerater;
           if bitno >=1 then decider;
           bitno:=bitno+1;
           END;
         END;
      END;

(* This is the start of the main program.                 *)
BEGIN
  bitno:=0;
  Fo:=35;
  BI:=1;
writeln('Enter a value for a');
read(a);
writeln('Enter a value for b');
read(b);
F1:=10.0E6;
  rewrite(datafile,'freqdata');
  for t1:=0 to 3 do
  BEGIN
    for t2:=0 to 139 do
    BEGIN
    ang1:=2*pi*Fo*(t2/140+t1);
    ang2:=pi*(t2/140+t1)/2;
    sines[t2+140*t1]:=sin(ang1)*sin(ang2);
    coses[t2+140*t1]:=cos(ang1)*cos(ang2);
```

```
    END;
  END;
  inputpage(a1,a2);
  if a1=1 then
      BEGIN
      writeln('Randon Generation Option Selected');
      randomgeneration;
      END;
  if a1=2 then
      BEGIN
      writeln('Set Bit Generation');
      writeln('Type In 8 Bits eg. 10011100');
      setbitgen;
      END;
rmsS:=sqrt(rmsS/1120);
rmsN:=sqrt(rmsN/1120);
noiseratio:=20*ln(rmsS/rmsN)/ln(10)+10*ln(ENB/br)/ln(10);
writeln(noiseratio);
writeln(BER);
END.
```